PAN AFRICAN UNIVERSITY

INSTITUTE FOR BASIC SCIENCES, TECHNOLOGY AND INNOVATION

MATHEMATICAL MODELS FOR INFLUENZA A VIRUS AND PNEUMOCOCCUS: WITHIN–HOST AND BETWEEN–HOST INFECTION

By

Fulgensia Kamugisha Mbabazi

A Thesis Submitted in Partial Fulfillment of the Requirements for the Award of the Degree of Doctor of Philosophy in Mathematics of Pan African University Institute for Basic Sciences, Technology and Innovation

April 1, 2019

DECLARATION

I, **Fulgensia Kamugisha Mbabazi** declare that this submission is my own work towards the Ph.D mathematics and that, to the best of my knowledge it contains no material previously published by another person nor material which has been accepted for the award of any other degree of the University or College elsewhere, except where due acknowledgment has been made in the text.

Signature ..... Date .....

This thesis has been under our supervision and has approval for submission:
Certified by:

Signature ..... Date .....

Professor, Joseph Y.T Mugisha
Makerere University,
College of Natural Sciences,
Mathematics Department,
P.O.BOX 7062,
Kampala, Uganda.

Signature ..... Date .....

Doctor, Kimathi Mark
Department of Mathematics,
Statistics and Actuarial Sciences, Machakos University,
P. O. Box, 136–90100, Machakos, Kenya.

DEDICATION

I dedicate this research work to my dear parents late Gabrael Rwitoka, Tekyera Beturumura and Mary Kebita Okuja. May their souls rest in peace.

ACKNOWLEDGMENT

I give glory to the Almighty God who has made it possible for me to accomplish this research and wish to extend my sincere thanks and appreciation to the following people and institutions.

Pan African University Institute for Basic Sciences, Technology and Innovation, Nairobi–Kenya, Busitema University, Tororo–Uganda and Uganda Martyrs University, Nkozi–Uganda, for the financial support.

My Supervisors Professor Joseph Y.T. Mugisha and Doctor Kimathi Mark for their dedicated guidance, encouragement, devotion, tolerance and all the necessary support rendered to me especially in the field of Mathematical Modeling and Computational Mathematics. May God, bless you plentifully. Professor L.S. Luboobi, your parental guidance and technical support has been a road mark in my achievement, be blessed always!

My husband Major Kamugisha Joram Kembo for loving, encouraging, supporting and accepting me to undertake the programme; may God bless you. My children: Asea James, Kyokusiima Racheal, Kagaiga Joel and Katungi Emmanuel for the care, encouragement, prayers, jokes and loving stories you have always offered; may God guide you to grow into responsible citizens. My friends, thank you for your support in advising me during the programme and paying visits to my children. May God reward you abundantly.

TABLE OF CONTENTS

DECLARATION i

DEDICATION ii

ACKNOWLEDGMENT iii

LIST OF FIGURES viii

LIST OF TABLES xiii

ACRONYMS xv

NOMENCLATURE xvi

ABSTRACT xxi

Chapter One: INTRODUCTION 1

1.1 Basic information about influenza A virus 1

1.2 Basic information about pneumococcus 3

1.3 Co–infection of influenza A virus and pneumoccus 4

1.4 Attempts to control pneumococcal pneumonia 7

1.5 Important definitions 8

1.6 Statement of the problem 10

1.7 Study Objectives 11

1.7.1 General objective 11

1.7.2 Specific objectives 11
1.8 Justification of the study 11
1.9 Methodologies for model analysis 12
1.9.1 Autonomous system 12
1.9.2 Stability of steady states 13
1.9.3 Global stability of steady states (Equilibrium points)–Lyapunov functions 14
1.10 Organization of the Thesis 15

Chapter Two: LITERATURE REVIEW **17**

2.1 Introduction 17
2.2 Within–host Co–infection for infectious diseases 17
2.3 Mathematical models of infectious diseases, with time delays, antibiotic resistance awareness and treatment 19

Chapter Three: WITHIN–HOST CO–INFECTION MODEL OF INFLUENZA A VIRUS AND PNEUMOCOCCUS **23**

3.1 Introduction 23
3.2 Description, formulation and basic qualitative properties of the model 23
3.3 Model assumptions 25
3.4 Basic qualitative properties 28
3.4.1 Positivity of solution trajectories of model (3.1) 28
3.4.2 Boundedness of the solutions 29

3.5 Well–possedness of influenza A virus sub–model 30

3.5.1 Computation for influenza A viral fitness (R_0^1) 32

3.5.2 Stability analysis of influenza A virus steady state 34

3.5.3 Global stability of the influenza A virus free steady states 36

3.5.4 Existence of Influenza A virus endemic state 39

3.5.5 Pathogen fitness (R_{IP}) 44

3.6 Existence and uniqueness of steady states 50

3.6.1 Infection–free steady state (IFSS) 50

3.6.2 Endemic steady state (ESS) 50

3.7 Stability of steady states 52

3.7.1 Local stability of the infection–free steady state (IFSS) . . 52

3.7.2 Local stability of the endemic steady state (ESS) 54

3.7.3 Global stability of the infection–free steady state (IFSS) . 56

3.7.4 Global stability of endemic steady state 59

3.7.5 Sensitivity analysis of the model parameters on the pathogens' fitness 65

3.7.6 The impact of pneumococcus on Influenza A virus 69

3.7.7 The impact of Influenza A virus on pneumococcus 69

3.8 Model results and discussion 71

Chapter Four: BETWEEN–HOST PNEUMOCOCCAL PNEUMONIA MODEL WITH TIME DELAYS 78

4.1 Introduction 78

4.2 Model formulation 78
4.3 Model assumptions 79
4.3.1 Positivity of solutions 81
4.3.2 Boundedness 84
4.3.3 The control reproduction ratio 84
4.4 Stability of equilibria 85
4.4.1 Local stability of the disease–free equilibrium point 87
4.4.2 The transcendental equation 88
4.4.3 Delay–free system 90
4.5 Existence of Hopf–bifurcation 91
4.5.1 Delay only in latent period ($\tau_1 > 0, \tau_2 = 0$) 92
4.5.2 Delay only in seeking medical care by the infectious ($\tau_1 = 0, \tau_2 > 0$) 96
4.5.3 Delay in latent period and seeking medical care ($\tau_1 = \tau_2 = \tau > 0$) 100
4.6 Model results and discussion 102

Chapter Five: MODELING EFFECTS OF ANTIBIOTIC RESISTANCE AWARENESS AND SATURATED TREATMENT OF PNEUMOCOCCAL PNEUMONIA 111

5.1 Introduction 111
5.2 Model formulation 111
5.3 Model assumptions 113
5.3.1 Positivity of solution trajectories in model (5.1) 116

5.3.2 Invariant region 117
5.3.3 Existence and uniqueness of the steady states 117
5.3.4 The basic reproductive number 119
5.3.5 Local stability behavior of the disease–free steady states . 120
5.3.6 Local stability of endemic steady state 122
5.4 Global stability of the equilibria 123
5.4.1 Global stability of the disease–free steady state 124
5.4.2 Global stability of the endemic–steady state 125
5.4.3 Sensitivity analysis of model epidemiological parameters on the control reproduction number 127
5.5 Model results and discussion 130

Chapter Six: CONCLUSION AND RECOMMENDATIONS 134

6.1 Conclusion 134
6.2 Recommendations 135
6.3 Future research direction 136

REFERENCES 137

APPENDICES 157

LIST OF FIGURES

1.1 Pathophysiological interactions between influenza and bacterial respiratory pathogens and various clinical expressions (Metersky et al., 2012). 6

3.1 A schematic diagram for model (3.1). The dotted lines indicate cell–pathogen interaction and solid lines with arrows not starting from the compartments show the release of pathogens from infected cells. The solid lines with arrows show transfer from one compartment to another. 27

3.2 Simulation of model (3.1), the free–infection steady state, with populations $I_v = I_b = I_{vb} = B = V = 0$. The rest of the parameters are as in Table 3.2 and Table 3.1. 53

3.3 A weighted simple digraph for influenza A virus and pneumococcus co–infection 62

3.4 Phase potraits for the dynamics of influenza A virus and pneumococcal bacteria, (a) with parameter values $n_v = 10^3, n_b = 10^5$, variables $S(0) = 4.8 \times 10^5$, $I_v = 10^2, I_b = I_{vb} = B = V = 10^3$ and (b) with parameter values $n_v = 10^4, n_b = 10^3$, variables $S(0) = 4.8 \times 10^5$, $I_v = 10^3, I_b = 10, I_{vb} = B = V = 10^3$ and other parameters remain as in Table 3.1 and Table 3.2. 70

3.5 Simulation of model (4.8), global stability for populations of infected cells (I_v) as function of time with parameter values: $\Lambda = 6.25 \times 10^5, m = 95, n_v = 10^2, \beta_b = 1.2 \times 10^{-3}, \tau_v = 1.2 \times 10^{-2}, \tau_{vb} = 1.1 \times 10^-4, \beta_v^* = 7.3 \times 10^{-10}$; variables $I_v = I_b = B = 10^3, I_{vb} = 10^4$ (thus $R_P = 17.1774 > 1$ and $R_I = 2.4218 > 1$), and other parameters remain as in Table 3.1 and Table 3.2. 71

3.6 Simulation of model (3.1)(a) showing chronic levels of infected cells I_b for different values of β_b as function of time with parameter values:$\Lambda = 6.25 \times 10^5, \beta_b = 1.2 \times 10^-4, n_b = 10^5, a = 2.0 \times 10^{-2}, b = 0.6, \mu_b = 1.34 \times 10^{-2}, \tau_b = 1.102 \times 10^{-5}$, variables; $S(0) = 4.0 \times 10^3$, $I_v = I_{vb} = 10^2$, $I_b = B = 10^3, V = 10^7$ (thus $R_P = 2235.9654 > 1$ and $R_I = 8.6950 > 1$). (b) Chronic levels of infected cells I_v for different values of β_v as function of time with parameter values: $n_b = 10^3, \tau_{vb} = 2.4 \times 10^{-3}, \beta_v^* = 7.3 \times 10^{-8}, \beta_b^* = 4.1 \times 10^-7, \tau_v = 8.6 \times 10^-2$, variables; $S(0) = 4.8 \times 10^7, I_v = 10^4, I_b = 10^2, \tau_{vb} = 10, B = 10^6, V = 10^4$ and other parameters remain as in Table 3.1 and Table 3.2, hence $R_p = 2.2359 > 1$ and $R_I = 86.9477 > 1$ . . . 72

3.7 Simulation of model (3.1)(a) Global stability of the positive endemic steady state of co–infected cells (I_{vb}), showing varying values of maximum number of bacteria alveolar macrophage (m) can consume (that is $m = 60$ ($R_p = 3.7407$), $m = 80$ ($R_P = 2.2360$), $m = 100$ ($R_P = 1.5945$), with variables: $S(0) = 4.0 \times 10^{-1}, I_v = I_b = I_{vb} = 10^3, B = 10^4, V = 10^6$. (b) Global stability for the co–infected population with changing effect of phagocytosis rate γ_a that is $\gamma_a = 8.877 \times 10^{-1}$ (R_P=2.2360), γ_a=9.877×10^{-1} ($R_P = 1.8927$), γ_a=7.877×10^{-1} ($R_P = 2.7310$), with variables $I_v = 10, I_b = I_{vb} = 10^3, B = 10^4, V = 10^3$. The rest of the parameters are as in Table 3.1 and Table 3.2. 74

3.8 Solution trajectories for Epithelial population with variables: (a)$a = 0.02, b = 0.6, S(0) = 4.0 \times 10^7, I_v(0) = 10^4, V(0) = 10^7, V(0) = 10^6$ ($R_I = 0.86967$) (b) $a = 0, b = 0.6, I_v(0) = 10^5, V(0) = 10^4 (R_I = 1.739 \times 10^7)$, (c)$b = 0, a = 0.01$ $R_I = 1.7393$ with variables $I_v(0) = 10^5, V(0) = 10^4$. The rest of the parameters are as in Table 3.1 and Table 3.2. 74

3.9 Solution trajectories for Epithelial population with variables: (c)$a = 0.02, b = 0, S(0) = 4.0 \times 10^7, I_v(0) = 10^4, V(0) = 10^7, V(0) = 10^6$ ($R_I = 0.86967$) (d) $a = 0, b = 0, \Lambda = 6.25 \times 10^4, S(0) = 4.0 \times 10^3, I_v(0) = 10^4, V(0) = 10^5 (R_I = 17393)$, The rest of the parameters are as in Table 3.1 and Table 3.2. 75

4.1 A schematic diagram showing the dynamics of pneumococcal pneumonia. The dotted lines represent contacts made by individuals in the respective classes and the solid lines show transfer from one class to another. 80

4.2 Simulation of model (4.1), the disease–free equilibrium, with populations parameters: $\phi = 3.57144 \times 10^{-1}, \beta = 1.0102 \times 10^{-5}, \gamma = 3.3333 \times 10^{-2}$ (with $R_0 = 0.7873, R_0^u = 0.1382, R_0^v = 0.6490$). . . . 88

4.3 (a& b) Stability of the endemic equilibrium showing Hopf–bifurcation, with initial variables: $S(0) = 5586, V(0) = 22, C(0) = 64, I(0) = 11, E(0) = 100$. (c& d) The evolution of the infected, the susceptible and corresponding I-S portrait and 3-D phase trajectories, (with $R_0 = 15.4, R_0^u = 15.14, R_0^v = 0.271$ parameters:$\mu = 2.0547 \times 10^{-4}, \phi = 3.574 \times 10^{-2}$. The rest of the parameters remain fixed as in Table 4.1. 104

4.4 Simulation of model (4.1) for $\tau_2 = 0$ and $\tau_1 > 0$, with initial variable values: $(S(0), V(0), E(0), C(0), I(0)) = (3280, 30, 10, 10, 100)$. The rest of the parameters are as in Table 4.1. 105

4.5 Stability of the endemic equilibrium P^* for $\tau_1 = \tau_2 = 2$ days. The rest of the parameters are as in Table 4.1. 106

4.6 The effect of varying τ_2 on the dynamics of model (4.1). The delay τ_2 was chosen as $\tau_2 = 2.5, 3, 3.5$. All other parameters remain as stated in Table 4.1. 107

4.7 The effect of varying time delay τ_1 on the dynamics of model (4.1). The delay τ_1 was chosen as $\tau_1 = 0.5, 2, 8.5$. All the parameter values are the same as in Table 4.1. 108

5.1 A transition diagram showing the dynamics of pneumococcal pneumonia, with $T(I) = \frac{I}{1+\tau I}, g(I) = (\beta I - \frac{\beta_1 m I}{m+I})$. 115

5.2 Sensitivity indices of R_0, in relation to epidemiological parameters. 129

5.3 Stability of the disease–free steady state (a) With parameter values $\beta = 0.0001865$ and $\beta_1 = 0.00046$. (b) With parameter values $\beta = 0.0417, \gamma = 0.00145, \beta_1 = 0.046$ and $\beta_2 = 0.00007498$. Choosing initial values $S_u = 103, S_a = 24896, I = 0, R = 0$ and all the parameter values are the same as in Table 5.2 130

5.4 Stability of the endemic–steady state (a)Initial variables $S_u^* = 606, S_a^* = 581, I^* = 10, R^* = 8$. (b) Variables:$S_u^* = 40, S_a^* = 20, I^* = 1, R^* = 1$ Parameter values $\beta = 0.0417, \gamma = 0.00145, \beta_1 = 0.046$ and $\beta_2 = 0.00007498$. Initial values $S_u = 103, S_a = 24896, I = 0, R = 0$ and all the parameter values are the same as in Table 5.2 131

5.5 Effect of antibiotic resistance awareness and loss of information on awareness on the control reproduction number 132

LIST OF TABLES

3.1 Parameter values for influenza A virus and Streptococcus pneumoniae 66

3.2 Parameter values for pneumococcus co–infection models 67

3.3 Sensitivity indices of R_I/R_P to parameters of IAV and Pneumococcus (SP), computed at the baseline parameter values given in Table 3.2 and Table 3.1 68

4.1 Parameter values 103

5.1 Parameters values 128

5.2 Sensitivity index (S.I) of R_0 w.r.t the parameters 129

ACRONYMS

ODE	Ordinary Differential Equation
DDE	Delay Differential Equation
MATLAB	Matrix Laboratory
HIV	Human Immunodeficiency Virus
AIDS	Acquired Immunodeficiency Syndrome
IAV	Influenza A Virus
IBV	Influenza B Virus
ICV	Influenza C Virus
IDV	Influenza D Virus
NA	Neuraminidase
HA	Hemagglutinin
IPD	Invasive Pneumococcal Diseases
AM	Alveolar Macrophages
PCV's	Pneumococcal Conjugate Vaccines
SP	Streptococcus Pneumoniae
SIS	Susceptible–Infective–Susceptible
SEI	Susceptible–Exposed–Infective
SIR	Susceptible–Infective–Recovered
SEIR	Susceptible–Exposed–Infective–Recovered

NOMENCLATURE

Withinhost co–infection model of IAV and pneumococcus

S	Population density of uninfected cells
I_v	Population density of infected cells not yet producing IAV
I_b	Density of infected cells not yet producing pneumococcus
I_{vb}	Population density of co–infected cells
V	Total number of influenza A virus
B	Total number of pneumococcus bacteria
A	Alveolar macrophage population
Λ	Recruitment of epithelial cells from the pool of precursor cells
μ_s	Natural death rate for uninfected epithelial cell
r	Bacterial growth rate
γ_a	Phagocytosis rate
τ_b	Creation rate of bacterium by infected epithelial cells
μ_b	Mortality rate of pneumococcus infected cells
β_b	Epithelial cell infection rate per bacterium
δ_b	Toxic death rate due to pneumococcus bacterium
n_b	Released pneumococcus particles from lysis of infected cells

n_v	Released infectious IAV particles from lysis of infected cells
n_{vb}	Free co–infected particles liberated from lysis of infected cells
β_v	Epithelial cell infection rate per virion
β_v^*	Infectivity rate of infected cells by pneumococcus with IAV
β_b^*	Infectivity rate of infected cell by IAV with pneumococcus
α_v	Loss of IAV due to interaction of uninfected cells with SP
α_b	Loss of SP due interaction of uninfected cell with IAV
τ_v	IAV production rate
τ_{vb}	Creation rate of co–infected cells
δ_v	Toxic death rate due to influenza A virus
μ_v	Mortality rate of influenza A virus infected cells
μ_{vb}	Mortality rate of co–infected cells
m	Maximum number of bacteria an AM can catch in a unit time

Between–host pneumococcal pneumonia model with time delays

$S(t)$	Number of susceptible individuals at time t
$V(t)$	Number of vaccinated individuals at time t
$E(t)$	Number of asymptomatic individuals at time t
$C(t)$	Number of people with one sero–type not covered by the vaccine
$I(t)$	Number of infectious individuals at time t
b	Recruitment rate
ν	Effective vaccination rate
γ	Transfer rate from E to I class
μ	Natural mortality rate from causes unrelated to the infection
δ	Disease–induced mortality rate
ρ	Progression rate from C to I class
ϕ	Per capita rate of recovery
ζ	Waning rate of vaccine
ϑ	Proportion of the sero–type not covered by vaccine
β	Transmission coefficient
τ_1	Delay for the incubating individual
τ_2	Delay in seeking medical care

A model for the effect of antibiotic resistance awareness and saturated treatment for pneumococcal pneumonia

$S_u(t)$	Unaware individuals
$S_a(t)$	Aware individuals
$I(t)$	Infected individuals receiving treatment
$R(t)$	Infected individuals but resistant to first line of treatment
$N(t)$	Total population
B	Recruitment by birth/immigration
β	Maximal effective contact rate before awareness
β_1	Maximal reduced effective contact rate due to media alerts
β_2	Contact rate of aware susceptibles with infectives
γ	Rate of relapse encountered in administering treatment
m	Efficiency of awareness through media coverage
δ	Excess death due to disease
ξ	Loss of information about disease by aware susceptibles
Φ	Recovery rate due to treatment
D	Number of days delayed in receiving appropriate treatment
τ	Rate of delay to receive appropriate treatment

p	Probability of acquiring resistance during treatment
v	Rate at which unaware susceptibles become aware

ABSTRACT

Infectious diseases have become problematic throughout the world, threatening individuals who come into contact with pathogens responsible for transmitting diseases. Pneumoccocal pneumonia, a secondary bacterial infection follows an influenza A infection, responsible for morbidity and mortality in children, elderly and immuno–comprised groups. The aims of this Thesis are to; develop a mathematical model for within–host co–infection of influenza A virus and pneumococcus, model between–host pneumococcal pneumonia in order to determine the effect of time delays due to latency and seeking medical care, and study the effect of antibiotic resistance awareness and saturated treatment in the control of pneumococcal pneumonia. Analysis of the stability of steady states of influenza A virus and pneumococcal co–infection, pnemococcal pneumonia with time delays and antibiotic resistance awareness is done. The graph theoretic method, combined linear and quadratic Lyapunov functions, Goh–Voltera Lyapunov function are used to get suitable Lyapunov functions for global stability of steady states. The results show that the endemic equilibrium of pneumococcal pneumonia is locally stable without delays and stable if the delays are under conditions. The results suggest that as the respective delays exceed some critical value past the endemic equilibrium, the system loses stability and yields Hopf–bifurcation. The results of influenza A virus and pneumococcal co–infection show that, there exist a biologically important steady state where the two pathogens of unequal strength co–exist and replace each other in the epithelial cell population when the pathogen fitness for each infection exceeds unity. The impact of influenza A virus onto pneumococcus and vice–versa yields a bifurcation state. The results show that, the presence of antibiotic resistance awareness and treatment during the spread of pneumococcal pneumonia drastically reduces the basic reproduction number R_0 to less than unity, hence the disease could be eradicated.

CHAPTER 1

INTRODUCTION

1.1 Basic information about influenza A virus

Infectious diseases commonly known as communicable diseases, have always besieged animals and humans. Pathogenic microorganisms, such as bacteria, viruses, parasites or fungi spread diseases, directly or indirectly, from one person to another. Examples of bacterial diseases include pneumococcal, Tuberculosis ; Viral infections among others include influenza A virus and HIV/AIDS. Of the main important pathogens affecting humans today are influenza A virus and pneumococcus (Ackleh & Allen, 2003). Infectious diseases are significant and frequently cause human illness that lead to mortality across the globe.

Influenza commonly known as 'flu' is an infectious disease caused by a virus that is categorized in four different types A, B, C and D (IAV, IBV, ICV and IDV), but only influenza A and B viruses cause clinically significant human disease and seasonal epidemics (Ferguson et al., 2015). Influenza is one of the most studied viral infections, interactions and co–infections for respiratory viruses in general (Boianelli et al., 2015). It causes yearly chronic epidemic outbreaks, and individuals become infected several times over their lifetime (Beauchemin & Handel, 2011). They are distinguished by differences in two major virus surface proteins; HA and NA (Kamal et al., 2017). There are 16 diverse types of HA and 9 diverse types of NA. Thus there are potentially 144 diverse subtypes of influenza A viruses (Shi et al., 2010). With these types, virus A is epidemiologically essential for humans because it can recombine its genes with those of strains circulating in animal populations (birds, swine and horses).

Influenza is highly infectious, transmitted through contact with droplets from the nose and throat of an infected person who is coughing and sneezing (Krishnapriya et al., 2017). Influenza A is a short–lived infection with an incubation period of approximately 2 days with viral shedding in respiratory secretions starting approximately 1 day before the onset of symptoms (Carrat et al., 2008). The typical pattern of virus kinetics is characterized by fast exponential growth, with climax in viral load up to 1–3 days post infection, followed by a decline over the subsequent 3–5 days (Chang & Young, 2007).

IAV has been observed to be a significant threat to public health, giving rise to 15–65 million infections and more than 200,000 hospitalizations each year during seasonal epidemics in the United States (Smith & Smith, 2016). Influenza–related acute lower respiratory infection is responsible for at least 28,000 to 111, 500 deaths in children less than 5 years old accounting for more than 90% of deaths due to influenza in young children in developing countries (Nair et al., 2011). The outbreaks reported as the Asiatic Flu (H2N8) (1889–1890), Spanish Flu (H1N1) (1918–1920), Asian Flu (H2N2) (1957–1958), Hong Kong Flu(H3N2) (1968–1969) and the swine Flu (H1N1) of (2009) revealed a high morbidity and mortality rate Boianelli et al. (2015); Rynda-Apple et al. (2015); Pawelek et al. (2016) of whom, over 50% of the people who died showed histologic and microbiologic evidence of bacterial pneumonia (Joseph et al., 2013). The 1918–1919 epidemic was among the deadliest public health crises in human history, killing approximately 675,000 people in the United States and about 50 to 100 million people worldwide (Chertow & Memoli, 2013). In 2003, avian influenza A virus subtype (H5N1) caused human deaths and massive poultry die–offs globally, including west and north Africa (Katz et al., 2012; Radin et al., 2012). An outbreak of H7N9 bird influenza occurred in China between February 2013 and May 2014, 400 infected human

cases by this avian H7N9 virus were reported to have contracted the virus from exposure to live poultry or potentially contaminated environments, especially trading markets where live poultry was sold for food (Xing et al., 2017).

1.2 Basic information about pneumococcus

Pneumococcus is the classic example of a highly invasive, gram–positive, extracellular bacterial pathogen that colonizes the upper respiratory tract, which includes the nose, nasal cavity, pharynx, and larynx (Henriques-Normark & Tuomanen, 2013). Viruses that appear the nasopharynx of asymptomatic individuals can facilitate both colonization of bacteria and promote viral presence (Bosch et al., 2013). Pneumococci are different, with 90 recognized sero–types; several of these serotypes are capable of causing invasive disease (Chertow & Memoli, 2013). Pnemococcus cause the following types of illnesses depending on the affected part of the body: IPD such as meningitis, bacteremia and bacteremic pneumonia; lower respiratory tract infections (e.g., pneumonia), and upper respiratory tract infections (e.g., otitis media and sinusitis) (Lamb et al., 2011; Bichara et al., 2012). Pneumococcal infections may follow a viral infection, like a cold or flu (influenza) (Mbabazi et al., 2018). The wide spread of the disease may be promoted by potentially asymptomatic persons Sun et al. (2015); Li et al. (2016) and an individual remains in the exposed class for a certain latent period prior to becoming infective (Cooke & Van Den Driessche, 1996; Xu & Ma, 2010).

Pneumonia is the most common form of severe pneumococcal disease, accounting for 15 % of all deaths of children under 5 years and killing an estimated 922,000 in 2015, and is the leading cause of death in this age group (Waheed et al., 2016). Death due pneumonia is attributed to bacterial infections, mostly Streptococcus

pneumonia (32.7%) and Haemophilus influenzae (15.7%), influenza viruses add considerably, accounting for 7% of all severe pneumonia episodes and 10.9% of pneumonia deaths (Mina & Klugman, 2014). According to Walker et al. (2013), 1.3 million (81%) of death are associated with pneumonia that occurs in the first 2 years of life. Worldwide, pneumococcal pneumonia disease continues to be a major cause of morbidity and mortality in persons of all ages and the leading cause of bacterial childhood disease, despite a century of study and the development of antibiotics and vaccination (Domínguez et al., 2017). With an estimated 14.5 million episodes of serious pneumococcal disease occurring each year among children under 5 years of age, resulting in approximately 500,000 deaths, most of which occur in low and middle–income countries (O'Brien et al., 2009; Rodgers & Klugman, 2016; Iroh Tam et al., 2018).

1.3 Co–infection of influenza A virus and pneumoccus

Influenza A virus and pneumococcus are pathogens that cause epidemics of recurrent infections driven by seasonality (Weinberger et al., 2014). Influenza A virus and pneumococcus co–infections manifest in difficult–to–treat disease processes that require extensive antimicrobial therapy and cause significant excess mortality (Mina & Klugman, 2014). During influenza infection the resident AM depletion takes place and this creates a position for secondary pneumococcus infection by altering early cellular innate immunity in lungs, that results into pneumococcal development and lethal pneumonia (Ghoneim et al., 2013). In the process of co–infection by the same host, highly virulent viral strains play the role of colonizers, because they kill cells faster and thus reproduce faster, which allows faster spread and colonization of new cells (Ojosnegros et al., 2012).

Competition in the host occurs when different pathogens selects for the fastest replicating strain which could be more virulent (Ackleh & Allen, 2003; Bichara et al., 2012). At population level an intermediate replication rate that maximizes transmission takes place (May & Anderson, 1983). Of the 317 pediatric deaths that occurred in the United States from April, 2009 to January, 2010 showed, 28% evidence of bacterial co–infection, predominantly streptococcus aureus and pneumococcus (Cox et al., 2011). The interaction of influenza and bacterial respiratory pathogens and various clinical outcome is shown in Figure 1.1.

Control strategies have been instituted in an effort to fight the co–infection. Vaccines against bacterial pathogens can reduce the co–infection element, but their efficiency is limited to the vaccine serotypes (McCullers, 2011; Mina et al., 2013; Metzger et al., 2015). Vaccines for influenza A virus and pneumococcus are not effective because they do not include pandemic strains and offer little protection against viruses with novel coat proteins (Cauley & Vella, 2015; McCullers, 2006). Watanabe et al. (2012) and Belser et al. (2011) reported increasing frequent infections due to new strains of avian influenza virus (including H5N1 and H7N9), stressing the possibility that another pandemic could arise. Emphasis on development of new and effective vaccines that target drug–resistant strains during secondary infection should be given priority (Chung & Huh, 2015).

Treatment with antimicrobial agents may also reduce infection progress and eliminate secondary bacterial infection incidence (McCullers, 2004; Ghoneim et al., 2013).

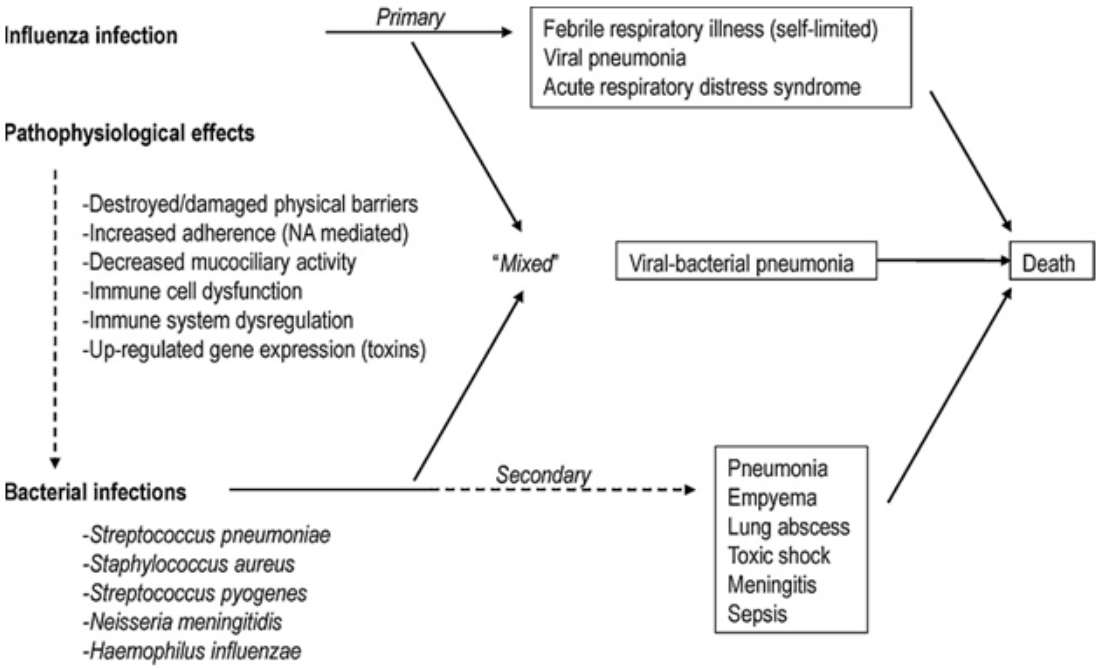

Figure 1.1: Pathophysiological interactions between influenza and bacterial respiratory pathogens and various clinical expressions (Metersky et al., 2012).

1.4 Attempts to control pneumococcal pneumonia

Pneumococcal pneumonia is preventable through vaccination, diagnostic testing, environmental control measures, and appropriate treatment (Kizito & Tumwiine, 2018). Vaccination is a highly efficient means of preventing diseases and death (Rémy et al., 2015). Decrease of IPD has been managed by PCV's, and they are among the many ongoing control interventions of vaccine successes around the world. One dose of vaccine does not protect all receivers because vaccine–induced immunity is lost after some period of time (Gjorgjieva et al., 2005; Samanta et al., 2016).

Mass media plays a vital role in changing behavior related to public health (Redman et al., 1990). Enhanced levels of awareness, for example: practice of better hygiene, voluntary quarantine, application of preventive medicine or vaccination and avoidance of places containing large numbers of people may reduce the spread and contraction of the disease (Greenhalgh et al., 2015). The spread of an infectious disease is reported by the media, such as television programs, newspapers, radio or online social networks, whenever it outbreaks. Daily updates and reports about infections and mortality have significant effects on the necessity of control of an epidemic (Liu et al., 2016). Campaigns mainly focus on increasing individual's knowledge about disease transmission and control measures that may reduce likelihood of being infected (Misra et al., 2011). Mathshidiso (2018) described antibiotic resistance as a grave threat to future of global health as World Health Organization joined the global community to observe the World antibiotic awareness week from 12th–18th November 2018, with the overall theme 'Think Twice'.

Epidemiological data of influenza A virus–pneumococcal co–infection is major challenge. Yet, modeling studies have been limited by the poor knowledge about respiratory viruses and bacteria circulating in the community, especially because little is known about prevalence, incidence, at risk populations, and even epidemic profiles in different populations (Opatowski et al., 2018).

During co–infection of the same host highly virulent viral strains play the role of colonizers, because they kill cells faster and thus reproduce faster, which allows faster spread and colonization of new cells (Samuel et al., 2012). Concurrent infection with multiple pathogens as for the case of influenza A and pneumococcal greatly contribute to disease severity especially with supper–infections of the lung and middle ear (Greenhalgh et al., 2015). Multiple infections cause intra–host competition among strains and thus lead to an increase in the average level of virulence above the maximal growth rate for a single pathogenic strain (Bosch et al., 2013). Further, co–infections are believed to reduce treatment efficacy and increase treatment costs (Griffiths et al., 2014).

Individuals continue to practice self medication Resti et al. (2009); Pajuelo et al. (2018), which leads to delays in the administration of adequate antimicrobial treatment, increase resistance to antibiotics that lead to increased hospital mortality (Kollef et al., 1999).

1.5 Important definitions

Pathogen fitness: is the number of secondary infections generated during the whole infectious period (Ciupe & Heffernan, 2017).

Basic reproductive ratio number: is the number of new infections generated in the lifetime of an infected individual when introduced into a completely susceptible population (Ojosnegros et al., 2012).

Co–infection: A processes where either multiple parasite strains or species infect a single host (May & Nowak, 1995).

Multi–parasite hosts: Single host species exploited by several concurrent parasite species, either during their whole life cycle or during a given stage within it, at both the individual and population levels (Rigaud et al., 2010).

Mathematical model: is a set of formulas and/or equations based on a quantitative explanation of real phenomena and formed in anticipation that the behavior it predicts will be similar to the real behavior on which it is based.

Hopf–bifurcation: is a critical point where a system's stability switches and a periodic solution arises.

A differential equation: is an equation which involves an unknown function $f(x)$ and at least one of its derivatives.

A Lyapunov function: is a scalar function defined on the phase space, which can be used to prove the stability of an equilibrium point.

A graph $G = (V(G), E(G),$ $\tilde{G}(.))$ is a pair of sets $V(G)$ and $E(G)$ and an incidence relation $\tilde{G}(.)$ that maps pairs of elements of $V(G)$ (not necessarily distinct) to elements of $E(G)$ (Kandel et al., 2007).

A directed graph, or digraph, G**:**, is a set of vertices $V(G)$, a set of arcs $A(G)$, and a function which assigns each arc A an ordered pair of vertices (i, j) (Din et al., 2016).

In–degree $d^{-}G(i)$ **of vertex** i**:** is the number of arcs (p, i), $p \in V$ that terminate at V.

Out–degree $d^{+}G(i)$ **of vertex** i**:** is the number of arcs (i, p), $p \in V$ that start at V (Shuai & Driessche, 2013).

Delay differential equations: At time t, evolution of the system depends on t,

current state of the system and state of the system some time $\tau_i > 0$ in the past $\dot{x} = f(x(t), x(t-\tau_1), x(t-\tau_2), \ldots, x(t-\tau_n))$; where the quantities τ_i are positive constants (Kuang, 1993).

1.6 Statement of the problem

Pathogens are everywhere, affect every feature imaginable in life of their hosts including fitness. Influenza A virus and Pneumococcus cause viral pneumonia and bacterial pneumonia respectively, these are silent killer diseases of children under 5 years of age and the elderly whose immune system might be compromised. The incidence is grave when an individual is co–infected by both diseases leading to a viral–bacterial pneumonia. If an individual initially has a viral pneumonia, delay in the latency stage increases the possibility of acquiring a viral–bacterial pneumonia. Failure to take prescribed medicine on time and continuous practices of self medication due to medicines disposal in pharmacies by infected individuals escalates the cost of treatment and increase fatalities. Infected individuals delaying to seek medical care expose individuals severe cases that may be hard to treat.

Antibiotic resistance and ineffective treatment of infections are a serious and a growing problem. It is worse in developing where herbs are used to treat the infections. Infected individuals usually relapse and become infected with new resistant strains that are hard to treat and involve high costs.
Mathematical techniques can be used to study the ffects of co–and various control interventions.Increase in antibiotics resistance lead to increased hospital mortality.

1.7 Study Objectives

The research objectives are classified into general and specific objectives respectively

1.7.1 General objective

To mathematically study the dynamics of both within–host influenza A virus and pneumococcus co–infection, and between–host of pneumococcal pneumonia.

1.7.2 Specific objectives

The specific objectives of this study are:

(i) To develop a model of within–host co–infection of IAV and pneumococcus

(ii) To design a mathematical model for pneumococcal pneumonia that determines the effect of time delays due to latency and seeking medical care

(iii) To determine the effects of antibiotic resistance awareness and saturated treatment in the control of pneumococcal pneumonia

(iv) To determine severity of IAV and pneumococcus co–infection to a host

1.8 Justification of the study

Over the years mathematical modeling has been extensively used to analyze the dynamics of various infectious diseases for example; HIV, Malaria, cholera, Tuberculosis, dengue fever, influenza, ebola, of recent zika fever and many others.

Mathematical models are extremely important, they help in increasing the understanding of the dynamics of diseases and provide policy directions for interventions. Interactions between pathogens in the host may cause considerable effects on both host and parasite fitness through host vulnerability, infection length, infection intensity, morbidity and mortality rates (Lakshmikantham et al., 1989).

Influenza A and pneumococcal are two infectious diseases of global concern and are two of the many medical conditions responsible for pneumonia illness in tropical and subtropical regions affecting children and the elderly that lead to death if untreated. Understanding the within–host dynamics is paramount to inform health workers on how best dual infections can be prevented and controlled.

1.9 Methodologies for model analysis

In this work, models of within–host of influenza A virus and pnueococcus, and between–host pneumococcal pneumonia are analyzed using various techniques described in the subsections that follow

1.9.1 Autonomous system

Let x to be the state of a dynamical system. A deterministic model that involves x is given by:

$$\dot{x} = f(x, t, \lambda) \tag{1.1}$$

with $x \in \mathbb{R}^n$, $t =$ time and $\lambda =$ the parameters upon which the evolution of the system depends.

In this thesis models are represented by autonomous systems written in the form:

$$\dot{x} = f(x) \tag{1.2}$$

with $x = (x_1, x_2, \ldots, x_n)$ and $\dot{x} = \frac{dx}{dt}$ (point–wise time–derivatives of the state variable x)

Description of a biological systems in a given dynamical system is given as; A system of differential equations is a collection of n interrelated differential equations of the form

$$\begin{aligned}
\dot{x}_1 &= f_1(t, x_1, x_2, x_3, \ldots, x_n), \\
\dot{x}_2 &= f_2(t, x_1, x_2, x_3, \ldots, x_n), \\
\ldots \quad &\ldots \quad \ldots\ldots\ldots\ldots\ldots\ldots \\
\dot{x}_{n-1} &= f_{n-1}(t, x_1, x_2, x_3, \ldots, x_n), \\
\dot{x}_n &= f_n(t, x_1, x_2, x_3, \ldots, x_n).
\end{aligned} \tag{1.3}$$

Where the functions f_j are real–valued functions of the $n+1$ variables $x_1, x_2, \ldots, x_n$, and t and assume that thef_j are C^∞ functions (M. W. Hirsch et al., 2012). Therefore, the partial derivatives of all orders of the f_j exist and are continuous.

1.9.2 Stability of steady states

Steady states (equilibrium points) of dynamical systems: A state $\bar{x}$ is said to be a steady state of the model if $f(\bar{x}) = 0$. Mathematical models are becoming more and more complicated when higher degree of nonlinearity is believed to address real–world problems. Locating explicit solutions of these models is difficult. Despite the fact that numerical simulations may provide good approximations to solutions with fixed parameters, the general solution may remain unidentified.

When a general solution is impossible to achieve, stability analysis may be an option to get a logic solution of the dynamical system's behavior. Actually, stability analysis can forecast the long time behaviour of the dynamical system's solution accurately. Broadly, there are two types of stability analysis, local and global. Local stability deals with behaviour of the dynamical system's solution near a steady state (equilibrium point), while global stability explains the dynamical system's solution behaviour in the entire region.

The Jacobian matrix of a dynamical system is given by:

$$J = Df(x) = \begin{pmatrix} \frac{\partial f_1}{\partial x_1} & \frac{\partial f_1}{\partial x_2} & \dots & \frac{\partial f_1}{\partial x_{n-1}} & \frac{\partial f_1}{\partial x_n} \\ \frac{\partial f_2}{\partial x_1} & \frac{\partial f_2}{\partial x_2} & \dots & \frac{\partial f_2}{\partial x_{n-1}} & \frac{\partial f_2}{\partial x_n} \\ \vdots & \vdots & \dots & \vdots & \vdots \\ \frac{\partial f_{n-1}}{\partial x_1} & \frac{\partial f_{n-1}}{\partial x_2} & \dots & \frac{\partial f_{n-1}}{\partial x_{n-1}} & \frac{\partial f_{n-1}}{\partial x_n} \\ \frac{\partial f_n}{\partial x_1} & \frac{\partial f_n}{\partial x_2} & \dots & \frac{\partial f_n}{\partial x_{n-1}} & \frac{\partial f_n}{\partial x_n} \end{pmatrix}. \tag{1.4}$$

1.9.3 Global stability of steady states (Equilibrium points)–Lyapunov functions

Let the autonomous systems

$$\begin{aligned} x' &= f(x) \\ \frac{dx_i}{dt} &= f_i(x_1, x_2, \dots, x_n), i = 1, 2, \dots, n, \end{aligned}$$

with steady state (E^*).

Suppose a continuously differentiable function is given by: $V(x) = V(x_1, x_2, \ldots, x_n)$

We define a total derivative

$$\frac{dV}{dt} = \frac{\partial V}{\partial x_1}\frac{dx_1}{dt} + \frac{\partial V}{\partial x_2}\frac{dx_2}{dt} + \cdots + \frac{\partial V}{\partial x_n}\frac{dx_n}{dt} \tag{1.5}$$

Examples of Lyapunov functions include:

(i) The logarithmic Lyapunov function by Goh for Lotka–Voltera systems
$L(x_1, x_2, \ldots, x_n) = \sum_{i=1}^{n} c_i(x_i - x_i^* - x_i^* \ln \frac{x_i}{x_i^*})$.

(ii) Common quadratic Lyapunov function for nonlinear and linear functions
$V(x_1, x_2, x_3, \ldots, x_n) = \sum_{i=1}^{n} \frac{c_i}{2}(x_i - x_i^*)^2$.

(iii) Composite–Voltera function
$W(x_1, x_2, , \dot{x}_n) = c\Big(\sum_{i=1}^{n}(x_i - x_i^*) - \sum_{i=1}^{n} x_i(\ln \frac{\sum_{i=1}^{n}(x_i)}{\sum_{i=1}^{n}(x_i)})\Big)$.

1.10 Organization of the Thesis

This thesis is organized as follows:

In Chapter 1, the basic information about influenza A virus, pneumococcus, co–infection of influenza A virus and pneumococcus, and attempts to control pneumococcal pneumonia is given. The methods used in the study have also been highlighted.

In Chapter 2, the mathematical framework of other scholars is presented. The review includes; Within–host Co–infection for infectious diseases and mathematical models of infectious diseases, with time delays, antibiotic resistance awareness

and treatment

Chapter 3 presents a nonlinear mathematical model for a within–host co–infection of influenza A virus and pneumococcus.

In Chapter 4, a between–host model of pneumococcal pneumonia with time delays is proposed and analyzed.

Chapter 5, presents a mathematical model of pneumococcal pneumonia for the effect of antibiotic awareness and saturated treatment.

In Chapter 6, conclusions and recommendations are given. In the Appendices, important equations, computations and codes that were used to arrive at the results are given. In all models qualitative and numerical analysis are done.

To this end, the next chapter gives an overview of studies done by other researchers that use mathematical techniques in modeling infectious diseases.

CHAPTER 2

LITERATURE REVIEW

2.1 Introduction

Mathematical modelling is one of the most useful tools to explore the inner mechanism of disease outbreak and spread of infectious diseases, and has been extensively used to study different types of epidemics, for example; human immunodeficiency virus (HIV) and tuberculosis, cholera, influenza A, hepatitis B (Gakkhar & Chavda, 2012; Sun et al., 2017; Krishnapriya et al., 2017; Khan et al., 2018). Deterministic models have a long history of being applied to the study of infectious disease epidemiology (Roberts et al., 2015). This Chapter presents the mathematical framework and literature/theoretical review. The theoretical review covers the contribution of other scholars on within–host co–infection of influenza A virus–pneumococcus and the dynamics of pneumococcal pneumonia.

2.2 Within–host Co–infection for infectious diseases

Within–host interaction can sustain co–existence of various parasite strains in a population (Bosch et al., 2013; Mosquera & Adler, 1998). Within–host models are dynamical models that represent and explain the interaction of the pathogen with the host reproduction machinery or immune defenses within a single host individual (Martcheva et al., 2015), thus enhance our understanding of the mechanistic interactions that govern acute infections with pathogens such as Influenza A virus and pneumococcus (Ciupe & Heffernan, 2017). The within–host models can be categorized into three groups: models that describe the pathogen reproduction process within–host; models that describe the pathogen interaction with the

immune responses; and models that include both the replication of the pathogen and the immune responses.

Erwin (2017) investigated the mechanisms behind diseases and the immune responses required for successful disease resolution. Hadjichrysanthou et al. (2016), formulated a simple within–host model of viral dynamics and investigated the within–host dynamics of influenza A virus infection in humans. The Beddington–DeAngelis functional response in Beddington (1975) and DeAngelis et al. (1975) is used to model the viral course with healthy target cells because relationship between virus and host cell is nonlinear. The Beddington–DeAnglis functional response ($\frac{\alpha x_1 x_2}{a+x_1+bx_2}$), where a = a saturation constant, b = mutual interference term, x_1 and x_2 represent species in the interaction and α=rate constant describing infected cells in parasite–host interactions. Huang et al. (2009) used Beddington–DeAngelis functional response in describing the infection rate between HIV–1 virus and CD4–CT cells.

Cheng et al. (2017) used a probabilistic approach to derive a within–host dynamic model of co–infection with influenza A virus and SP integrated with dose–response and found out that the day of secondary SP infection had much more impact on the severity of inflammatory responses in pneumonia compared to the effects caused by initial virus titers and bacteria loads.

A study by Shrestha et al. (2013), explored an immune–mediated model of the viral–bacterial interaction that quantifies the timing and the intensity of the interaction. Results predicted that with pneumococcal bacteria introduced, following influenza infection during a 4–6 day window yields invasive pneumonia at significantly lower innoculum size than in hosts not infected with influenza. Other studies done on within–host influenza A virus and pneumococcus co–infection

include: Smith (2017); Smith & Smith (2016) and demonstrate a practical understanding of the dynamics for influenza A virus and pneumococcal co–infection in animals. At population level co–infection models of Hussaini et al. (2016); Lawi et al. (2013); Nthiiri et al. (2015), provide an understanding of important biological parameters responsible in disease development.

Smith et al. (2013) described the co–dynamics of viral–bacterial infection. However, the model system doesn't include the model equation of co–infected cells, yet it is an important subsystem that helps in showing which pathogen survives during the interaction of the two pathogens.

2.3 Mathematical models of infectious diseases, with time delays, antibiotic resistance awareness and treatment

During treatment of pneumonia, microorganisms occasionally persevere, emerge or re–merge despite of good clinical responses. Thus, recovered individuals may relapse and return to the infective class (Kiem & Schentag, 2013). The recurrence of disease is a significant feature of some animal and human diseases; for example, malaria, herpes, tuberculosis in both humans and animals (Van Den Driessche et al., 2007). Patients with HIV/AIDS commonly have a recurrence of pneumococcal bacteremia due to pre–existing drug resistance (Zuo & Liu, 2014; Agaba et al., 2017). Pneumococcal pneumonia patients infected with chronic diseases such as HIV/AIDS, are more likely to relapse compared to individuals without chronic diseases (Campo et al., 2005).

In events of acute side effects, patients tend to discard their treatment, only to return to the hospital with persistent infections of a more virulent and resistant strain of the bacteria (Okeke et al., 1999). To control antibiotic resistance, vaccines have been proposed as an essential intervention, complementing improvements in antibiotic stewardship and drug pipelines (Atkins et al., 2017). Disease appropriate awareness in a population can control an infection efficiently (Levy et al., 2017).

Time delays are significant in the transmission process of epidemics and arise due to delayed feedback especially the period for waning vaccine–induced immunity, latent period of infection, the infectious period and the immunity period (Rao & Kumar, 2015). Among the mathematical tools currently used, delay differential models with time delay have attracted attention in the field of science especially modeling infectious diseases. Delays change the dynamical systems' stability by giving rise to Hopf–bifurcations (Zhao & Zhao, 2017).

Rao & Kumar (2015) proposed a model for infectious diseases spread having susceptible, infected and recovered populations, and observed that incubation delays have influence on the system even under enhanced vaccination. Zhao & Zhao (2017), proposed an SIR epidemic model incorporating media coverage with time delay, and the results showed that the time delay in media coverage affects the stability of the endemic equilibrium and produces limit cycle oscillations when the basic reproduction number is greater than unity. Zhao et al. (2014), proposed an SIRS epidemic model by incorporating media coverage with time delay, the results showed that time delay in media coverage could affect the endemic equilibrium giving rise to a family of periodic orbits bifurcating from the endemic equilibrium when the time delay increases through a critical value. Misra et al. (2012) used a mathematical model for the control of cholera epidemic, to show that the disease may be controlled by spraying insecticides but a longer delay in

spraying insecticides may destabilize the system.

An SIS model that divides the susceptible class into two subclasses: aware susceptible and unaware susceptible due to individuals' behavioral changes because of media coverage influence was used to investigate the effect of awareness coverage and delay in controlling infectious diseases (Al Basir et al., 2018). The results showed that the disease–free equilibrium is stable if the basic reproduction number is smaller than unity and the endemic equilibrium exhibits Hopf–bifurcation, in both delayed and non-delayed system, whenever it exists.

A research by Al Basir (2018), on the dynamics of infectious diseases with media coverage and two time delays; one for the time lag in reporting number of infected individuals and another for the delay between the awareness campaign and the time of taking measures by susceptible individual. The author noted that if the number of campaigns due to the awareness program is increased then the disease transmission amongst the susceptible population declines. However, if both delays increase, the system shows limit cycle oscillations, which pose a challenge to control the epidemic. Lu et al. (2017), conducted a study about the impact of media coverage on spread and control of infectious diseases using an SEI model, including individuals' behavior changes in their contacts due to the influences of media coverage. The results showed that, the media coverage may decrease the peak value of the infectives' or the average number of the infectives in various cases.

The above studies have considered mathematical models of infectious diseases in an attempt to suggest strategies that can reduce the disease incidence in human populations. Nonlinear ODE's and DDE's are considered. The total population is subdivided into susceptible, infective, vaccinated, carrier, treated and recovered. However, none of them has done a study about within–host model for the

co–infection of IAV and pneumococcus that has a subpopulation of co–infected cells and a Beddington DeAngelis functional response (infection rate). To the best of our knowledge no study has undertaken the dynamics of pneumococcal pneumonia with time delays in the latency and infective subpopulations. Further, no study has been conducted about pneumococcal pneumonia with subdivided susceptible and infective subpopulations, with antibiotic resistance awareness and saturated treatment. This is why we are motivated to undertake this study to bridge the existing gap.

In the next Chapter, a within–host co–infection of IAV and pneumococcus model is constructed, analytically and numerically analyzed, with an aim of finding out the most virulent pathogen.

CHAPTER 3

WITHIN–HOST CO–INFECTION MODEL OF INFLUENZA A VIRUS AND PNEUMOCOCCUS

3.1 Introduction

Co–infection typically means two or more pathogens infecting the human (or animal) host, but nature is full of surprises and one clinically important type of co–infection turns out to involve viral infection of the principal pathogen (McArdle et al., 2018). Humans and animals are continuously exposed to multiple potential pathogens. Most people are chronically or latently infected (be it with virus, bacteria, fungi), and usually carry possible pathogens in their colonizing microbial flora (Pradeu, 2016). This implies that almost every new occurring infection, probably constitutes sort of a co–infection. A frequent problem of respiratory viral disease can be secondary bacterial infection. Bacterial co/secondary bacterial infection, as the name suggests, is a bacterial infection that occurs during or after an infection from another pathogen, commonly viruses (Morris et al., 2017).

3.2 Description, formulation and basic qualitative properties of the model

We formulate a within–host co–infection of influenza A virus and pneumococcus model. The epithelial cell population at time t, represented by N, is sub–divided into four mutually compartments consisting of uninfected cells (S), infected cells

with influenza A virus, (I_v) infected cells with pneumococcus (I_b), co–infected cells (I_{vb}). The pathogen population is sub–divided into two subclasses: pneumococcus (B) and influenza A virus (V). Uninfected cells S are recruited from the pool of precursor cells at a constant rate Λ and have a natural death rate μ_s. The infection rate by influenza A virus is the Beddington–DeAngelis functional response, and infection rate by pneumococcus is $\beta_b B$ per cell. The infected cells with influenza A virus, have increased death rate μ_v. The infected epithelial cells with pnemococcus (I_b), have a contact between pneumococcus and uninfected epithelial cells that occurs at a rate proportional to both their incidences and have increased death rate μ_b. The co–infected epithelial cells (I_{vb}), have increased death rate μ_{vb}.

Pneumococcus proliferate logistically at a maximum rate r, with a tissue carrying capacity K.'The growth rate approaches zero when the bacterial culture approaches the value of the capacity $B = K$'. Pneumococcus have increased bacterial loss due to increased toxic death δ_b, and infection resulting from the interaction of uninfected epithelial cells with influenza A virus α_v. The pneumococcus is decreased at a ratio–dependency term $\frac{mA}{A+hB}$, where m is the maximum number of bacteria an Alveolar macrophage can catch in a unit time t, and h is a handling time for the alveolar macrophage.

Influenza A virus (V) are maintained by both the production of influenza A virus infected epithelial cells, $\tau_v n_v$ from I_v lysis of infected epithelial cells, $\tau_{vb} n_{vb}$ from I_{vb} lysis of co–infected cells. Influenza A virus have increased viral loss due to toxic death (δ_v) and infection resulting from the interaction of uninfected epithelial cells with pneumococcus α_b. The infected epithelial cells release n_v, n_b and n_{vb} virions during their life time.

The mathematical model in this study, adopts a nonlinear incidence of the Bedding-

ton–DeAngelis functional response, where the contact rate depends on saturation and mutual interference factors and mass–action incidence. The Beddington DeAngelis response term adopted in this model is of the form $\frac{\beta_v SV}{1+aS+bV}$, where b is a measure of inhibition effect due to treatment like oseltamivir neuraminidase by infected individuals and a is a measure of inhibition effect, such as preventive health care taken by susceptible individuals for disease prevention, as opposed to disease treatment, the Beddington DeAngelis response term can be used to derive other important response terms by setting some parameters to zero for example;

(i) Setting $a = b = 0$, yields $f(S, V) = \beta_v SV$, commonly known as a standard bilinear form (Zhonghua & Yaohong, 2010).

(ii) Setting $b = 0$, gives $f(S, V) = \frac{\beta_v SV}{1+aS}$, described as the saturated incidence rate with respect to the susceptible individuals. The inhibition effect due to the saturation factor arises because of the preventive health care precautions to control the spread of the epidemic (Korobeinikov & Maini, 2005).

(iii) Setting $a = 0$, then $f(S, V) = \frac{\beta_v SV}{1+bV}$, known as saturated incidence rate with respect to the infected individuals (Xu et al., 2015). Under such circumstances, the contact between infective and susceptible individuals may saturate at high infection level due to congestion of infective individuals or due to protection given to susceptible individuals (Laarabi et al., 2012).

3.3 Model assumptions

The following assumptions are stated to guide in the development of model equations:

(i) The interaction within–host is between IAV and pneumococcus pathogens and the target cells

(ii) A typical viral/bacteria pathogen replicates within the machinery of host cells called the target cells

(iii) The infection in a given population is spread only by free pathogens: IAV and pneumococcus bacteria

(iv) The bacteria population (B) have a logistic growth because there are limits to growth in all known biological systems.

(v) The pneumococcus population is phagocytosed by alveolar macrophages

(vi) Co–infection in the epithelial cell population is due to IAV and pneumococcus.

Within–host model deals with interaction of cell and pathogen populations, therefore, the associated state variables and parameters are positive. The related state variables and parameters of the model are given in the Nomenclature, and the transition diagram for the model is given in Figure 3.1.

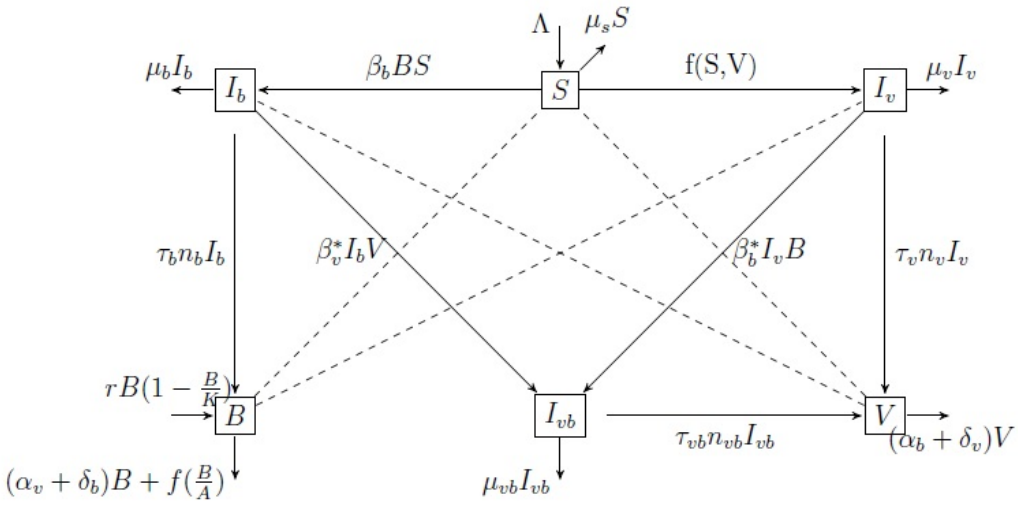

Figure 3.1: A schematic diagram for model (3.1). The dotted lines indicate cell–pathogen interaction and solid lines with arrows not starting from the compartments show the release of pathogens from infected cells. The solid lines with arrows show transfer from one compartment to another.

where $f(S,V)=\frac{\beta_v SV}{1+aS+bV}$ is the Beddington–DeAngelis functional response and $f(\frac{B}{A})=\frac{mA}{A+hB}$ is the ratio–dependency term.

From Figure 3.1 we get a system of nonlinear differential equations by the balance law of compartments stated as: rate of change=inflow transition rate−outflow transition rate that is: $\dot{X}$ = sum of inflow transition rates− sum of outflow transition rates, hence we have

$$\begin{aligned}
\dot{S} &= \Lambda-\frac{\beta_v SV}{1+aS+bV}-\beta_b SB-\mu_s S,\\
\dot{I}_v &= \frac{\beta_v SV}{1+aS+bV}-(\beta_b^* B+\mu_v)I_v,\\
\dot{I}_b &= \beta_b SB-(\mu_b+\beta_v^* V)I_b,\\
\dot{I}_{vb} &= \beta_v^* I_b V+\beta_b^* I_v B-\mu_{vb} I_{vb},\\
\dot{B} &= rB\left(1-\frac{B}{K}\right)+\tau_b n_b I_b-\frac{\gamma_a mAB}{A+hB}-(\alpha_v+\delta_b)B,\\
\dot{V} &= \tau_v n_v I_v+\tau_{vb} n_{vb} I_{vb}-(\alpha_b+\delta_v)V.
\end{aligned} \tag{3.1}$$

with initial conditions $S(0) = S_0 \geq 0$, $I_v(0) = I_{v0} \geq 0$, $I_b(0) = I_{b0} \geq 0$, $I_{vb}(0) = I_{vb0} \geq 0, B(0) = B_0 \geq 0, V(0) = V_0 \geq 0$.

The model was built on the previous work of Smith (2017), by incorporating important epidemiological and biological features of each infection. The major inputs are: the sub–population compartment for influenza A virus and pneumococcus co–infection, a Beddington–DeAngelis nonlinear incidence term, the ratio–dependent term because bacteria grow rapidly for initial doses that would be rapidly cleared in the absence of virus, the recruitment of healthy epithelial cells, toxic death rates to each class and number of infectious particles released from lysis of infected cells.

3.4 Basic qualitative properties

3.4.1 Positivity of solution trajectories of model (3.1)

In this Section, the existence of non–negative solutions for all time $0 < t < \infty$ is shown by contradiction. Given that values of the state variables the are non–negative, that is

$$S(0) \geq 0,\ I_v(0) \geq 0,\ I_b(0) \geq 0,\ I_{vb}(0) \geq 0,\ V(0) \geq 0,\ B(0) \geq 0,$$

the variables remain so $\forall t > 0$. That is $S(t) \geq 0$, $I_v(t) \geq 0$, $I_b(t) \geq 0$, $I_{vb}(t) \geq 0$, $V(t) \geq 0$, $B(t) \geq 0$.

Suppose, the following possibility at a given time hold:

(i) t_1 is such that S(t_1)=0 and $\dot{S}(t_1) < 0$ whenever; $I_v(t) > 0$, $I_b(t) > 0$, $I_{vb}(t) > 0$, $B(t) > 0$ and $V(t) > 0$ for $0 < t < t_1$.

From possibility (i) and model (3.1) we obtain

$$\dot{S(t_1)} = \Lambda - \frac{\beta_v S(t_1)V(t_1)}{1+aS(t_1)+bV(t_1)} - \beta_b S(t_1)B(t_1) - \mu_s S(t_1).$$

Then

$$\dot{S}(t_1) = \Lambda > 0. \tag{3.2}$$

Equation (3.2) is a contradiction of assumption (i) that is

$$S(t_1) = 0 \text{ and } \dot{S}(t_1) < 0.$$

In other words, there exists no such "t_1". Hence it follows that for t; $0 < t < t_1$ we have $S(t) > 0$. We can extend this t_1 to ∞. Similarly, it can be shown that the variables $I_v; I_b; I_{vb}; B$ and V remain positive for all $t > 0$. This approach was also used by e.g Magombedze et al. (2010) and references therein.

3.4.2 Boundedness of the solutions

Since model (3.1) describes host cell–pathogen interaction, it is essential to show that our solutions are bounded in the proper subset $\Omega \subset \mathbb{R}^4 \times \mathbb{R}^2$. The overall epithelial cell population size at time t is N given by $N = S + I_v + I_b + I_{vb}$ and the overall pathogen population at time t is $P = B + V$.

Proposition 3.3.1. *The solution of model* (3.1) *is ultimately bounded in* $\Omega \subset \mathbb{R}^4 \times \mathbb{R}^2$.

Proof. From the first equation of model (3.1), we have $\dot{S} \leq \Lambda - \mu_s S$. This implies $\limsup_{t\to\infty} S \leq \frac{\Lambda}{\mu_s}$. Since $N = S + I_v + I_b + I_{vb}$, then

$$\dot{N} \leq \Lambda - \delta_1 N,$$

where $\delta_1 = \min\{\mu_s, \mu_v, \mu_b, \mu_{vb}\}$. Hence, $\limsup_{t\to\infty} N \leq \frac{\Lambda}{\delta_1}$. It follows that $\limsup_{t\to\infty} I_v \leq l_1$, $\limsup_{t\to\infty} I_b \leq l_1$ and $\limsup_{t\to\infty} I_{vb} \leq l_1$, where $l_1 = \frac{\Lambda}{\delta_1}$. Therefore, the global attractor of the epithelial cell population is contained in Ω_c On the other hand,

$$\dot{P} \leq \phi l_1 - \delta_2 P,$$

where $\phi = \tau_b n_b + \tau_v n_v + \tau_{vb} n_{vb}$ and $\delta_2 = min\{(\alpha_b + \delta_v), (\alpha_v + \delta_b)\}$. Hence, $\limsup_{t\to\infty} P \leq \frac{(\tau_b n_b + \tau_v n_v + \tau_{vb} n_{vb}) l_1}{\delta_2}$. It follows that $\limsup_{t\to\infty} B \leq l_2$, $\limsup_{t\to\infty} V \leq l_2$, where $l_2 = \frac{(\tau_b n_b + \tau_v n_v + \tau_{vb} n_{vb}) l_1}{\delta_2}$. Thus, the global attractor of the pathogen population is contained in Ω_p. Hence the feasible solution set of model (3.1) remain in the region $\Omega = \Omega_c \cup \Omega_p$ where $\{\Omega_c = (S, I_v, I_b, I_{vb}) \in \mathbb{R}^4_+ : N \leq \frac{\Lambda}{\delta_1}$ and $\Omega_p = \{(B, V) \in \mathbb{R}^2_+ : P \leq \frac{\phi}{\delta_2}\}$.

Therefore, no epithelial cell and pathogen populations becomes negative or grows without bound. Thus, model (3.1) is epidemiologically and mathematically well–posed and its dynamics can be considered in a proper subset Ω (Hethcote, 2000).

3.5 Well–possedness of influenza A virus sub–model

The influenza A virus steady state (E_1) occurs when populations for $I_b = I_{vb} = B = 0$, thus $E_1 = (S_0, I_v^*, 0, 0, 0, V^*)$. From the full system (3.1) we get

$$\begin{aligned} \dot{S} &= \Lambda - \frac{\beta_v S V}{1 + aS + bV} - \mu_s S, \\ \dot{I}_v &= \frac{\beta_v S V}{1 + aS + bV} - \mu_v I_v, \\ \dot{V} &= \tau_v n_v I_v - (\alpha_b + \delta_v) V. \end{aligned} \tag{3.3}$$

System (3.3) illustrates the dynamics of influenza A virus with the epithelial cell population and therefore, it can be shown that the related state variables are non–negative for all time $t \geq 0$ and that all solutions of the system (3.3) with positive initial data remains positive for all time $t \geq 0$. By assuming the related parameters as non–negative for all time $t \geq 0$. We show that all feasible solutions are uniformly bounded in a proper subset Φ.

Proposition 3.4.1. *Solutions of the system* (3.3)*are contained in the region* Φ

Proof. Suppose all feasible solutions are uniformly–bounded in a proper subset Φ, let $(S(t), I_v(t), V(t)) \in \mathbb{R}^3_+$ be any solution with non–negative initial conditions. Using the differential inequality Cheng et al. (2017), it follows that; $\limsup_{t\to\infty} S(t) \leq \frac{\Lambda}{\mu_s}$.

Given $N(t) = S(t) + I_v(t) + V(t)$ and taking its time derivative along the solution path of system (3.3), we obtain

$$\frac{N(t)}{dt} = \Lambda + \tau_v n_v I_v - \mu_v I_v - \mu_s S - (\alpha_b + \delta_v) V. \tag{3.4}$$

Let $\phi^* = \Lambda + \tau_v n_v I_v$ and $\delta_0 = min(\mu_s, \mu_v, (\alpha_b + \delta_v))$, such that $\frac{N(t)}{dt} \leq \phi^* - \delta_0 N(t)$. Hence, from the differential inequality it follows that

$0 \leq N(t) \leq \frac{\phi^*}{\delta_0} + k_0 e^{-\delta_0 t}$, where k_0 is a constant of integration, thus $0 \leq N(t) \leq \frac{\phi^*}{\delta_0}(1 + k_1 e^{-\delta_0 t}) \leq \frac{\phi^*(1+k_1)}{\delta_0}, \forall t > 0$, with $k_1 = \frac{k_0 \delta_0}{\phi^*}$.

This indicates that as $t \to \infty$, we have $0 \leq N(t) \leq \frac{\phi^*(1+k_1)}{\delta_0}$.

Therefore, N(t) is bounded and all the feasible solutions of influenza A virus

sub–model starting in the region Φ approach, enter or stay in the region, where $\Phi = (S(t), I_v(t), V(t)) : N(t) \leq \frac{\phi}{\delta_0}$.

Therefore, Φ is positively invariant under the flow induced by system (3.3). Hence, existence, uniqueness and results that follow also hold for system (3.3) in Φ. Thus, system (3.3) is mathematically and epidemiologically well–posed and it is necessary to consider its solutions in Φ.

3.5.1 Computation for influenza A viral fitness (R_0^1)

The pathogen fitness is derived as a spectral radius of (FV^{-1}) where F are the new uprising infections in the infectious compartment. V is the outgoing infections from the infectious compartment. Using the next generation operator method Van Den Driessche & Watmough (2002) on system (3.3), let $f_i(x_i) = f - v$, where $f = [f_{ij}]$ and $x_i = I_v$, f is a group of new infections and $v = [v_{ij}]$ (the outgoing infections from the infectious compartments).

Let

$$F = \left[\frac{\partial f_i(x_i)}{\partial x_i}\Big|_{x_i=E_1}\right], V = \left[\frac{\partial f_i(x_i)}{\partial x_i}\Big|_{x_i=E_1}\right].$$

Thus, the pathogen fitness, $R_0 = \rho(FV^{-1})$ evaluated at infection free state

$$f = \begin{bmatrix} \\ \frac{\beta_v SV}{1+aS+bV} \\ \\ 0 \\ \end{bmatrix}.$$

By linearization approach, the associated matrix at infection–free steady state is given by

$$F = \begin{bmatrix} 0 & \frac{\beta_v \Lambda}{\mu_s + a\Lambda} \\ 0 & 0 \end{bmatrix}.$$

Suppose the outgoing infections from the infectious compartments are given by

$$v = \begin{bmatrix} \mu_v I_v \\ (\alpha_b + \delta_v)V - \tau_v n_v I_v \end{bmatrix}.$$

Again by linearization we obtain

$$V = \begin{bmatrix} \mu_v & 0 \\ -\tau_v n_v & \alpha_b + \delta_v \end{bmatrix}.$$

Therefore the inverse of the outgoing infections from the infectious compartments is given by

$$V^{-1} = \begin{bmatrix} \frac{1}{\mu_v} & 0 \\ \frac{\tau_v n_v}{\mu_v(\alpha_b + \delta_v)} & \frac{1}{\alpha_b + \delta_v} \end{bmatrix}.$$

Therefore:

$$F \times V^{-1} = \begin{bmatrix} \frac{\tau_v n_v \beta_v \Lambda}{\mu_s \mu_v (\alpha_b + \delta_v)} & \frac{\beta_v \Lambda}{\mu_s (\alpha_b + \delta_v)} \\ 0 & 0 \end{bmatrix}. \tag{3.5}$$

By finding the eigenvalues of expression (3.20) we get

$$\lambda_1 = 0, \lambda_2 = \frac{\beta_v \Lambda \tau_v n_v}{(\mu_s + a\Lambda)\mu_v(\alpha_b + \delta_v)}.$$

then

$$R_0^1 = \max(\lambda_1, \lambda_2) = \frac{\beta_v \Lambda \tau_v n_v}{(\mu_s + a\Lambda)\mu_v(\alpha_b + \delta_v)}. \tag{3.6}$$

For a steady state to be locally asymptotically stable, all the roots of the characteristic polynomial must be located in $\mathbb{C}^- = \{z \in \mathbb{C} : Re(z) < 0\}$.

3.5.2 Stability analysis of influenza A virus steady state

A dynamical system (3.3) with free infection state (E_1) is said to be stable if all real parts of the eigenvalues computed from the Jacobian matrix of the system are less than zero and unstable otherwise.

Theorem 3.5.1 *If $R_0^1 < 1$, the Infection–free steady state for system* (3.3) (E_1) *is locally asymptotically stable and E_1 is unstable if $R_0^1 > 1$*

Proof. Linearizing system (3.3) to generate the Jacobian

$$J_{E_0} = \begin{bmatrix} -\mu_s & 0 & -\frac{\beta_v \Lambda}{\mu_s + a\Lambda} \\ 0 & -\mu_v & \frac{\beta_v \Lambda}{\mu_s + a\Lambda} \\ 0 & \tau_v n_v & -(\alpha_b + \delta_v) \end{bmatrix}. \tag{3.7}$$

Evaluating the determinant of the Jacobian J_{E_1} yields a characteristic expression

$$P(\lambda) = \lambda^3 + w_2\lambda^2 + w_1\lambda + w_0. \tag{3.8}$$

with $w_2 = ((\alpha_b + \delta_v) + \mu_v + \mu_s), w_1 = ((\alpha_b + \delta_v)(\mu_v + \mu_s) + \mu_v\mu_s - \frac{\tau_v n_v \beta_v \Lambda}{\mu_s + a\Lambda}),$
$w_0 = -\mu_s(\frac{\beta_v \Lambda \tau_v n_v}{\mu_s + a\Lambda} + (\alpha_b + \delta_v)\mu_v).$
We solve for the eigenvalues by equating the characteristic polynomial (3.8) to zero to obtain

$$\lambda_1 = -\mu_s, \lambda_{2,3} = \frac{-\mu_v}{2} - \frac{(\alpha_b + \delta_v)}{2} \pm \frac{\sqrt{(\mu_v^2 - 2\mu_v(\alpha_v + \delta_v) + (\alpha_b + \delta_v)^2 + \frac{4\beta_v \Lambda \tau_v n_v}{\mu_s + a\Lambda})}}{2}, \tag{3.9}$$

Clearly λ_1 is negative, however λ_2 and λ_3 take up two signs hence by finding appropriate combinations of the two eigenvalues we get

$$\lambda_2 + \lambda_3 = -(\mu_v + (\alpha_b + \delta_v)) < 0,$$
$$\lambda_2 \times \lambda_3 = (\frac{\mu_v}{2} + \frac{\alpha_b + \delta_v}{2})^2 - \frac{1}{4}(\mu_v^2 - 2\mu_v(\alpha_b + \delta_v) + (\alpha_b + \delta_v)^2 + \frac{4\beta_v \Lambda \tau_v n_v}{\mu_s + a\Lambda}) \tag{3.10}$$

Expanding and simplifying expression (3.10) we obtain

$$\lambda_2 \times \lambda_3 = \mu_v(\alpha_b + \delta_v) - \frac{\beta_v \Lambda \tau_v n_v}{\mu_s + a\Lambda}$$

Lemma 3.5.1. $\lambda_2 \times \lambda_3 < 0$, if $\mu_v(\alpha_b + \delta_v) < \frac{\beta_v \Lambda \tau_v n_v}{\mu_s + a\Lambda}$

By dividing throughout system by $\mu_v(\alpha_b + \delta_v)$

we obtain $1 < \frac{\beta_v \Lambda \tau_v n_v}{(\mu_s + a\Lambda)\mu_v(\alpha_b + \delta_v)}$.

Let $R_0^1 = \frac{\beta_v \Lambda \tau_v n_v}{(\mu_s + a\Lambda)\mu_v(\alpha_b + \delta_v)}$,

be the viral fitness for influenza A virus, then $R_0^1 > 1$.

Lemma 3.5.2. *suppose* $\lambda_2 \times \lambda_3 > 0$, then this will happen if

$\mu_v(\alpha_b + \delta_v) > \frac{\beta_v \Lambda \tau_v n_v}{\mu_s + a\Lambda}$.

Dividing by $\mu_v(\alpha_b + \delta_v)$, on both sides we obtain

$$\frac{\beta_v \Lambda \tau_v n_v}{(\mu_s + a\Lambda)\mu_v(\alpha_b + \delta_v)} < 1,$$

hence $R_0^1 < 1$. Therefore E_1 is locally asymptotically stable whenever $R_0^1 < 1$ and unstable for $R_0^1 > 1$. This ends the proof of the Theorem 3.5.1.

3.5.3 Global stability of the influenza A virus free steady states

Theorem 3.5.2. *When $R_0^1 < 1$, the infection steady state for influenza A virus, is globally asymptotically stable in region Φ*

Proof. In order for us to show that influenza A virus free–steady state is globally stable inside region (Φ), we apply the method of fluctuation employed in (W. M. Hirsch et al., 1985; Jiang et al., 2009). Suppose $g_\infty = \lim_{t\to\infty} g(t)$ and $g^\infty = \limsup_{t\to\infty} g(t)$ for any continuous and bounded function $g : [0, \infty) \to \mathbb{R}$.

We have already shown that the solutions of $S(t)$, $I_v(t)$ and $V(t)$ are always non–negative and bounded from above for any given well–posed conditions. Therefore, $\liminf_{t\to\infty}$ and $\limsup_{t\to\infty}$ always exist for each individual state. Theorems of fluctuations in Thieme (2003) are re–stated:
If there exists sequences t_n and s_n such that if $t_n \to \infty$ whenever $n \to \infty$, then

$$\begin{aligned} \lim_{n\to\infty} X(t_n) = X^\infty, \lim_{n\to\infty} \dot{X}(t_n) = 0, \\ \lim_{n\to\infty} X(s_n) = X_\infty, \lim_{n\to\infty} \dot{X}(s_n) = 0 \end{aligned} \tag{3.11}$$

Suppose $t = t_n$, equation (1) of system (3.3) becomes

$$\dot{S} + \frac{\beta_v S(t_n) V(t_n)}{1 + aS(t_n)} + \mu_s S(t_n) = \Lambda. \tag{3.12}$$

We note that as $n \to \infty$ and applying (3.11), expression (3.12) reduces to

$$\frac{\beta_v S^\infty V_\infty}{1 + aS^\infty + \mu_s S^\infty} + \mu_s S^\infty = \Lambda.$$

This implies that

$$\mu_s S^\infty \leq \frac{\beta_v S^\infty V_\infty}{1 + aS^\infty + bV_\infty} + \mu_s S^\infty \leq \Lambda. \tag{3.13}$$

Considering equation (2) of system (3.3), we obtain

$$\dot{I}_v(t_n) - \frac{\beta_v S(t_n) V(t_n)}{1 + aS(t_n) + bV(t_n)} = -\mu_v I_v(t_n)$$

we note that as $n \to \infty$ we get

$$\mu_v I_v^\infty \leq \frac{\beta_v S^\infty V_\infty}{1 + aS^\infty + bV_\infty} \tag{3.14}$$

Thus, from equation (3.14) we have

$$I_v^{\infty} \leq \frac{\beta_v S^{\infty} V_{\infty}}{\mu_v(1 + aS^{\infty} + bV_{\infty})}. \tag{3.15}$$

From equation (3) of system (3.3), let $t = t_n$, then we get

$$\dot{V}(t_n) + (\alpha_b + \delta_v)V(t_n) \leq \tau_v n_1 I_v(t_n)$$

as n$\rightarrow \infty$ we apply identities in equation (3.11) to obtain

$$(\alpha_b + \delta_v)V^{\infty} \leq \tau_v n_1 I_v^{\infty}. \tag{3.16}$$

From equation (3.16), we obtain V^{∞} and make a substitution of I^{∞} from equation (3.15) to have

$$V^{\infty} \leq \frac{\tau_v n_v \beta_v S^{\infty} V_{\infty}}{\mu_v(\alpha_b + \delta_v)(1 + aS^{\infty} + bV_{\infty})} \tag{3.17}$$

Dividing equation (3.17) through by V_{∞} we obtain

$$1 \leq \frac{\tau_v n_v \beta_v S^{\infty}}{\mu_v(\alpha_b + \delta_v)(1 + aS^{\infty} + bV_{\infty)}}. \tag{3.18}$$

From equation (3.13), if no pathogen to cause infection in the longrun i.e. $V_{\infty} = 0$. Then $S^{\infty} \rightarrow \frac{\Lambda}{\mu_s}$ for $b = 0$ and equation (3.18) is given as $1 \leq \frac{\beta_v \tau_v n_v \Lambda}{\mu_v(\alpha_b+\delta_v)(\mu_s+a\Lambda)}$.
We note that $R_0^1 = \frac{\beta_v \tau_v n_v \Lambda}{\mu_v(\alpha_b+\delta_v)(\mu_s+a\Lambda)}$ hence equation (3.18) becomes
$1 \leq R_0^1$, which contradicts "R_0^1", and this implies that if $S^{\infty} = 0$, then from equations (3.16) and (3.18) we have $I_v^{\infty} = 0$ and $V^{\infty} = 0$
Therefore, since the solutions to system (3.3) are non–negative and lim inf $\leq$ lim sup, we must have $S(t)$, $I_v(t)$, V(t)$\rightarrow 0$ as $t \rightarrow \infty$ because $S(t) \rightarrow 0$ asymptotically in equation (3) of system (3.3), that is $\dot{S} = \Lambda - \mu_s S$. This result is related

to that of Castillo-Chavez & Thieme (1994), the solution $S(t) \to \frac{\Lambda}{\mu_s}$ as $t \to \infty$ Hence, we observe that the local stability established earlier and the global attractive property herein, the proof of the Theorem 3.5.2 is complete!

3.5.4 Existence of Influenza A virus endemic state

The endemic state is a state for which the infection can spread in the epithelial cell population. The existence of the endemic state for influenza A virus which keep alive the infection propagating is now discussed.

Theorem 3.5.3. *The influenza A virus only model has a unique endemic equilibrium if and only if* $R_0^1 > 1$.

Proof. Equating the R.H.S of system (3.3) to zero, we get

$$\begin{aligned} \Lambda - \frac{\beta_v S^* V^*}{1 + aS^* + bV^*} - \mu_s S^* &= 0, \\ \frac{\beta_v S^* V^*}{1 + aS^* + bV^*} - \mu_v I_v^* &= 0, \\ \tau_v n_v I_v^* - (\alpha_b + \delta_v) V^* &= 0. \end{aligned} \tag{3.19}$$

Simultaneously solving a system of equation (3.19), we get

$$S^* = \frac{\Lambda b \tau_v n_v + \mu_v(\alpha_b + \delta_v)}{\tau_v n_v(\beta_v + \mu_s b) - \mu_v(\alpha_b + \delta_v)a}. \tag{3.20}$$

Dividing the R.H.S of equation (3.20) by $\mu_v(\alpha_b + \delta_v)$ we obtain

$$S^* = \frac{\frac{bR_0^1(\mu_s + a\Lambda)}{\beta_v} + 1}{\frac{R_0^1(\mu_s + a\Lambda)}{\beta_v \Lambda} + a}. \tag{3.21}$$

From the expression of S^* we observe two arising situations to be considered for functional response

$$S^* = \frac{1}{R_0^1(\frac{\mu_s+\Lambda a}{\beta_v \Lambda}) + a}. \tag{3.22}$$

Case I: *Saturation functional response, when* $a = 0$ *and* $b > 0$

It implies that, a less than linear response in V could occur when concentration of influenza A viruses increase, and yet the infectious proportion is high enough so that exposure is likely to happen (Castillo-Chavez et al., 2002).

Hence, $S^* = b\Lambda + \frac{\beta_v \Lambda}{R_0^1 \mu_s} = \Lambda(b + \frac{\beta_v}{R_0^1 \mu_s})$.

Case II: *Holling type II functional response, when* $b = 0$ *and* $a > 0$

We consider

$$I_v^* = \frac{\mu_v(\alpha_b + \delta_v)(\mu_s + a\Lambda) - \beta_v \tau_v n_v \Lambda}{\mu_v(\mu_v(\alpha_b + \delta_v))a - \tau_v n_v(\beta_v + \mu_s b)}. \tag{3.23}$$

Dividing the R.H.S of equation (3.23) by $\mu_v(\mu_s + a\Lambda)(\alpha_b + \delta_v)$, we obtain

$$I_v^* = \frac{1 - R_0^1}{\frac{\mu_v a}{\mu_s + a\Lambda} - \frac{R_0^1 \mu_v(\beta_v + \mu_s b)}{\beta_v \Lambda}}.$$

Therefore, we consider

(i) $a = 0$ and $b > 0$ such that $I_v^* = \frac{(1-R_0^1)\beta_v \Lambda}{-R_0^1 \mu_v(\beta_v + \mu_s b)} = \frac{\beta_v \Lambda}{\mu_v(\beta_v + \mu_s b)} \left(1 - \frac{1}{R_0^1}\right)$.

(ii) $b = 0$ and $a > 0$ such that $I_v^* = \frac{1 - R_0^1}{\frac{\mu_v a}{\mu_s + a\Lambda} - \frac{R_0^1 \mu_v \beta_v}{\beta_v \Lambda}}$.

This implies that

$$I_v^* = \frac{\Lambda(1 - R_0^1)}{\mu_v(\frac{a\Lambda}{\mu_s + a\Lambda}) - R_0^1}. \tag{3.24}$$

whenever, $R_0^1 > \mu_v(\frac{a\Lambda}{\mu_s+a\Lambda})$ holds.

We consider a state for

$$V^* = \frac{\tau_v n_1(a\mu_v(\alpha_b+\delta_v))(\mu_s+a\Lambda) - \beta_v\tau_v n_v\Lambda}{\mu_v(\alpha_b+\delta_v)(\mu_v(\alpha_b+\delta_v)a - \tau_v n_v(\beta_v+\mu_s b))}. \tag{3.25}$$

Dividing the R.H.S of equation (3.25) by $\mu_v(\alpha_b+\delta_v)(\mu_s+a\Lambda)a$, we get

$$V^* = \frac{\tau_v n_1}{\mu_v(\alpha_b+\delta_v)}\left(\frac{1-\frac{\beta_v\tau_v n_v\Lambda}{\mu_v(\alpha_b+\delta_v))(\mu_s+a\Lambda)a}}{\frac{1}{\mu_s+a\Lambda}-\frac{\tau_v n_v(\beta_v+\mu_s b)}{\mu_v(\alpha_b+\delta_v)(\mu_s+a\Lambda)a}}\right),$$

which simplifies to

$$V^* = R_0^1\left(\frac{a-R_0^1}{\frac{\beta_v\Lambda a}{\mu_s+a\Lambda}-R_0^1}\right). \tag{3.26}$$

We observe that when $a=0$, $b>0$ exist a saturation functional response, $V^* = R_0^1$ Finally, from equations (3.21), (3.24) and (3.26), the endemic steady state in the presence of both saturated functional responses and Holling type II functional response is given as

$$E_1^* = \left(\frac{\frac{bR_0^1(\mu_s+a\Lambda)}{\beta_v}+1}{\frac{R_0^1(\mu_s+a\Lambda)}{\beta_v\Lambda}+a}, \frac{1-R_0^1}{\frac{\mu_v a}{\mu_s+a\Lambda}-\frac{R_0^1\mu_v(\beta_v+\mu_s b)}{\beta_v\Lambda}}, R_0^1(\frac{a-R_0^1}{\frac{\beta_v\Lambda a}{\mu_s+a\Lambda}-R_0^1})\right). \tag{3.27}$$

However, the endemic steady state (3.27) can be expressed in terms of no saturation functional response in the presence of Holling type II functional response and vice–versa as below. The endemic steady state for influenza A virus (E_1^*) in the absence of saturation functional response when Holling type II functional response is positive is given as

$$E_1^* = (S^*, I_v^*, V^*) = \left(\Lambda(b+\frac{\beta_v}{R_0^1\mu_s}), \frac{\beta_v\Lambda}{\mu_v(\beta_v+\mu_s b)}\left(1-\frac{1}{R_0^1}\right), R_0^1\right), \tag{3.28}$$

and the endemic state for influenza A virus when the saturation function response is present,

$$E_2^* = (S^*, I_v^*, V^*) = \left(\frac{1}{R_0^1(\frac{\mu_s+\Lambda a}{\beta_v \Lambda}) + a}, \frac{\Lambda(1-R_0^1)}{\mu_v(\frac{a\Lambda}{\mu_s+a\Lambda}) - R_0^1}, 0 \right). \tag{3.29}$$

Linearizing system (3.3) near the equilibrium E_2^* and using the Routh–Hurwitz criterion, we obtain the following conditions for local asymptotic stability of this steady state

$$J_{E_2^*} = \begin{bmatrix} -\beta_v V^* - \mu_s & 0 & -\beta_v S^* \\ \beta_v V^* & -\mu_v & \beta_v S^* \\ 0 & \tau_v n_v & -(\alpha_b + \delta_v). \end{bmatrix}$$

The characteristic equation of the Jacobian matrix of the linearized system evaluated at this point E_2^* is

$$P(\lambda) = \lambda^3 + a_1\lambda^2 + a_2\lambda + a_3 = 0, \tag{3.30}$$

where

$a_1 = (\alpha_b + \delta_v) + \mu_v + \mu_s + \beta_v V^*$, $a_2 = \mu_v(\alpha_b - \tau_v n_v \beta_v S^* + \delta_v) + ((\alpha_b + \delta_v) + \mu_v)(\mu_s + \beta_v V^*)$, $a_2 > 0$, $a_3 = \tau_v n_v \beta_v^2 V^* S^* + ((\alpha_b + \delta_v)(\mu_v) - \tau_v n_v \beta_v S^*)(\beta_v V^* + \mu_s)$,

provided $\mu_v(\alpha_b + \delta_v) > \tau_v n_v \beta_v S^*$, $\mu_v(\alpha_b + \delta_v) > \tau_v n_v \beta_v S^*$,

which means that, the overall death rate of infected epithelial cells is greater than the total number of new virions generated from the interaction with the uninfected epithelial cells.

The local stability of the endemic steady state in equation (3.28), can't be easily identified. Instead we use Routh–Hurwitz criterion to analyze it's local stability. The criterion states that the corresponding steady state is locally asymptotically stable if and only if all Hurwitz determinants of the characteristic polynomial are positive (Hinrichsen & Pritchard, 2005). We define the three Hurwitz matrices using the coefficients a_1, a_2, a_3, of polynomial (3.29).

$$H_1 = \begin{bmatrix} \\ a_1 \\ \\ \end{bmatrix}, H_2 = \begin{bmatrix} a_1 & 1 \\ \\ 0 & a_2 \end{bmatrix}, H_3 = \begin{bmatrix} a_1 & 1 & 0 \\ \\ a_3 & a_2 & a_1 \\ \\ 0 & 0 & a_3 \end{bmatrix}$$

Since $n = 3$, we compute the $\det(H_3) = a_1a_2 - a_3$, the eigenvalues of the matrix have negative real parts if and only if the inequalities for $a_1 > 0, a_3 > 0$ and $a_1a_2 > a_3$ hold, for the coefficients of the characteristic equation.

Making substitutions of $a_i|_{i=(1,2,3)}$ in $\det H_3$ we get

$a_1 \times a_2 - a_3 = (\mu_v + (\alpha_b + \delta_v))(\alpha_b + \delta_v)\mu_v + \mu_s(\alpha_b + \delta_v)\mu_v + (\mu_v + \mu_s + (\alpha_b + \delta_v))((\alpha_b + \delta_v) + \mu_v)(\beta_v V^* + \mu_s) + \beta_v V^*(\alpha_b + \delta_v)\mu_v + \beta_v V^*((\alpha_b + \delta_v) + \mu_v)(\beta_v V^* + \mu_s) - (\alpha_b + \delta_v)\mu_v\tau_v n_v\beta_v S^* - \beta_v^2 V^*\tau_v n_v S^* - [\tau_v n_v\beta_v^2 V^* S^* + ((\alpha_b + \delta_v)(\mu_v) - \tau_v n_v\beta_v S^*)(\beta_v V^* + \mu_s)]$.

Therefore, with simplification of terms we get

$a_1a_2 - a_3 = (\mu_v + (\alpha_b + \delta_v))(\alpha_b + \delta_v)\mu_v + (\mu_v + \mu_s + (\alpha_b + \delta_v))((\alpha_b + \delta_v) + \mu_v)(\beta_v V^* + \mu_s) + \beta_v V^*((\alpha_b + \delta_v) + \mu_v)(\beta_v V^* + \mu_s) - (\alpha_b + \delta_v)\mu_v\tau_v n_v\beta_v S^* + \tau_v n_v\beta_v S^*(\mu_s - \beta_v V^*) > 0$

provided $\mu_s > \beta_v V^*$. Since $a_1 > 0, a_2 > 0, a_1a_2 > a_3$, then the characteristic equation (3.30) has negative real parts, thus E_1 is locally asymptotically stable provided conditions $\mu_v(\alpha_b + \delta_v) > \tau_v n_1\beta_v S^*$ and $\mu_s > \beta_v V^*$ hold. Therefore the endemic steady state E_2^*, where it exists, is always locally asymptotically stable.

3.5.5 Pathogen fitness (R_{IP})

The threshold quantity R_{IP} is the pathogen fitness of the infection (Gilchrist et al., 2004). The threshold number cannot be determined from the structure of the mathematical model alone, but depends on the definition of infected and uninfected compartments (Van Den Driessche & Watmough, 2002). Pathogen fitness gives information about the infection growth and control. If the pathogen fitness R_{IP} is less than unity, then the infection–free steady state is locally as well as globally stable. If R_{IP} is less than unity, the infection can be controlled through different ways like treatment and vaccination. On other hand if R_{IP} is greater than unity, the chronic–infection steady state becomes stable locally as well as globally and the infection exists permanently in the population.

We use the next generation operator method Van Den Driessche & Watmough (2002) on model (3.1) to compute the pathogen fitness. Suppose $\dot{x}_i = f_i(x) = F_i(x) - V_i(x)$, i=1,....,n, where $\mathbf{V}_i = V_i^- - V_i^+$ and $F = [f_{ij}]$ and $x = I_v, I_b, I_{vb}, B, V$ a group of new infections and $V = [v_{ij}]$ (the outgoing infections from the infectious compartments).

Let $F = \frac{\partial F_i(x)}{\partial x_i}|_{x_i=E_1}$ and $V = \frac{\partial V_i(x)}{\partial x}|_{x_i=E_1}$.

By restating the five conditions given as A(1)–A(5) in Van Den Driessche & Watmough (2002) as

The functions described above satisfy these conditions.

A(1): If $x \geq 0$, then $\mathbf{F}_i$; $\mathbf{V}_i^+, \mathbf{V}_i^- \geq 0$ for i=1,...,n,

A(2): If $x_i = 0$, then $(V_i^-$, in particular, if $x \in X_s$ then $\mathbf{V}_i^- = 0$ for i=1,...,m,

A(3): $\mathbf{F}_i = 0$, if $i > m$,

A(4): If $x \in X_s$, then $\mathbf{F}_i = 0$ and $\mathbf{V}_i^+(x) = 0$,

A(5): If $\mathbf{F(x)}$ is set to zero, then all eigenvalues of $Df(x_0)$ have negative real parts.

From model (3.1), we obtain a Jacobian, $J = D_{X_i} f_i(E_0)$ where $X_i = (S, I_v, I_b, I_{vb}, B, V) \in$

$\mathbb{R}^6$, $D_{X_i} f_i(E_0) = \frac{\partial f_i}{\partial X_i}|_{E_0=(\frac{\Lambda}{\mu_s},0,0,0,0)}$, $f_i = (\dot{S},\, \dot{I}_v,\, \dot{I}_b,\, \dot{I}_{vb},\, \dot{B},\, \dot{V})$ and E_0 is the infection–free steady state

Therefore, we obtain

$$J(E_0) = \begin{bmatrix} -\mu_s & 0 & 0 & 0 & -\frac{\beta_b \Lambda}{\mu_s} & -\frac{\beta_v \Lambda}{\mu_s + a\Lambda} \\ 0 & -\mu_v & 0 & 0 & 0 & \frac{\beta_v \Lambda}{\mu_s + a\Lambda} \\ 0 & 0 & -\mu_b & 0 & \frac{\beta_b \Lambda}{\mu_s} & 0 \\ 0 & 0 & 0 & -\mu_{VB} & 0 & 0 \\ 0 & 0 & \tau_b n_b & 0 & r - (\alpha_v + \delta_b + \gamma_a m) & 0 \\ 0 & \tau_v n_v & 0 & \tau_{vb} n_{vb} & 0 & -(\alpha_b + \delta_v) \end{bmatrix} \tag{44}$$

Hence using the conditions above we partition the matrix $J(E_0)$

Since each transfer has directed individual then;

$$\mathbf{F} = \begin{bmatrix} \frac{\beta_v SV}{1+aS+bV} \\ \beta_b SB \\ 0 \\ 0 \\ 0 \end{bmatrix}$$

we evaluate the Jacobian at infection–free state to obtain:

$$F = \begin{bmatrix} 0 & 0 & 0 & 0 & \frac{\beta_v \Lambda}{(\mu_s + a\Lambda)} \\ 0 & 0 & 0 & \frac{\beta_b \Lambda}{\mu_s} & 0 \\ 0 & 0 & 0 & 0 & 0 \\ 0 & 0 & 0 & 0 & 0 \\ 0 & 0 & 0 & 0 & 0 \end{bmatrix}$$

Suppose the outgoing infections from the infectious compartments are given by:

$$\mathbf{V} = \begin{bmatrix} \mu_v I_v + \beta_b^* B I_v \\ \mu_b I_b + \beta_v^* V I_b \\ \mu_{vb} I_{vb} - \beta_v^* I_b V - \beta_b^* I_b B \\ (\alpha_v + \delta_b) B + \frac{\gamma_a m A B}{A + hB} - rB(1 - \frac{B}{K}) - \tau_b n_b I_B \\ (\alpha_b + \delta_v) V - \tau_v n_v I_v - \tau_{vb} n_2 I_{vb} \end{bmatrix}$$

Moreover, computing the Jacobian at infection–free we obtain:

$$V = \begin{bmatrix} \mu_v & 0 & 0 & 0 & 0 \\ 0 & \mu_b & 0 & 0 & 0 \\ 0 & 0 & \mu_{vb} & 0 & 0 \\ 0 & -\tau_b n_b & 0 & (\alpha_v + \delta_b + \gamma_a m) - r & 0 \\ -\tau_v n_v & 0 & -\tau_{vb} n_{vb} & 0 & \alpha_b + \delta_v \end{bmatrix}$$

Therefore the inverse of the outgoing infections from the infectious compartments is given by:

$$V^{-1} = \begin{bmatrix} \frac{1}{\mu_v} & 0 & 0 & 0 & 0 \\ 0 & \frac{1}{\mu_b} & 0 & 0 & 0 \\ 0 & 0 & \frac{1}{\mu_{vb}} & 0 & 0 \\ 0 & -\frac{\tau_b n_b}{\mu_b((\alpha_v+\delta_b+\gamma_a m)-r)} & 0 & \frac{1}{(\alpha_v+\delta_b+\gamma_a m)-r} & 0 \\ \frac{\tau_v n_v}{\mu_v(\alpha_b+\delta_v)} & 0 & \frac{\tau_{vb} n_{vb}}{\mu_{vb}(\alpha_b+\delta_v)} & 0 & \frac{1}{\alpha_b+\delta_v} \end{bmatrix}$$

Therefore, we compute the product

$$F \times V^{-1} = \begin{bmatrix} J_{11} & 0 & J_{13} & 0 & J_{15} \\ 0 & J_{22} & 0 & J_{24} & 0 \\ 0 & 0 & J_{33} & 0 & 0 \\ 0 & 0 & 0 & 0 & 0 \\ 0 & 0 & 0 & 0 & 0 \end{bmatrix} \tag{3.31}$$

with $J_{11} = \frac{\beta_v \tau_v n_v \Lambda}{\mu_v(\mu_s+a\Lambda)(\alpha_b+\delta_v)}$, $J_{13} = \frac{\tau_{vb} n_{vb} \beta_v \Lambda}{\mu_{vb}(\mu_s+a\Lambda)(\alpha_b+\delta_v)}$, $J_{15} = \frac{\beta_v \Lambda}{(\mu_s+a\Lambda)(\alpha_b+\delta_v)}$, $J_{22} = \frac{\tau_b n_b \beta_b \Lambda}{\mu_s \mu_b((\alpha_v+\delta_b+\gamma_a m)-r)}$, $J_{24} = \frac{\beta_b \Lambda}{\mu_s((\alpha_v+\delta_b+\gamma_a m)-r)}$, $J_{33} = \frac{1}{\mu_{vb}}$.

Thus from equation (3.31), the eigenvalues are evaluated as $\lambda_i|_{i=(1,2,3)} = 0$,

$\lambda_4 = \frac{\beta_v \tau_v n_v \Lambda}{\mu_v(\mu_s + a\Lambda)(\alpha_b + \delta_v)} = R_I$,

and $\lambda_5 = \frac{\tau_b n_b \beta_b \Lambda}{\mu_s \mu_b((\alpha_v + \delta_b + \gamma_a m) - r)} = R_P$.

Since conditions A(1)–A(5) have been satisfied, then the viral fitness for the pathogens is $R_{IP} = \rho(FV^{-1}) = \max\{R_I, R_P\}$, where R_I and R_p are

$$\begin{aligned} R_I &= \frac{\beta_v \Lambda \tau_v n_v}{\mu_v(\mu_s + a\Lambda)(\alpha_b + \delta_v)}, \\ R_P &= \frac{\beta_b \Lambda \tau_b n_b}{\mu_s \mu_b((\alpha_v + \delta_b) + \gamma_a m - r)}. \end{aligned} \tag{3.32}$$

and $\rho(FV^{-1})$ is the spectral radius.

The pathogen fitness for influenza A virus and pneumococcus is interpreted as: The pathogen fitness for influenza A virus R_I is the product of the uninfected respiratory epithelial cell infection rate β_v, the average number of newly infected cells $\frac{\Lambda}{\mu_s + a\Lambda}$, the number of infectious IAV particles liberated from lysis of infected cells n_v, the average duration of exposure $\frac{1}{(\alpha_b + \delta_v)}$ and the chance that the infected cell survives toxicity and interaction with bacteria during replication $\frac{\tau_v}{(\alpha_b + \delta_v)}$.

The pathogen fitness for pneumococcus R_P is the product of the uninfected respiratory epithelial cell infection rate β_b, the number of infectious pneumococcus particles released from lysis of infected cells n_b, the average number of newly infected cells $\frac{\Lambda}{\mu_s}$, the average duration of exposure $\frac{1}{(\alpha_v + \delta_b) + \gamma_a m - r}$, and the probability that the infected cell survives toxicity and interaction with bacteria and alveolar macrophage phagocytosis $\frac{\tau_b}{(\alpha_v + \delta_b) + \gamma_a m - r}$.

3.6 Existence and uniqueness of steady states

3.6.1 Infection–free steady state (IFSS)

The infection–free steady state is a set of points of model (3.1) obtained in the absence of the virion or bacterium. The IFSS for our model thus is given by

$$E_0 = (S, I_v, I_b, I_{vb}, B, V) = (\frac{\Lambda}{\mu_s}, 0, 0, 0, 0, 0).$$

We state the following lemma

Lemma 3.6.1. *There is a unique infection–free steady state* E_0 *for model* (3.1)

Illustration. By this Lemma we substitute E_0 into model (3.1). The results indicate that all the derivatives of the sub–populations are equal to zero, thus the infection–free steady state is unique.

3.6.2 Endemic steady state (ESS)

Model (3.1) has an endemic steady state $E^*_{IP} = (S^*, I^*_v, I^*_b, I^*_{vb}, B^*, V^*)$ and exists if the entire population in each sub–population is positive that is $S^* > 0, I^*_v > 0, I^*_b > 0, I^*_{vb} > 0, B^* > 0, V^* > 0$. By equating the R.H.S of model (3.1) to zero and solving the resulting system of equations, at the endemic equilibrium E^*_{IP} as

$$
\begin{aligned}
S^* &= \frac{\Lambda(1+bV^*)}{\beta_v V^* + \beta_b B^* + \mu_s}, \\
I_v^* &= \frac{\beta_v V^*}{(\beta^* B^* + \mu_v)(\beta_v V^* + \beta_b B^* + (\mu_s + \Lambda a))}, \\
I_b^* &= \frac{\beta_b B^* \Lambda(1+bV^*)}{(\mu_b + \beta_v^* V^*)(\mu_s + \beta_v V^* + \beta_b B^*)}, \\
I_{vb}^* &= \frac{\beta^* V^* + \beta_b^* I_v^* B^*}{\mu_{vb}}, \\
B^* &= B^{*+}, \\
V^* &= \frac{\tau_v n_v I_v^* + \tau_{vb} n_{vb} I_{vb}^*}{(\alpha_b + \delta_v)}
\end{aligned}
$$

where B^{*+} is the positive real root of the following equation as to B^*:

$$
F(B^*) \equiv b_2 B^{*2} + b_1 B^* + b_0 = 0, \tag{3.33}
$$

with $b_2 = hr(\mu_b + \beta_v^* V^*)(\beta_v V^* + \mu_s + \beta_b)$,

$b_1 = (\mu_b + \beta_v^* V^*)(\beta_v V^* + \mu_s)\Big(r(A - kh) + \beta_b k(A(\alpha_v + \delta_b + \gamma_a m) + h(\alpha_v + \delta_b)) - k\Lambda\tau_b n_b \beta_b (1 + bV^*)\Big)$,

$b_0 = (\mu_b + \beta_v^* V^*)\Big(\beta_b r(A - k(h + A)) + k(\beta_v V^* + \mu_s)(\beta_b[A(\alpha_v + \delta_b) + \gamma_a m] + (\alpha_v + \delta_b)h - rA)\Big) - A\beta_b \Lambda \tau_b n_b k(1 + bV^*)$.

Obviously our model has two possible steady states given by

$E_{IP(1)}^* = (S^*, I_v^*, I_b^*, I_{vb}^*, B^{*+}, V^*)$ and $E_{IP(2)}^* = (S^*, I_v^*, I_b^*, I_{vb}^*, B^{*-}, V^*)$

We note that if $b_0 < 0$, there are two positive equilibria $\beta^{*+} = \frac{-b_1 - \sqrt{b_1^2 - 4b_2 b_0}}{2b_0}$ and $\beta^{*+} = \frac{-b_1 + \sqrt{b_1^2 - 4b_2 b_0}}{2b_0}$. Therefore, if $b_0 < 0$ and $b_2 > 0$ by Descartes' rule of sign, the quadratic equation (3.34) has a unique positive real root β^{*+}, hence there is a unique chronic–infection steady state $E_{IP(1)}^* = (S^*, I_v^*, I_b^*, I_{vb}^*, B^{*+}, V^*)$ if $R_{IP} > 1$.

3.7 Stability of steady states

3.7.1 Local stability of the infection–free steady state (IFSS)

Theorem 3.7.1. *If $\alpha_v + \delta_b + \gamma_a m > r$ holds, the IFSS of model (3.1), given by E_0, is locally asymptotically stable (LAS) if the effective pathogen fitness $R_{IP} < 1$ ($R_I < 1$ & $R_P < 1$), and unstable if $R_{IP} > 1$ ($R_I > 1$ & $R_P > 1$).*

Proof. The variational matrix for model (3.1) at the infection–free steady state E_0 is given by

$$J_m = \begin{pmatrix} -\mu_s & 0 & 0 & 0 & -\frac{\beta_b \Lambda}{\mu_s} & -\frac{\beta_v \Lambda}{\mu + a\Lambda} \\ 0 & -\mu_v & 0 & 0 & 0 & \frac{\beta_v \Lambda}{\mu + a\Lambda} \\ 0 & 0 & -\mu_b & 0 & \frac{\beta_b \Lambda}{\mu_s} & 0 \\ 0 & 0 & 0 & -\mu_{vb} & 0 & 0 \\ 0 & 0 & \tau_b n_b & 0 & -A(\alpha_v + \delta_b + \gamma_a m - r) & 0 \\ 0 & \tau_v n_v & 0 & \tau_{vb} n_{vb} & 0 & -(\alpha_b + \delta_v) \end{pmatrix} \tag{3.34}$$

The infection–free steady state is asymptotically stable if and only if the trace $(J_m) < 0$ and the $\det(J_m) > 0$. Therefore, from the variational matrix (3.34), we obtain

$$\begin{aligned} trace(J_m) &= -\Big(\mu_s + \mu_v + \mu_{vb} + A(\alpha_v + \delta_b + \gamma_a m - r) + (\alpha_b + \delta_v)\Big) < 0, \\ \det(J_m) &= \xi(1 - R_p)(1 - R_I) > 0 \end{aligned} \tag{3.35}$$

with $\xi = \mu_s^2\mu_{vb}\mu_b(\alpha_v + \delta_b + \gamma_a m - r)(\mu_v(\alpha_b + \delta_v))$.

Since parameters $\mu_s, \mu_v, \mu_{vb}, A, \alpha_v, \delta_b, \gamma_a m, r, \alpha_b$ and δ_v are positive, then

$-\Big(\mu_s + \mu_v + \mu_{vb} + A(\alpha_v + \delta_b + \gamma_a m - r) + (\alpha_b + \delta_v)\Big) < 0.$

Hence, trace$(J_m) < 0$. Additional, for $R_P < 1$ and $R_I < 1$ the det$(J_m) > 0$.

Since trace $(J_m) < 0$ and det$(J_m) > 0$ in equation (3.35) have been satisfied, then the IFSS (E_0) is locally asymptotically stable whenever $R_{IP} < 1$. □

Numerical simulations of the model (3.1) in Figure 3.2, depicts an infection–free

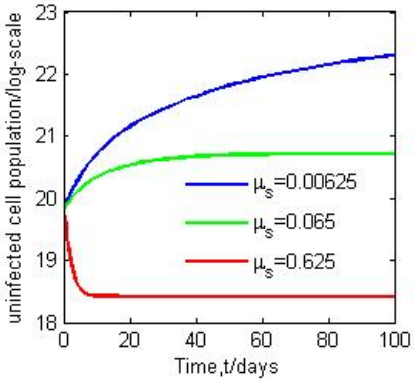

Figure 3.2: Simulation of model (3.1), the free–infection steady state, with populations $I_v = I_b = I_{vb} = B = V = 0$. The rest of the parameters are as in Table 3.2 and Table 3.1.

steady state. The threshold condition is $R_{IP} = 1$, and for $R_{IP} < 1$, the uninfected steady state is locally stable and unstable otherwise. The natural death rate exposes the basal cell layer and basement membrane, allowing for bacterial adherence and invasion (Chertow & Memoli, 2013). Increasing the natural death rate ($\mu_s = 0.0625$ ($R_P = 2.235 > R_I = 0.8695$) to $\mu_s = 0.625$ ($R_p = 0.2236 < R_I = 0.8695$) implies a reduction in the total number of uninfected cells, and decreasing the natural death rate ($\mu_s = 0.0625$ ($R_P = 2.235 > R_I = 0.8695$) to $\mu_s = 0.00625$ ($R_p = 22.3597 > R_I = 0.8695$) implies an increment in the number of uninfected cells. The results are in line with Theorem 3.7.1.

The biological implication of Theorem 3.7.1 is that the spread of the disease can be effectively controlled if the initial sizes of the sub–populations of the model (3.1) are in the basin of attraction of the DFE (E_0), that is in general if R_{IP} is less than unity, the infection can't establish itself in the respiratory cell population, thus the infection dies out in the long run. Whereas if $R_{IP} > 1$ the infection will persist in the population leading to disease establishment in the host.

3.7.2 Local stability of the endemic steady state (ESS)

The local stability of the ESS will be analytically studied by analyzing the eigenvalues of the variational matrix at endemic steady state using Routh–Hurwitz criterion.

Theorem 3.7.2. *The unique endemic steady state of model* (3.1) *is locally asymptotically stable, if* $R_{IP} > 1$

Proof. The variational matrix $J_m(S^*, I_v^*, I_b^*, I_{vb}^*, B^*, V^*)$ associated with the

endemic steady state $(E^* = S^*, I_v^*, I_b^*, I_{vb}^*, B^*, V^*)$ is given by

$$J_m = \begin{pmatrix} k_0 & 0 & 0 & 0 & -\beta_b S^* & k_1 \\ k_2 & k_3 & 0 & 0 & -\beta_b^* I_v^* & k_4 \\ \beta_b B^* & 0 & k_5 & 0 & \beta_b S^* & -\beta_v^* I_b \\ 0 & \beta_b^* B^* & \beta_v^* V^* & -\mu_{vb} & \beta_b^* I_v & \beta_v^* I_b \\ 0 & 0 & \tau_b n_b & 0 & k_6 & 0 \\ 0 & \tau_v n_v & 0 & \tau_{vb} n_{vb} & 0 & -(\alpha_b + \delta_v) \end{pmatrix}. \tag{3.36}$$

with $k_0 = -\Big(\mu_s + \beta_b S^* B^* + \frac{\beta_v V^*(1+bV^*)}{(1+aS^*+bV^*)^2}\Big)$, $k_1 = -\frac{\beta_v S^*(1+aS^*)}{(1+aS^*+bV^*)^2}$, $k_2 = \frac{\beta_v V^*(1+bV^*)}{(1+aS^*+bV^*)^2}$,
$k_3 = -(\mu_v + \beta_b^* B^*), k_4 = \frac{\beta_v S^*(1+aS^*)}{(1+aS^*+bV^*)^2}, k_5 = -(\mu_b + \beta_v^* V^*)$,
$k_6 = -\Big(\frac{2rB^*}{k} + \frac{\gamma_a mA(A+hB^*)+\gamma_a mAB^* h}{(A+hB^*)^2} + (\alpha_v + \delta_b) - r\Big)$
The characteristic polynomial corresponding to $J_m(S^*, I_v^*, I_b^*, I_{vb}^*, B^{*+}, V^*)$ about $E^* = (S^*, I_v^*, I_b^*, I_{vb}^*, B^{*+}, V^*)$ is given by

$$H(y) = h_6 y^6 + h_5 y^5 + h_4 y^4 + h_3 y^3 + h_2 y^2 + h_1 y + h_0, \tag{3.37}$$

The coefficient h_6 of y^6 in equation (3.37), is always positive. If all preceding coefficients are positive by Descartes' rule of signs implies that there is no zero of the polynomial in equation(3.37) with a positive real number. Whereas if $h_0 < 0$, the polynomial equation (3.37) has one or more sign change among consecutive parameters with at most six (6) positive roots of y or equivalent of six negative roots of y. Therefore, all zeros of the polynomial (3.37) have negative real parts.

The Routh–Hurtwiz criterion for polynomial equation (3.37) gives six negative eigenvalues if the conditions $h_i > 0$, for i = 1, 2, 3,. . . , 6 are satisfied. The relevant Routh–Hurtwiz criteria in Linda (2007) could be used to demonstrate that the model (3.1) is locally asymptotically stable when $R_{IP} > 1$.

3.7.3 Global stability of the infection–free steady state (IFSS)

For effective viral–bacterial infection elimination in the epithelial cell population, a global asymptotic stability result has to be proved for the IFSS.

Theorem 3.7.3. *If $R_{IP} < 1 (R_I < 1$ & $R_P < 1)$, then the infection–free steady state $E_0 = \{X^*, 0\}$ of model (3.1) is globally asymptotically stable in Ω and there is no unique endemic steady state.*

Proof. Let $X = S \in \mathbb{R}$ be a representative of uninfected epithelial cell population and $Z = (I_v, I_B, I_{vb}, B, V \in \mathbb{R}^5)$ be a representative of the infected population. The co–infection model (3.1) can be re–written as

$$\begin{cases} \frac{dX}{dt} = F(X, Z), \\ \\ \frac{dZ}{dt} = G(X, Z), \quad G(X, 0) = 0. \end{cases} \tag{3.38}$$

where

$$F(X, Z) = \begin{pmatrix} \Lambda - \frac{\beta_v SV}{1+aS+bV} - \beta_b SB - \mu_s S \end{pmatrix},$$

$$G(X,Z) \;=\; \begin{pmatrix} \frac{\beta_v SV}{1+aS+bV} - (\beta_b^* B + \mu_v) I_v \\ \beta_b SB - (\mu_b + \beta_v^* V) I_b \\ \beta_v^* I_b V + \beta_b^* I_v B - \mu_{vb} I_{vb} \\ rB\left(1 - \frac{B}{K}\right) + \tau_b n_b I_b - \left(\alpha_v + \delta_b + \frac{\gamma_a m A}{A+hB}\right) B \\ \tau_v n_v I_v + \tau_{vb} n_{vb} I_{vb} - (\alpha_b + \delta_v) V \end{pmatrix}.$$

We consider a reduced system

$$\frac{dX}{dt}|_{Z=0} = \Lambda - \mu_s X. \tag{3.39}$$

This implies that $(X^*, 0) = \frac{\Lambda}{\mu_s}$ is a globally asymptotically stable steady state. Equation (3.39) gives

$S = \frac{\Lambda}{\mu_s} + (S(0) - \frac{\Lambda}{\mu_s})e^{-\mu_s t}$, which approaches X^* as $t \to \infty$, this shows global convergence of solution of (3.39) in Ω. We re–state the two conditions given as H2 in Castillo-Chavez et al. (2002), that guarantee global asymptotic stability as follows:

(a) $\frac{dX}{dt} = G(X, 0), X^*$

(b) G(X,Z)=$LZ - \tilde{G}(X, Z)$, such that $\tilde{G}(X, Z) \geq 0$ for $(X, Z) \in \Omega$

where $L = D_z G(X^*, 0)$ is an M–matrix (the off–diagonal elements of L are non–negative) and Ω is the region where the model has a biological meaning. If system (4.5) satisfies conditions (a) and (b) then, Theorem 3.7.3 holds.

By linearization of $G(X, Z)$, we obtain a matrix

$$L = \begin{pmatrix} -\mu_v & 0 & 0 & 0 & \frac{\beta_v \Lambda}{\mu_s + a\Lambda} \\ 0 & -\mu_b & 0 & \frac{\beta_b \Lambda}{\mu_s} & 0 \\ 0 & 0 & -\mu_{vb} & 0 & 0 \\ 0 & \tau_b n_b & 0 & r - (\alpha_v + \delta_b + \gamma_a m) & 0 \\ \tau_v n_v & 0 & \tau_{vb} n_{vb} & 0 & -(\alpha_b + \delta_v) \end{pmatrix}. \tag{3.40}$$

Therefore, $G(X, Z)$ can be expressed as $G(X, Z) = LZ - \bar{G}(X, Z)$, where

$$LZ = \begin{pmatrix} \frac{\beta_v \Lambda V}{\mu_s + a\Lambda} - \mu_v I_v \\ \frac{\beta_b \Lambda B}{\mu_s} - \mu_b I_b \\ -\mu_{vb} I_{vb} \\ \left(r - \left(\alpha_v + \delta_b + \frac{\gamma_a m}{A + hB}\right)\right) B + \tau_b n_b I_b \\ \tau_v n_v I_v + \tau_{vb} n_{vb} I_{vb} - (\alpha_b + \delta_v) V \end{pmatrix}, \tag{3.41}$$

and

$$\tilde{G}(X,Z) = \begin{pmatrix} \tilde{G}_1(X,Z) \\ \tilde{G}_2(X,Z) \\ \tilde{G}_3(X,Z) \\ \tilde{G}_4(X,Z) \\ \tilde{G}_5(X,Z) \end{pmatrix} = \begin{pmatrix} \beta_b^* B I_v \\ \beta_v^* V(t) I_b \\ -(\beta_v^* I_b V + \beta_b^* I_v B) \\ \frac{rB^2}{K} \\ 0 \end{pmatrix}. \tag{3.42}$$

Thus, from equation (3.42) $\tilde{G}_3(X,Z) < 0$, hence condition (b) is not satisfied. This indicates that the infection–free steady state for model (3.1) may not be globally asymptotically stable whenever $R_{IP} < 1$ ($R_I < 1$ & $R_P < 1$), hence the global asymptotic stability of the infection–free steady state fails from Theorem 3.7.3.

3.7.4 Global stability of endemic steady state

In this Section, we show the global stability of endemic steady state for model (3.1). We give specific coefficients of Lyapunov functions for the global stability of unique endemic equilibrium by the graph–theoretic method found in Guo et al. (2008) and Shuai & Driessche (2013).

Theorem 3.7.4. *The unique endemic steady state of model* (3.1) *is globally asymptotically stable.*

Proof. We adapt Lyapunov functions of the integral form $S - S^* - \int_{S^*}^{S} \frac{f(S^*,I^*)}{f(\tau,I^*)} d\tau$ used in Korobeinikov (2007); Huang et al. (2011); Elaiw & Azoz (2013).

By setting the vertice's corresponding to system (3.1) to be

$$\begin{aligned}
L_1 &= S - S^* - \int_{S^*}^{S} \left(\frac{f_1(S^*, V^*)}{f_1(\phi, V^*)} + \frac{f_2(S^*, B^*)}{f_2(\phi, B^*)} \right) d\phi, \\
L_2 &= (I_v - I_v^* - I_v^* \ln I_v), \\
L_3 &= (I_b - I_b^* - I_b^* \ln I_b) \\
L_4 &= (I_{vb} - I_{vb}^* - I_{vb}^* \ln I_{vb}), \\
L_5 &= (B - B^* - \ln B^*), \\
L_6 &= E(V - V^* - V^* \ln V).
\end{aligned} \tag{3.43}$$

Such that we have

$$\begin{aligned}
L(S, I_v, I_b, I_{vb}, B, V) &= S - S^* - \int_{S^*}^{S} \left(\frac{f_1(S^*, V^*)}{f_1(\phi, V^*)} + \frac{f_2(S^*, B^*)}{f_2(\phi, B^*)} \right) d\phi \\
&+ (I_v - I_v^* - I_v^* \ln I_v) + (I_b - I_b^* - I_b^* ln I_b) \\
&+ (I_{vb} - I_{vb}^* - I_{vb}^* \ln I_{vb}) + (B - B^* - \ln B^*) + (V - V^* - V^* \ln V).
\end{aligned}$$

We consider system (3.43) for vertex 1 and compute the time derivative of L_1 to get

$$\dot{L}_1 = (3 - \frac{f_1(S^*, V^*)}{f_1(S, V^*)} - \frac{S^*}{S})(\Lambda - \frac{\beta_v SV}{1 + aS + bV} - \beta_b SB - \mu_s S). \tag{3.44}$$

We simplify $\dot{L}_1$ to get

$$\begin{aligned}
\dot{L}_1 &= 3f_1(S^*, V^*)\Big(1 - \frac{f_1(S, V)}{f_1(S^*, V^*)}\Big) + 3\beta_b S^* B^* \Big(1 - \frac{SB}{S^* B^*}\Big) + 3\mu_s S^* \Big(1 - \frac{S}{S^*}\Big) \\
&- \frac{f_1(S^*, V^*)}{f_1(S, V^*)} \left(f_1(S^*, V^*)\Big(1 - \frac{f_1(S, V)}{f_1(S^*, V^*)}\Big) + \beta_b S^* B^* \Big(1 - \frac{SB}{S^* B^*}\Big) + \mu_S^* \Big(1 - \frac{S}{S^*}\Big) \right) \\
&- \frac{S^*}{S} \left(f_1(S^*, V^*)\Big(1 - \frac{f_1(S, V)}{f_1(S^*, V^*)}\Big) + \beta_b S^* B^* \Big(1 - \frac{SB}{S^* B^*}\Big) + \mu_s \Big(1 - \frac{S^*}{S}\Big) \right)
\end{aligned} \tag{3.45}$$

From equation (3.45), the arithmetic mean is greater than the geometric mean. Thus we obtain

$$\begin{aligned}\dot{L}_1 &\leq 3\left(f_1(S^*,V^*)\Big(1-\frac{f_1(S,V)}{f_1(S^*,V^*)}\Big)+\beta_b S^* B^*\Big(1-\frac{SB}{S^*B^*}\Big)\right)\\ &+ 3\mu_s S^*\Big(1-\frac{S}{S^*}\Big) : a_{12}G_{12}+a_{13}G_{13} \qquad (3.46)\end{aligned}$$

Let $f(y_i) = 1 - y_i + \ln y_i|_{(i=1,2,3)} < 0$ whenever $y_i > 1$.

Clearly $\dot{L}_1 < 0$ and $\dot{L}_1 = 0$ for $f_1(S^*, V^*) = f_1(S, V)$, $S = S^*$ and $B = B^*$.

We apply the same technique as shown in the Appendix 3 to obtain the remaining vertice's, hence

$$\begin{aligned}\dot{L}_2 &\leq \beta_b^* I_v^* B^*\Big(1-\frac{I_v B}{I_v^* B^*}\Big) : a_{24}G_{24},\\ \dot{L}_3 &\leq \beta_b S^* B^*\Big(1-\frac{I_b^* SB}{I_b S^* B^*}\Big) : a_{31}G_{31},\\ \dot{L}_4 &\leq \beta_b^* I_v^* B^*\Big(1-\frac{I_v B I_{vb}^*}{I_v^* B^* I_{vb}}\Big)+\beta_v^* I_b^* V^*\Big(1-\frac{I_b^* V I_{vb}^*}{I_b V^* I_{vb}}\Big) : a_{42}G_{42}+a_{43}G_{43},\\ \dot{L}_6 &\leq \tau_v n_1 I_v^*\Big(1-\frac{I_v V^*}{I_v^* V}\Big)+\tau_{vb} n_2 I_{vb}^*\Big(1-\frac{V^* I_{vb}}{V I_{vb}^*}\Big) : a_{62}G_{62}+a_{64}G_{64}. \qquad (3.47)\end{aligned}$$

However,

$$\dot{L}_5 \leq rB^*\left(1-\frac{B^*}{K}\right)\left(1-\frac{B(1-\frac{B}{K}}{B^*(1-\frac{B^*}{K}}\right)+\tau_b n_b I_b^*\left(1-\frac{I_b B^*}{I_b^* B}\right). \qquad (3.48)$$

has been ignored because it is a self loop.

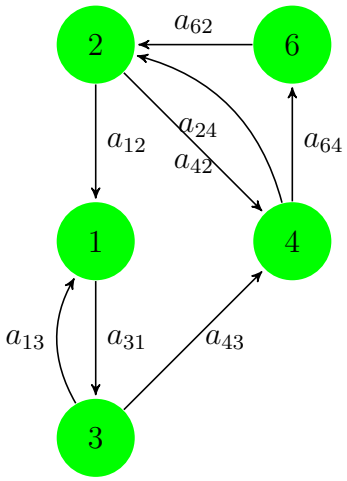

Figure 3.3: A weighted simple digraph for influenza A virus and pneumococcus co–infection

We assume that H is a spanning set of G having the same vertex sets, then H is called a sub–digraph of G. By assigning a positive weight to each edge, then the digraph G is said to be weighted. The weight $W(H)$ of a sub–digraph H is the product of the weights on all its arcs. Suppose G is a weighted digraph having n vertices. We consider an $n \times n$ weighted matrix denoted by $M = (a_{ij})$ such that $a_{ij} > 0$ equal to the weight of arc (j, i) if it exists and 0 otherwise.

From Figure 3.7.4, along each cycle we have

$$\begin{aligned} G_{13} + G_{31} &= 0, \\ G_{42} + G_{24} &= 0, \\ G_{12} + G_{31} + G_{43} + G_{24} &= 0. \end{aligned} \tag{3.49}$$

Applying Theorem (3.5) in Shuai & Driessche (2013), lemmas 4.1 & 4.3 in Din et al. (2016) and ignoring a vertex with a self loop, there exists c_i, $1 \leq i \leq 5$ such that $L(X) = \sum_{i=1}^{5} c_i L_i$ is a Lyapunov function of model (3.1). From Figure and using equation (3.49), we obtain the relations:

$d^-(4) = 2$; implying that $c_2a_{24} + c_6a_{64} = c_4a_{43} + c_4a_{42}$ but $a_{24} = a_{42}$, hence

$$(c_2 - c_4)a_{24} \quad = \quad c_4a_{43} - c_6a_{64}. \tag{3.50}$$

$d^+(1) = 1$; implying $c_3a_{31} = c_1a_{12} + c_1a_{13}$. We observe that, $a_{13} = a_{31}$ thus we get

$$c_1(a_{31} + a_{12}) = c_3(a_{31}). \tag{3.51}$$

By making substitutions from system (3.51) we obtain

$$c_1 \quad = \quad \frac{c_3\beta_b^*S^*B^*}{\beta_bS^*B^* + 3f_1(S^*, V^*)}. \tag{3.52}$$

$d^-(2) = 3$; implying $c_1a_{12} + c_4a_{42} + c_6a_{62} = c_2a_{24}$, however, $a_{24} = a_{42}$ thus we obtain

$$(c_2 - c_4)a_{24} \quad = \quad c_1a_{12} + c_6a_{62}. \tag{3.53}$$

$d^-(1) = 1$; implying $c_3a_{31} = c_4a_{43} + c_1a_{13}$, we note that $a_{13} = a_{31}$ hence the expression yields

$$(c_3 - c_1)a_{13} \quad = \quad c_4a_{43}. \tag{3.54}$$

From system (3.52), let $c_1 = 1$. Then we obtain $c_3 = \frac{\beta_bS^*B^*+3f_1(S^*,V^*)}{\beta_bS^*B^*}$.
We make substitutions of c_3 and c_1 in system (3.54) to obtain

$$c_4a_{43} \quad = \quad a_{13}\left(\frac{\beta_bS^*B^* + 3f_1(S^*, V^*)}{\beta_bS^*B^*} - 1\right). \tag{3.55}$$

FRom equation (3.55) we have

$$c_4 = \frac{3f_1(S^*, V^*)\beta_bS^*B^*}{\beta_bS^*V^*\beta_v^*I_b^*V^*} = \frac{3f_1(S^*, V^*)}{\beta_v^*I_bV^*}. \tag{3.56}$$

Combining system (**??**) and (3.52) gives

$$c_6 = \frac{c_4 a_{43} - c_1 a_{12}}{a_{62} + a_{64}}.$$

Substituting for c_1, a_{43}, a_{12}, leads to

$$c_6 = \frac{3f_1(S^*, V^*) - 3f_1(S^*, V^*)}{a_{62} + a_{64}} = 0.$$

Substituting for c_6 in system (3.52) we get

$$c_2 = c_4 + \frac{c_1 a_{12}}{a_{24}}.$$

Hence

$$c_2 = \frac{3f_1(S^*, V^*)}{\beta_v^* I_b^* V^*} + \frac{3f_1(S^*, V^*)}{\beta_b^* I_v^* B^*} = 3f_1(S^*, V^*) \left(\frac{\beta_b I_v^* B^* + \beta_v I_b^* V^*}{\beta_v^* I_b^* V^* \beta_b^* I_v^* B^*} \right).$$

Therefore,

$$L(X) = \sum_{i=1}^{5} c_i L_i = L_1 + 3f_1(S^*, V^*) \left(\frac{\beta_b I_v^* B^* + \beta_v I_b^* V^*}{\beta_v^* I_b^* V^* \beta_b^* I_v^* B^*} \right) L_2 + \frac{\beta_b S^* B^* + 3f_1(S^*, V^*)}{\beta_b S^* B^*} L_3 + \frac{3f_1(S^*, V^*)}{\beta_v^* I_b V^*} L_4. \tag{3.57}$$

with $X = (S, I_v, I_b, I_{vb}, B, V)$

Hence, $L(X)$ is a Lyapunov function for model (3.1). One can verify that $\{E^*\}$ is the only invariant set in int(Ω) where $L'(X) = 0$, therefore, E^* is globally asymptotically stable in int (Ω). The epidemiological implication of the result is that the infection will establish itself in the respiratory epithelial cell population whenever $R_{IP} > 1$ irrespective of the initial number of the infectious epithelial cell population, ultimately the co–infected cell population approaches a constant level.

3.7.5 Sensitivity analysis of the model parameters on the pathogens' fitness

Under this section, model parameters are varied with respect to the pathogen fitness threshold, $R_{IP} = \max\{R_I, R_P\}$ of the model (3.1). We carry out a sensitivity analysis of the pathogen fitness to the model parameter. This will help us in identifying and verifying model parameters that most influence the pathogen fitness threshold for the pathogens. Further, values obtained for sensitivity indexes indicate which parameters should be targeted most for intervention purposes.

The normalized forward sensitivity index of a variable to a parameter is the fraction of the relative change in the variable to the relative change in the parameter (Chitnis et al., 2008). If the variable is a differentiable function of the parameter, the sensitivity index may be defined using partial derivatives. The normalized forward sensitivity index technique outlined in Tilahun et al. (2017) is used to obtain indices of R_I and R_P. Therefore, $\triangle_p^{R_0} = \frac{\partial R_0}{\partial p} \times \frac{p}{R_0}$
with R_0 =variable of either R_I or R_P, $\triangle_p^{R_0}$ the sensitivity index of either R_I or R_P with respect to a given parameter and $p =$ is a differentiable parameter.

Since the availability of literature and data especially on within–host influenza A virus and pneumococcus co–infection is limited, the qualitative predictions of our model (3.1) is dependent on estimating some of the parameter values shown in Table 3.1 and Table 3.2.

Table 3.1: Parameter values for influenza A virus and Streptococcus pneumoniae

Parameter	value	Reference
Influenza A virus		
$S(0)$	4.0×10^8	(Baccam et al., 2006)
Λ	6.25×10^7	(Bocharov & Romanyukha, 1994)
$I(0)$	0	
$V(0)$	10^7	(Chen et al., 2012)
μ_v	8.9×10^{-1}	(Cheng et al., 2017)
μ_s	6.25×10^{-2}	(Chen et al., 2012)
n_v	$10^3 - 10^4$	(Hadjichrysanthou et al., 2016)
a	0.02	assumed
b	0.6	assumed
β_v	2.7×10^{-5}	(Baccam et al., 2006)
δ_v	0.5-2	(Xing et al., 2017)
α_b	3.2×10^{-4}	assumed
τ_v	8.6×10^{-1}	assumed
Streptococcus pneumoniae		
$B(0)$	10^3	(Cheng et al., 2017)
$I_b(0)$	0	
r	2.7×10^1	(Smith et al., 2013)
τ_b	1.102×10^{-6}	assumed
K	2.3×10^8	(Smith & Smith, 2016)
γ_a	8.877×10^{-1}	estimated

Table 3.2: Parameter values for pneumococcus co–infection models

Parameter	value	Reference
Streptococcus pneumoniae		
δ_b	2×10^{-2}	assumed
α_v	10^{-1}	assumed
n_b	1×10^{3}	assumed
h	5.0	(Metzger et al., 2015)
A	$10^{5.5}$	(Smith & Smith, 2016)
β_b	1.2×10^{-5}	assumed
μ_b	1.34×10^{-1}	assumed
Co–infection		
μ_{vb}	5.2×10^{-10}	(Smith, 2017; Cheng et al., 2017)
τ_{vb}	2.4×10^{-3}	assumed
n_{vb}	2.51×10^{1}	(Smith et al., 2013)
β_v^*	7.3×10^{-8}	assumed
β_b^*	4.1×10^{-6}	assumed

The positive sign of sensitivity index of the pathogen fitness with respect to the model parameters indicates that an increase (or decrease) in the value of each of the parameters in such a group will lead to an increase (or decrease) in the pathogen fitness of the infection. Whereas the negative sensitivity index of the pathogen fitness threshold with respect to the model parameter implies that an increase (or decrease) in the value of the parameter in this group, results into a corresponding decrease (or increase) in the pathogen fitness of the infection, and asymptotically results into persistence (or eradication) of the infection in the

Table 3.3: Sensitivity indices of R_I/R_P to parameters of IAV and Pneumococcus (SP), computed at the baseline parameter values given in Table 3.2 and Table 3.1

Parameter	S.I of R_I	Parameter	S.I of R_P
β_v	+1.0	m	-1.5
δ_v	-9.9×10^{-1}	γ_a	-1.6
τ_v	+1.0	Λ	+1.0
μ_v	-1.0	τ_b	+1.0
n_v	+1.0	μ_s	-1.0
a	-9.9×10^{-1}	β_b	+1.0
μ_s	-4.9×10^{-8}	n_b	+1.0
α_b	-2.1×10^{-4}	r	-5.9×10^{-1}
Λ	+4.9×10^{-8}	α_v	-7.0×10^{-6}
		δ_b	-3.3×10^{-2}

epithelial cell population (see, Theorem 3.7.4). For instance, $\triangle_{\beta_v}^{R_I} = 1$, means that, when β_v is increased (or decreased) by 10%, increases or decreases R_I by 10%. Therefore, with sensitivity analysis, one is able to get an insight on the suitable intervention strategies to prevent and control the spread of the influenza A virus and pneumococcus co–infection described by system (3.1).

Sensitivity analysis of model (3.1) revealed that the pathogen fitness for pneumococcus and influenza A virus is most sensitive to maximum number of bacteria an alveolar macrophage can catch (m), phagocytosis rate (γ_a), number of infectious influenza A virus particles and pneumococcus liberated from lysis of infected cells (n_v & n_b) and infection rates of pathogens β_b and β_v.

3.7.6 The impact of pneumococcus on Influenza A virus

To analyze the effects of streptococcus pneumoniae on influenza A virus and vice versa, we express R_P in terms of R_I. We solve for μ_s to obtain $\mu_s = \frac{A-a\Lambda R_I}{R_I}$. Substituting into (3.32) for R_P, we obtain $R_P = \frac{BR_I}{A-a\Lambda R_I}$,

where

$$A = \frac{\beta_v \Lambda \tau_v n_v}{\mu_v(\alpha_b + \delta_v)}, B = \frac{\beta_b \Lambda \tau_b n_b}{\mu_b((\alpha_v + \delta_b) + \gamma_a m - r)}. \tag{3.58}$$

Computing the partial derivative of R_P with respect to R_I leads to

$$\frac{\partial R_P}{\partial R_I} = \frac{AB}{(A - R_I a\Lambda)^2}. \tag{3.59}$$

If the R.H.S of (3.59) is equal to zero, this signifies that pneumococcus has no effect on the dynamics of influenza A. If result (3.59) is less than zero, this implies that a decrease in influenza A virus results into an increase of pneumococcus. Whereas if expression (3.59) is greater than zero, an increase in influenza A virus results in an increase of pneumococcus which implies an endemic steady state for which the pneumococcus–influenza A virus co–infection is likely to occur in the epithelial cell population.

3.7.7 The impact of Influenza A virus on pneumococcus

Similarly, expressing μ_s in terms of R_P, we obtain $\mu_s = \frac{B}{R_P}$. Substituting μ_s in equation (3.32), we obtain

$$R_I = \frac{AR_P}{B + a\Lambda R_P}.$$

By computing the partial derivative of R_I w.r.t R_P, we get

$$\frac{\partial R_I}{\partial R_P} = \frac{AB}{(B + a\Lambda R_P)^2}. \tag{3.60}$$

where A and B are as in equation (3.58). When expression (3.60) is equal to zero, this implies that pneumococcus bacteria has no impact on the transmission dynamics of influenza A. If result (3.60) is less than zero, a decrease in pneumococcus leads to an increase in influenza A virus, this implies that the infection due to pneumococcus can be wiped out of the epithelial cell population. Whereas if result (3.60) is greater than zero, it implies that an increase in pneumococcus density results into an increase in influenza A density that gives rise to a chronic infection. The implication of the above impact of influenza A virus and pneumococcal existence and vice–visa results into a bifurcation state (see Figure 3.4).

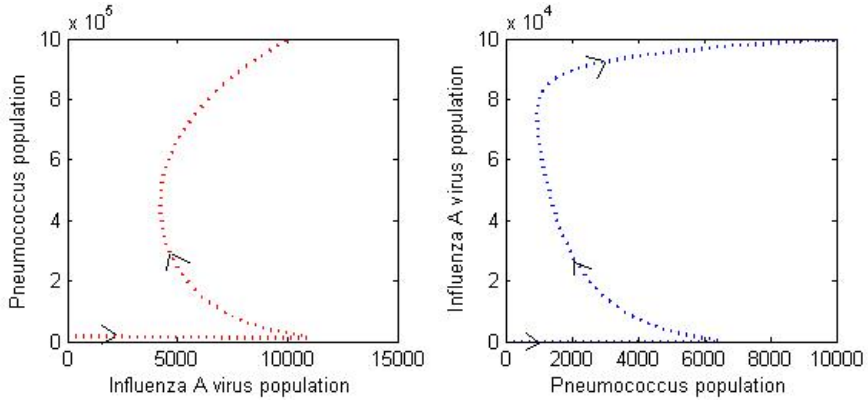

(a) (b)

Figure 3.4: Phase potraits for the dynamics of influenza A virus and pneumococcal bacteria, (a) with parameter values $n_v = 10^3, n_b = 10^5$, variables $S(0) = 4.8 \times 10^5$, $I_v = 10^2, I_b = I_{vb} = B = V = 10^3$ and (b) with parameter values $n_v = 10^4, n_b = 10^3$, variables $S(0) = 4.8 \times 10^5$, $I_v = 10^3, I_b = 10, I_{vb} = B = V = 10^3$ and other parameters remain as in Table 3.1 and Table 3.2.

3.8 Model results and discussion

In this section, the simulations of the model (5.1), are carried out in MATLAB's standard solver for ODEs, the inbuilt function ode45. The function implements a Runge–Kutta method with variable time step for efficient computation. The results arrived at and the results of the sensitivity analysis are illustrated by simulating the behaviour of model (3.1) using various initial conditions of parameter values in Table 3.1 and Table 3.2.

Computing R_I and R_P using the parameter values in Table 3.2 and Table 3.1, the respective values are 0.8694 and 2.2359, hence the infection would persist in the epithelial cell population for $R_{IP} = R_P = 2.2359 > 1$ and will die out if $R_{IP} = R_P < 1$.

Our numerical results provides a theoretical means to justify that assumptions made in the model development are biologically feasible. Figure 3.5 depicts re-

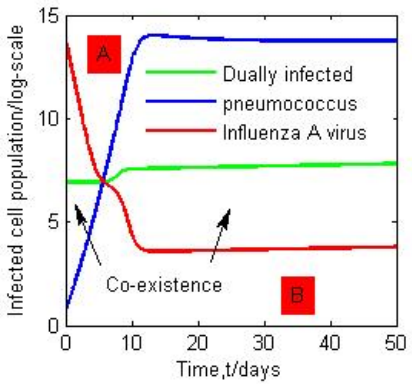

Figure 3.5: Simulation of model (4.8), global stability for populations of infected cells (I_v) as function of time with parameter values: $\Lambda = 6.25 \times 10^5, m = 95, n_v = 10^2, \beta_b = 1.2 \times 10^{-3}, \tau_v = 1.2 \times 10^{-2}, \tau_{vb} = 1.1 \times 10^{-}4, \beta_v^* = 7.3 \times 10^{-10}$; variables $I_v = I_b = B = 10^3, I_{vb} = 10^4$ (thus $R_P = 17.1774 > 1$ and $R_I = 2.4218 > 1$), and other parameters remain as in Table 3.1 and Table 3.2.

gion A with the existence of only pneumococcal infection after over powering

influenza A virus at endemic steady state E^*_{IP} and subsequently colonizing the respiratory cell population, whereas region B shows the existence of only influenza A virus that has been suppressed by pneumococcal infection. We note that the two pathogens continue to co–exist and replace each other in the respiratory cell population causing bacterial chronic infection. The intersection point is a Nash equilibrium, where the two pathogens payoff themselves while competing for the resources. The host's fitness is most affected at this equilibrium because of the presence of both pathogens at the same time. Figure 3.6 (a), depicts the effect of

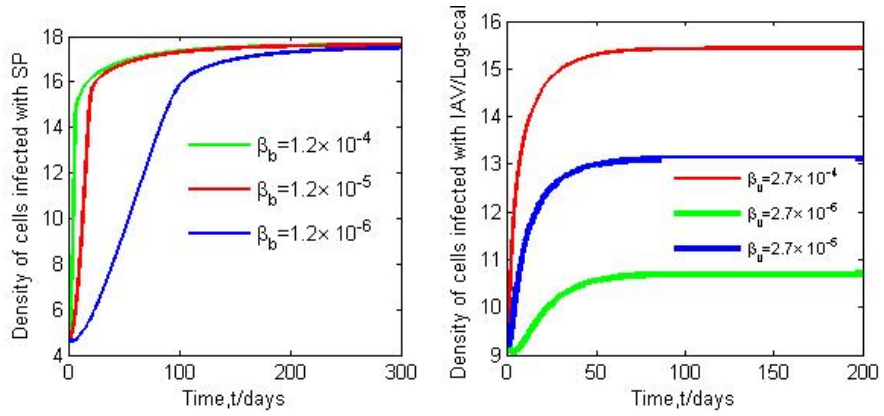

(a) (b)

Figure 3.6: Simulation of model (3.1)(a) showing chronic levels of infected cells I_b for different values of β_b as function of time with parameter values:$\Lambda = 6.25 \times 10^5, \beta_b = 1.2 \times 10^-4, n_b = 10^5, a = 2.0 \times 10^{-2}, b = 0.6, \mu_b = 1.34 \times 10^{-2}, \tau_b = 1.102 \times 10^{-5}$, variables; $S(0) = 4.0 \times 10^3$, $I_v = I_{vb} = 10^2$, $I_b = B = 10^3, V = 10^7$ (thus $R_P = 2235.9654 > 1$ and $R_I = 8.6950 > 1$). (b) Chronic levels of infected cells I_v for different values of β_v as function of time with parameter values: $n_b = 10^3, \tau_{vb} = 2.4 \times 10^{-3}, \beta^*_v = 7.3 \times 10^{-8}, \beta^*_b = 4.1 \times 10^-7, \tau_v = 8.6 \times 10^-2$, variables; $S(0) = 4.8 \times 10^7, I_v = 10^4, I_b = 10^2, \tau_{vb} = 10, B = 10^6, V = 10^4$ and other parameters remain as in Table 3.1 and Table 3.2, hence $R_p = 2.2359 > 1$ and $R_I = 86.9477 > 1$

varying the infection rate due to pneumococcal β_b. A high infection rate or low infection rate maintains the pneumococcus infection in the infected population and after a given period a constant unique chronic–infection level is attained that is, increasing $\beta_b = 1.2 \times 10^{-5}$ ($R_P = 22.3597$) to $\beta_b = 1.2 \times 10^{-4}$ ($R_P = 22.3597$). This implies that there is persistence of the infection due to pneumococcal in the

cell population. A decrease in transmission coefficient from $\beta_b = \beta_b = 1.2 \times 10^{-5}$ ($R_P = 22.3597$) to $\beta_b = 1.2 \times 10^{-6}$ ($R_P = 2.2360$), implies that the infection is persisting in the epithelial cell population. Therefore, the public health should put measures to combat the high endemicity of pneumococcal to reduce R_P to less than unity.

Figure 3.6 (b), shows the effect of varying β_v from 2.7×10^{-5} ($R_I = 86.9477$) to 2.7×10^{-4} ($R_I = 869.4774$), this implies that an increase in infection rate due to influenza A virus results into an increase in the population density of new uprising infections. It means that if the infection persists in the respiratory epithelial cell population, more susceptible cells will be infected even then the population will approach a constant level. However, the cases decrease with well managed prevention measures. Whereas decreasing β_v from 2.7×10^{-5} (R_I=86.9477) to 2.7×10^{-6} (R_I=8.6948) leads to a decrease in the population of newly infected epithelial cells that can eventually be phased out of the respiratory epithelial cell population. Figure 3.7(a), the region of parameter space where only the influenza A virus–pneumococcus co–infected exists and approaches a unique endemic steady state. To reduce the co–endemicity, the number of pneumocaccal bacteria that is caught by alveolar macrophage, the first arm of the immune system should be increased by reducing influenza A virus that leads to depletion of alveolar macrophage. To prevent such a co–infection, the alveolar macrophage (m) population can be partially restored via the immune modulator such as granulocyte macrophage colony stimulating factor (Smith, 2017).

Figure 3.7(b), shows the effect of varying the phagocytosis rate γ_a, the rate at which peumococcus is phagocytosed should be increased because pneumococcus viral load plays an important role in influenza A virus–pneumococcal co–existence.

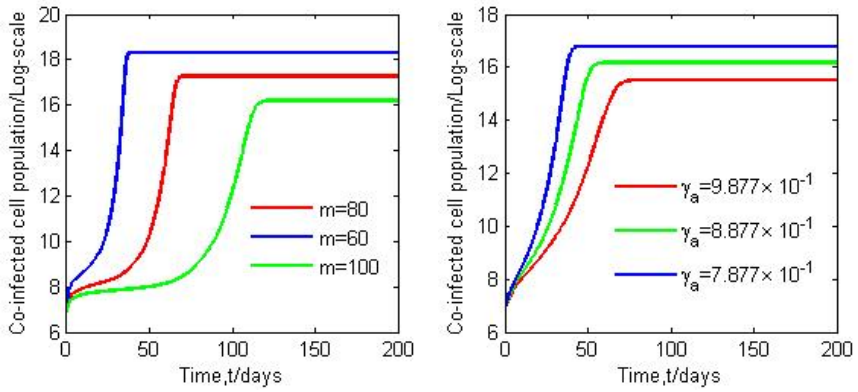

(a) (b)

Figure 3.7: Simulation of model (3.1)(a) Global stability of the positive endemic steady state of co–infected cells (I_{vb}), showing varying values of maximum number of bacteria alveolar macrophage (m) can consume (that is $m = 60$ ($R_p = 3.7407$), $m = 80$ ($R_P = 2.2360$), $m = 100$ ($R_P = 1.5945$), with variables: $S(0) = 4.0 \times 10^{-1}, I_v = I_b = I_{vb} = 10^3, B = 10^4, V = 10^6$. (b) Global stability for the co–infected population with changing effect of phagocytosis rate γ_a that is $\gamma_a = 8.877 \times 10^{-1}$ (R_P=2.2360), γ_a=9.877×10^{-1} ($R_P = 1.8927$), γ_a=7.877×10^{-1} ($R_P = 2.7310$), with variables $I_v = 10, I_b = I_{vb} = 10^3, B = 10^4, V = 10^3$. The rest of the parameters are as in Table 3.1 and Table 3.2.

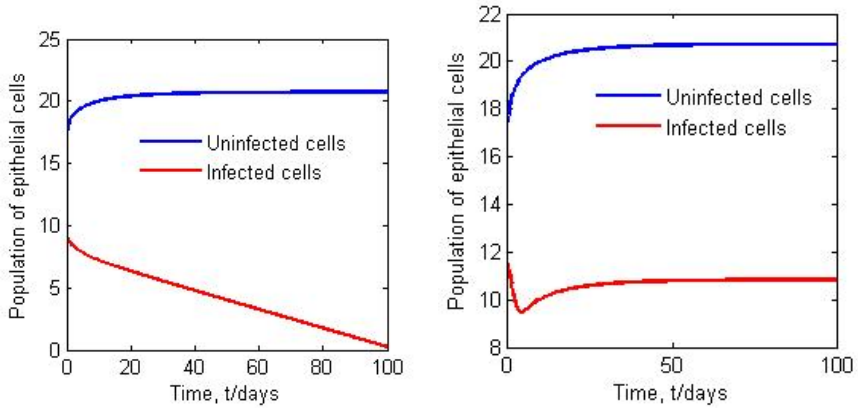

(a) (b)

Figure 3.8: Solution trajectories for Epithelial population with variables: (a)$a = 0.02, b = 0.6, S(0) = 4.0 \times 10^7, I_v(0) = 10^4, V(0) = 10^7, V(0) = 10^6$ ($R_I = 0.86967$) (b) $a = 0, b = 0.6, I_v(0) = 10^5, V(0) = 10^4 (R_I = 1.739 \times 10^7)$, (c)$b = 0, a = 0.01$ $R_I = 1.7393$ with variables $I_v(0) = 10^5, V(0) = 10^4$. The rest of the parameters are as in Table 3.1 and Table 3.2.

On the other hand if influenza A virus is assumed to be a resident strain implying that an individual initially has influenza A virus infection, we study the

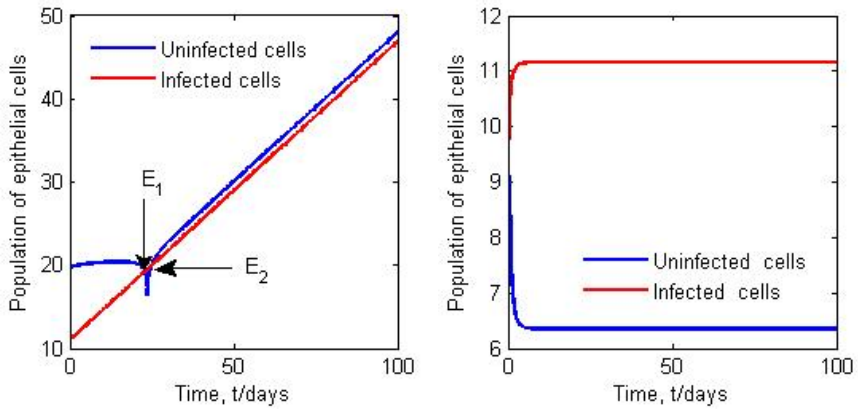

(a) (b)

Figure 3.9: Solution trajectories for Epithelial population with variables: (c)$a = 0.02, b = 0, S(0) = 4.0 \times 10^7, I_v(0) = 10^4, V(0) = 10^7, V(0) = 10^6$ $(R_I = 0.86967)$ (d) $a = 0, b = 0, \Lambda = 6.25 \times 10^4, S(0) = 4.0 \times 10^3, I_v(0) = 10^4, V(0) = 10^5 (R_I = 17393)$, The rest of the parameters are as in Table 3.1 and Table 3.2.

inhibition effects on the dynamics of influenza A virus. If $a = 0$ and $b = 0.6 > 0$, this implies that, a stable state is attained and the infectious proportion is high enough for the infection to persist in the cell population. Secondly, if $b = 0$ and $a > 0$ the infected cells and uninfected cells are globally stable, implying that influenza A virus keeps circulating in the population which can cause disease to the host. Thirdly, if $b = 0$ and $a > 0$ and $b = 0$ and $a = 0$ leads to a high endemicity. Therefore, control measures should be instituted to keep the pathogen fitness of influenza A virus below unity.

In this Chapter, a class of ODE within–host models with Beddington–DeAngelis nonlinear incidence rate and the standard bilinear incidence rate is investigated. The steady states for the infection–free steady state and endemic steady state exist and are unique. The pathogen fitness was computed by next generation operator method Van Den Driessche & Watmough (2002) and used in establishing the local stability of the infection–free steady state. The global stability of

the infection–free steady state of the model may not be globally asymptotically stable whenever the pathogen fitness R_{IP} is less than unity. A graph–theoretic approach was used to prove the global stability of the endemic steady state. The stability analysis of the given model (3.1) is carried out, when $R_{IP} < 1$, the infection–steady state E_o is locally asymptotically stable and unstable whenever R_{IP}.

Numerical simulations of the model (3.1) show that the two infections co–exist (with pneumococcus leading) when the pathogen fitness for each infection exceeds unity. The pneumococcus–endemic steady state, E^*, which exists when $R_{IP} = R_P > 1$, is LAS if $R_I < 1$, and unstable if $R_I > 1$. In other words, influenza A virus accelerates the persistence of pneumococcus growth when $R_I > 1$ because alveolar macrophage will be depleted and can't offer protection to the epithelial cell population. Co–infection typically occurs within a few days of influenza A virus infection, at times of high viral shedding, individuals develop co–infection between [1.3–11.1] days of influenza A virus infection. This result is consistent with (Chertow & Memoli, 2013).

The results further, show that pneumococcus and influenza A virus co–exist, as the steady state is bypassed, the pneumococcus replaces influenza A virus in it's region of existence. Due to co–existence of pneumococcus and influenza A virus in the cell population, each pathogen has an impact on the other. Maintaining pneumococcus or influenza A virus in the population increases the respective population and doesn't impact the same population, however a tipping point is reached when the topology of the dynamical system changes, resulting into a bifurcation.

Whenever two pathogens invade the respiratory cell population, assuming one pathogen to be resident strain (in this case influenza A virus) and the second to

be mutant (pneumococcal), one of the strains over powers the other and persists in the population leading to severe infection. For the two coexisting pathogens (conjecture 4.2) in Hussaini et al. (2016), one infection dominates the other whenever their pathogen fitness exceeds unity ($R_P > R_I = R_{IP} > 1$). This implies that the infection persists in the host cell that may result into bacteria pneumonia.

To this end, the next Chapter proposes a between–host pneumococcal pneumonia model, the fact that it's has been shown to be caused by the most virulent pathogen that overpowered IAV during the co–infection. The model considers two time delays that influence the stability of the endemic steady state during pneumococcal pneumonia spread.

CHAPTER 4

BETWEEN–HOST PNEUMOCOCCAL PNEUMONIA MODEL WITH TIME DELAYS

4.1 Introduction

Uncertainties in the burden of pneumococcal disease are largely determined by the proportion of pneumonia deaths attributable to pneumococcus (Wahl et al., 2018). Models of infectious diseases with time delays have attracted attention of scientists since time delays can alter the qualitative behavior of the system. A Hopf–bifurcation may occur, if a time delay is introduced into a dynamical system that could change the stability state of the equilibrium (stable equilibrium becomes unstable) and could cause fluctuations in the system (Bianca et al., 2013).

4.2 Model formulation

A model for the dynamics of the bacterial pneumonia (pneumococcal) in a human population with the total population size at time t denoted by $N(t)$ is formulated. The population is sub–divided into five mutually exclusive epidemiological classes: susceptible, vaccinated, exposed, carrier and infected denoted by $S(t)$, $V(t)$, $E(t)$, $C(t)$ and $I(t)$; respectively. The mathematical formulation adopts a mass–action incidence because it is important in deciding the dynamics of epidemic models where the contact rate depends on the size of the total human population. The force of infection for the vaccinated class is $\vartheta\beta I(t)$, where $0 \leq \vartheta < 1$ is the

proportion of the sero–type not covered by vaccine (Tilahun et al., 2017).

The increase in the number of susceptible individuals comes from a constant recruitment b through birth or migration and recovery of individuals. Several vaccines wane with time, and so vaccinated individuals return to the susceptible compartment, at a waning rate ζ. The susceptible individuals become infected through a force of infection $\beta I(t)$ and move to the latent class $E(t)$.

The latent class, $E(t)$ accounts for a time delay $\tau_1 > 0$ of the exposed individuals ie. the period between the time of an infection onset and the time of developing pneumococcal clinical symptoms. Exposed individuals transfer to the infectious class at a rate γ. Individuals in the carrier class $C(t)$ become symptomatic and join the infected class at a rate ρ.

The infectious class $I(t)$ accounts for a time delay $\tau_2 > 0$: the time taken by infected individuals to seek medical care. Infected individuals that delay to seek medical care die of pneumococcal pneumonia at a rate δ. Infectious individuals upon recovery transfer to the susceptible class at a rate ϕ. All classes exhibit a per capita natural mortality rate μ. The description of model variables and parameters is summarized in the nomenclature.

4.3 Model assumptions

The following assumptions are given to guide in the development of model equations:

(i) That every person in the population is susceptible to pneumococcal pneumonia disease

(ii) A continuous vaccination strategy is received by the recruited susceptible individuals at a rate ν, and that vaccination doesn't affect the infectious.

(iii) Vaccination is not 100% efficient, which means there is a chance of being infectious or carrier in small proportions

(iv) IAV is a resident (primary) pathogen and pneumococcus is secondary, and the interaction promotes severe pneumococcal pneumonia

(v) Individuals that survive natural mortality μ through latent period $[t-\tau_1, t]$ and infectious period $[t-\tau_2, t]$ have probability (survivorship function) $e^{-\mu\tau_1}$ and $e^{-\mu\tau_2}$ respectively.

The compartmental diagram of the model is shown in Figure 4.1.

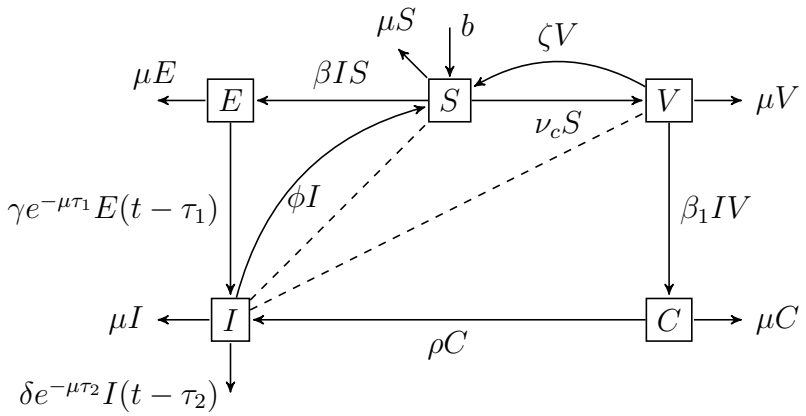

Figure 4.1: A schematic diagram showing the dynamics of pneumococcal pneumonia. The dotted lines represent contacts made by individuals in the respective classes and the solid lines show transfer from one class to another.

Based on the description of model variables, parameters, assumptions and from Figure 4.1, the dynamics of the model are governed by the balance law of compartments stated as: rate of change=inflow transition rate−outflow transition rate that is: $\dot{X}$ = sum of inflow transition rates− sum of outflow transition rates,

thus the system of equations given by

$$\begin{aligned}
\dot{S}(t) &= b + \zeta V(t) + \phi I(t) - (\nu + \mu + \beta I(t))S(t), \\
\dot{V}(t) &= \nu S(t) - (\mu + \zeta)V(t) - \beta_1 I(t)V(t), \\
\dot{E}(t) &= \beta I(t)S(t) - \gamma e^{-\mu\tau_1} E(t-\tau_1) - \mu E(t), \\
\dot{C}(t) &= \beta_1 I(t)V(t) - (\rho + \mu)C(t), \\
\dot{I}(t) &= \rho C(t) + \gamma e^{-\mu\tau_1} E(t-\tau_1) - \delta e^{-\mu\tau_2} I(t-\tau_2) - (\mu + \phi)I(t).
\end{aligned} \tag{4.1}$$

where, $\beta_1 = \vartheta\beta$.

To study the effect of time delays on the dynamics of pneumocccal pneumonia, the previous work by (Tilahun et al., 2017) helped in attributing knowledge to understand the current model. A new compartment of the latency is included in the model. Two time delays; the first delay is introduced in the latency subpopulation because there is delayed time from the time an individual is infected and when one becomes infectious. A second time delay of seeking medical care is included in the infectious subpopulation because not seeking medical attention leaves individuals' behaviors unchanged not to respond to existing control measures and more individuals become infected.

4.3.1 Positivity of solutions

System (4.1) is a representation of the dynamics of the human populations, thus it is required that all solutions are non–negative. We use the approach in Bodnar (2000) and Yang et al. (1996), we let C be a Banach space of continuous real valued functions $\psi : [-\tau, 0] \to \mathbb{R}^5_+$ equipped with the supremum norm, $||\psi||_C = \sup_{t\in[-\tau,0]}\{|\psi_1|, |\psi_2|, |\psi_3|, |\psi_4|, |\psi_5|\}$. The initial conditions of system (4.1)

are represented by

$$S(t) = \psi_1(t), V(t) = \psi_2(t), E(t) = \psi_3(t), C(t) = \psi_4(t), I(t) = \psi_5(t), \\ -\tau \leq t \leq 0, \qquad (4.2)$$

where $\tau = \max\{\tau_1, \tau_2\}$ and $\psi = (\psi_1, \psi_2, \psi_3, \psi_4, \psi_5)^T \in C$, such that $\psi_i(t) = \psi_i(0) \geq 0$ $(i = 1, 2, 3, 4, 5)$. The following Lemma establishes the positivity of the solutions of system (4.1).

Lemma 4.2.1. *Any solution of trajectories* (4.1) *with* $\psi_i(t) > 0$*;* $t \in [-\tau, 0]$ *remains positive whenever it exists.*

Proof. Suppose $S(t)$ was to lose positivity on some local existence interval $[0, T)$ for some constant $T > 0$, there would be a time at $t_1 = \sup\{t > 0 : S(t) > 0\}$ such that $S(t_1) = 0$.

From the first equation of system (4.1), it follows that

$$b + \zeta V(t) + \phi I(t) - (\nu + \mu)S(t) - \beta I(t)S(t) > 0.$$

This implies that $S(t) < 0$ for $t \in (t_1 - \varepsilon, t_1)$, where ε is an arbitrary small positive constant. This leads to a contradiction, it thus follows that $S(t)$ is always positive. Hence from the fundamental theory of differential equations, it is shown that there exists a unique solution for $S(t)$ of system (4.1) with initial data in $\mathbb{R}^5_+$ as follows

$$\frac{d}{dt}(S(t)e^{\int_0^t(\nu+\mu+\beta I(t))d\xi}) \;=\; e^{\int_0^t(\nu+\mu+\beta I(t))d\xi}(b + \zeta V(t) + \phi I(t)),$$

$$S(t) = \int_0^t \left((b + \zeta V(\sigma) + \phi I(\sigma))\, e^{-(\nu+\mu)t - \int_\sigma^t \beta I(\xi)d\xi} d\sigma \right. \\ \left. + \psi_1(0) e^{-(\nu+\mu)t - \int_0^t \beta I(\xi)d\xi}, \right.$$

Therefore,

$$\begin{aligned} S(t_1) &= \psi_1(0)e^{-(\nu+\mu)t_1-\int_0^{t_1}\beta I(\xi)d\xi} \\ &+ \int_0^{t_1}\left((b+\zeta V(\sigma)+\phi I(\sigma))\,e^{-(\nu+\mu)t_1-\int_\sigma^{t_1}\beta I(\xi)d\xi}d\sigma > 0. \right. \end{aligned} \tag{4.3}$$

Since $S(t_1) > 0$, then $S(t) > 0, t \geq 0$. This completes the proof.

Similarly, using the same technique we have

$$V(t_2) = \psi_2(0)e^{-(\mu+\zeta)t_2-\int_0^{t_2}\beta I(\xi)d\xi} + \int_0^{t_2} e^{\int_\sigma^{t_2}(\mu+\zeta+\beta_1 I(\xi))d\xi}\nu S(\sigma)d\sigma > 0. \tag{4.4}$$

$$E(t_3) = e^{-\mu t_3}\psi_3(0) + e^{-\mu t_3}\left(\int_0^{t_3} e^{\mu\xi}\left(\beta I(\xi)S(\xi) - \gamma e^{-\mu\tau_1}E(\xi-\tau_1)\right)d\xi\right) > 0 \tag{4.5}$$

$$C(t_4) = e^{-(\rho+\mu)t_4}\left(\psi_4(0) + \int_0^{t_4}\left(\beta_1 I(\xi)V(\xi)\right)e^{(\rho+\mu)\xi}d\xi\right) > 0. \tag{4.6}$$

and

$$\begin{aligned} I(t_5) &= \psi_5(0)e^{-(\mu+\phi)t_5} \\ &+ e^{-(\mu+\phi)t_5}\left(\int_0^{t_5}\left(\rho C(\sigma) + \gamma e^{-\mu\tau_1}E(\sigma-\tau_1) - \delta e^{-\mu\tau_2}I(\sigma-\tau_2)\right)e^{(\mu+\phi)\sigma}\right)d\sigma \end{aligned} \tag{4.7}$$

Therefore, from the above integral forms of equations (4.3) to (5.20) all solution trajectories are positive for all time $t > 0$ on $[0, +\infty]$.

4.3.2 Boundedness

For boundedness of system (4.1) with initial condition (4.2), we consider the following Lemma

Lemma 4.2.2. *The closed set*

$$\Omega_d = \{S(t), V(t), E(t), C(t), I(t)\} \in \mathbb{R}^5_+ : 0 \leq S(t), V(t), E(t), C(t), I(t); \\ S(t) + V(t) + E(t) + C(t) + I(t) \leq \frac{b}{\mu}$$

is positively invariant and absorbing with respect to the set of DDE's (4.1).

Proof. Summing all equations in system (4.1), yields

$$\frac{dN}{dt} = b - \mu N(t) - \delta e^{-\mu\tau_2} I(t).$$

Therefore, $\frac{dN}{dt} \leq b - \mu N(t)$ which implies that $\frac{dN}{dt} \leq 0$ if $N(t) \geq \frac{b}{\mu}$. Using the standard comparison test in Nagy (2011), we get $N(t) \leq N(0)e^{-\mu t} + \frac{b}{\mu}(1 - e^{-\mu t})$. Particularly, $N(t) \leq \frac{b}{\mu}$ if $N(0) \leq \frac{b}{\mu}$ for all time $t > 0$, hence Ω_d is positively invariant. Further, if $N(t) \geq \frac{b}{\mu}$, then either the solution enter at finite time or $N(t)$ is close to $\frac{\pi}{\mu}$ and the infected variables E, C and I tend to zero. Therefore, Ω_d is attracting implying that all solutions in $\mathbb{R}^5_+$ finally enter Ω_d Consequently, in Ω_d, system (4.1) is mathematically and epidemiologically well–posed.

4.3.3 The control reproduction ratio

The basic reproduction ratio identifies the number of secondary infections from the infected source and plays an important role in understanding the development of epidemics with a vaccination program in place. The control reproduction ratio R_0 is computed using an approach in Van Den Driessche & Watmough (2008) and

is given by $R_0 = R_0^u + R_0^v$,

where $R_0^u = \frac{\beta\gamma e^{-\mu\tau_1} S^0}{(\mu+\gamma e^{-\mu\tau_1})(\phi+\mu+\delta e^{-\mu\tau_2})}$, $R_0^v = \frac{\beta\rho\vartheta V^0}{(\rho+\mu)(\phi+\mu+\delta e^{-\mu\tau_2})}$. The quantity R_0^u measures the expected number of secondary cases generated by an index case for the susceptible individuals and R_0^v represents new cases arising from the vaccination program.

The control reproduction ratios with no delays ($\tau_1 = 0, \tau_2 = 0$) are given by $R_0^u = \frac{\beta\gamma S^0}{(\mu+\gamma)(\phi+\mu+\delta)}$ and $R_0^v = \frac{\beta\rho\vartheta V^0}{(\rho+\mu)(\phi+\mu+\delta)}$.

4.4 Stability of equilibria

Let $(S^*, V^*, E^*, C^*, I^*)$ be the corresponding partial populations at the eventual equilibrium point. Given that the values of the partial populations at the equilibrium are stable, the delay–dependency vanishes so that $\lim_{t\to\infty} I(t-\tau_2) = \lim_{t\to\infty} I(t) = I^*$ and $\lim_{t\to\infty} E(t-\tau_1) = \lim_{t\to\infty} E(t) = E^*$, such that at equilibrium, we have

$$\begin{aligned}
b + \zeta V^* + \phi I^* - (\nu + \mu + \beta I^*) S^* &= 0, \\
\nu S^* - (\mu + \zeta) V^* - \beta_1 I^* V^* &= 0, \\
\beta I^* S^* - (\gamma e^{-\mu\tau_1} + \mu) E^* &= 0, \\
\beta_1 I^* V^* - (\rho + \mu) C^* &= 0, \\
\rho C^* + \gamma e^{-\mu\tau_1} E^* - (\mu + \delta e^{-\mu\tau_2} + \phi) I^* &= 0, \\
\dot{S}^* + \dot{V}^* + \dot{E}^* + \dot{C}^* + \dot{I}^* = b - \mu N^* - \delta e^{-\mu\tau_2} I^* &= 0.
\end{aligned} \tag{4.8}$$

Hence, from system (4.8), we obtain the disease–free equilibrium $P_0 = (S^0, V^0, 0, 0, 0)$, where

$$S^0 = \frac{b(\mu+\zeta)}{(\mu+\zeta)(\nu+\mu)-\zeta\nu},\ V^0 = \frac{b\nu}{(\mu+\zeta)(\nu+\mu)-\zeta\nu}, \tag{4.9}$$

provided $(\mu+\zeta)(\nu+\mu) > \zeta\nu$.

It should be noted that for $\nu > 0$, the disease–free equilibrium is biologically feasible for any epidemiological parameters, whereas in the absence of vaccination strategy, i.e. for $\nu = 0$, E_0 is only feasible for epidemiological parameters in the susceptible class. From system (4.8) the endemic equilibrium $P^* = (S^*, V^*, E^*, C^*, I^*)$ is given as

$$\begin{aligned}
S^* &= \frac{b+\zeta V^*+\phi I^*}{\nu+\mu+\beta I^*},\\
V^* &= \frac{\nu(b+\phi I^*)}{(\nu+\mu+\beta I^*)(\mu+\zeta+\beta_1 I^*)-\nu\zeta},\\
E^* &= \frac{\beta(\zeta\nu+a_1)(bI^*+\phi I^{*2})}{a_1(\gamma e^{-\mu\tau_1}+\mu)(\nu+\mu+\beta I^*)},\\
C^* &= \frac{\nu\beta_1 I^*(b+\phi I^*)}{a_1(\rho+\mu)},\\
I^* &= I^*.
\end{aligned} \tag{4.10}$$

where $a_1 = (\nu+\mu+\beta I^*)(\mu+\zeta+\beta_1 I^*) - \nu\zeta$.

4.4.1 Local stability of the disease–free equilibrium point

Suppose that $P_0 = (S^0, V^0, 0, 0, 0)$ is a disease–free equilibrium point of system (4.1), then the linearization matrix J_{P_0} is given by

$$J_{P_0} = \begin{vmatrix} -(\mu+\nu) & \zeta & 0 & 0 & \phi - \beta S^0 \\ \nu & -(mu+\zeta) & 0 & 0 & -\beta\vartheta V^0 \\ 0 & 0 & -\mu & 0 & \beta S^0 \\ 0 & 0 & 0 & -(\rho+\mu) & \beta\vartheta V^0 \\ 0 & 0 & 0 & \rho & -(\mu+\phi) \end{vmatrix} = 0.$$

Clearly $y_1 = -\mu$ is one of the negative roots (eigenvalues) that guarantee local stability of the disease–free equilibrium P_0. The remaining eigenvalues are obtained from the characteristic polynomial given by

$$g(y) = y^4 + e_3 y^3 + e_2 y^2 + e_1 y + e_0 = 0, \tag{4.11}$$

where $e_3 = 4\mu+\nu+\zeta+\rho+\phi, e_2 = (\mu+\zeta)(2\mu+\rho+\nu)+(\mu+\phi)(2\mu+\nu+\zeta)-\beta\vartheta\rho V^0$,
$e_1 = (\mu+\zeta)(\mu+\rho)(2\mu+\nu+\phi) + (\mu+\nu)(\mu+\phi)(2\mu+\zeta+\rho) - \zeta\nu(2\mu+\rho+\phi) - \beta\rho\vartheta(2\mu+\nu+\zeta)$,
$e_0 = (\mu+\nu)(\mu+\zeta)\Big((\rho+\mu)(\mu+\phi) - \beta\rho\vartheta V^0\Big) + \zeta\nu(\beta\rho\vartheta V^0 - (\rho+\mu)(\mu+\phi)$.

Thus computing the roots of polynomial (4.11) gives
$y_2 = -\mu, y_3 = -(\mu+\zeta+\nu)$, $y_4 = -\frac{1}{2}\Big((2\mu+\rho+\phi) + \sqrt{(\rho-\phi)^2 + 4\beta\rho\vartheta V^0}\Big)$,

$$y_5 = -\tfrac{1}{2}\Big((2\mu+\rho+\phi) - \sqrt{(\rho-\phi)^2+4\beta\rho\vartheta V^0}\Big).$$

Since the rest of the roots are negative, root y_5 is negative provided $(\mu+\phi)(\rho+\mu) > \beta\rho\vartheta V^0$, holds implying that $R_0^v = \dfrac{\beta\rho\vartheta b\nu}{(\mu+\phi)(\rho+\mu)\Big((\mu+\zeta)(\nu+\mu)-\zeta\nu\Big)} < 1.$

Thus we have the result below

Proposition 4.3.1. *The disease–free equilibrium P_0 is locally asymptotically stable if the control reproduction ratio $R_0 < 1$, whenever conditions $(\mu+\zeta)(\mu+\nu) > \zeta\nu$ and $R_0^v < 1$ are satisfied, and unstable otherwise.*

To illustrate the stability of disease–free equilibrium, we use parameter values in Table 4.1 with corresponding population estimates of $S(0) = 10604, V(0) = 103, E(0) = C(0) = I(0) = 0$ and the resulting simulation is given in Figure 4.2. The biological implication of Proposition 4.4.1, means that in the long run the vac-

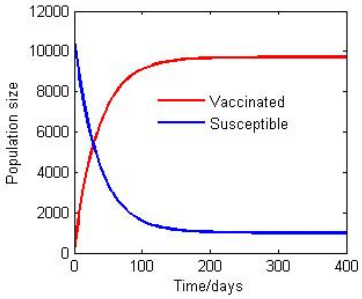

Figure 4.2: Simulation of model (4.1), the disease–free equilibrium, with populations parameters: $\phi = 3.57144 \times 10^{-1}, \beta = 1.0102 \times 10^{-5}, \gamma = 3.3333 \times 10^{-2}$ (with $R_0 = 0.7873, R_0^u = 0.1382, R_0^v = 0.6490$).

cinated and susceptible populations will be stable and pneumococcal pneumonia will be under control.

4.4.2 The transcendental equation

We obtain the expression for the transcendental equation by linearizing system (4.1) around

$P^* = (S^*, V^*, E^*, C^*, I^*)$, to obtain

$$\begin{pmatrix} \dot{S}(t) \\ \dot{V}(t) \\ \dot{E}(t) \\ \dot{C}(t) \\ \dot{I}(t) \end{pmatrix} = \begin{pmatrix} a_1 & a_2 & 0 & 0 & a_3 \\ a_4 & a_5 & 0 & 0 & a_6 \\ a_7 & 0 & a_8 & 0 & a_9 \\ 0 & a_{10} & 0 & a_{11} & a_{12} \\ 0 & 0 & 0 & a_{13} & a_{14} \end{pmatrix} \begin{pmatrix} S(t) \\ V(t) \\ E(t) \\ C(t) \\ I(t) \end{pmatrix} + \begin{pmatrix} 0 & 0 & 0 & 0 & 0 \\ 0 & 0 & 0 & 0 & 0 \\ 0 & 0 & a_{15} & 0 & 0 \\ 0 & 0 & 0 & 0 & 0 \\ 0 & 0 & a_{16} & 0 & a_{17} \end{pmatrix} \begin{pmatrix} 0 \\ 0 \\ E_{\tau_1} \\ 0 \\ I_{\tau_2} \end{pmatrix}, \tag{4.12}$$

$a_1 = -((\mu + \nu) + \beta I^*), a_2 = \zeta, a_3 = \phi - \beta S^*, a_4 = \nu, a_5 = -((\mu + \zeta) + \beta \vartheta I^*), a_6 = -\beta \vartheta V^*,$

$a_7 = \beta I^*, a_8 = -\mu, a_9 = \beta S^*, a_{10} = \beta \vartheta I^*, a_{11} = -(\rho + \mu), a_{12} = \beta \vartheta V^*, a_{13} = \rho,$

$a_{14} = -(\mu + \phi), a_{15} = -\gamma e^{-\mu \tau_1}, a_{16} = \gamma e^{-\mu \tau_1}, a_{17} = -\delta e^{-\mu \tau_2}, E_{\tau_1} = E(t - \tau_1)$ and

$I_{\tau_2} = I(t - \tau_2)$.

The variational matrix of (4.12) is given by

$$J_g = \begin{pmatrix} a_1 & a_2 & 0 & 0 & a_3 \\ a_4 & a_5 & 0 & 0 & a_6 \\ a_7 & 0 & a_8 - \gamma e^{-(\mu+\lambda)\tau_1} & 0 & a_9 \\ 0 & 0 & 0 & a_{11} & a_{12} \\ 0 & 0 & \gamma e^{-(\mu+\lambda)\tau_1} & a_{13} & a_{14} - \delta e^{-(\mu+\lambda)\tau_2} \end{pmatrix} = 0,$$

Then, we obtain the transcendental equation of the linearized system at P^*

$$\begin{aligned} g(\lambda, e^{-\lambda\tau_1}, e^{-\lambda\tau_2}) = \lambda^5 + k_4\lambda^4 + k_3\lambda^3 + k_2\lambda^2 + k_1\lambda + k_0 \\ +(\lambda^4 + l_3\lambda^3 + l_2\lambda^2 + l_1\lambda + l_0)\gamma e^{-(\mu+\lambda)\tau_1} \\ +(\lambda^4 + m_3\lambda^3 + m_2\lambda^2 + m_1\lambda + m_0)\delta e^{-(\mu+\lambda)\tau_2} \\ +(\lambda^3 + n_2\lambda^2 + n_1\lambda + n_0)\gamma\delta e^{-(\mu+\lambda)(\tau_1+\tau_2)} = 0. \end{aligned} \tag{4.13}$$

with coefficients of the transcendental equation (4.13) given in Appendix A3(a).

4.4.3 Delay–free system

Here, to show the local stability of P^*, we consider a situation where there are no delays during the latent period ($\tau_1 = 0$) and in seeking medical care ($\tau_2 = 0$). By

letting $\tau_1 = \tau_2 = 0$, equation (4.13) reduces to

$$g(\lambda) = \lambda^5 + b_4\lambda^4 + b_3\lambda^3 + b_2\lambda^2 + b_1\lambda + b_0 = 0. \tag{4.14}$$

with coefficients of polynomial equation in Appendix A3(b).

Proposition 4.3.2. *The endemic equilibrium P^* is locally asymptotically stable in the absence of delays*

$\tau_1 = \tau_2 = 0$, iff the following Routh–Hurwitz conditions are satisfied

$b_0 > 0, b_4b_3 - b_2 > 0, b_2(b_4b_3 - b_2) - b_4(b_4b_1 - b_0) > 0$ *and* $b_1(b_2(b_4b_3 - b_2) - b_4(b_4b_1 - b_0)) - b_0(b_3(b_4b_3 - b_2) - (b_4b_1 - b_0)) > 0$, with b_4, b_3, b_2, b_1 and b_0 defined in Appendix A3(b).

Using parameter values in Table 4.1 the characteristic equation (4.14) is given as $\lambda^5 + 0.7364\lambda^4 - 148.4\lambda^3 - 4.9408\lambda^2 - 0.3965\lambda - 0.0001806 = 0$.

The resulting eigenvalues are given by: $\lambda_1 = 11.8, \lambda_2 = -0.0005, \lambda_3 = -12.5357$, $\lambda_{4,5} = -0.01641 \pm 0.4885i$.

Since there exist a positive root for model (4.1), there is a stability change from unstable to stable of the endemic equilibrium point $P^* = (S^*, V^*, E^*, C^*, I^*) = (2099, 6, 54, 2, 100)$ that gives rise to a Hopf–bifurcation.

4.5 Existence of Hopf–bifurcation

Under this subsection, we discuss the stability of the endemic equilibrium point of model (4.1). We use the approach in Song & Wei (2004) to prove the conditions for continuation of unstable or stable switches at the endemic equilibrium point. By choosing time delay $\tau = \max = \{\tau_1, \tau_2\}$ as a bifurcation parameter.

4.5.1 Delay only in latent period ($\tau_1 > 0, \tau_2 = 0$)

In such a situation the transcendental equation (4.13) reduces to

$$\begin{aligned} &\lambda^5 + k_4\lambda^4 + k_3\lambda^3 + k_2\lambda^2 + k_1\lambda + k_0 \\ &+(\gamma\lambda^4 + h_3\lambda^3 + h_2\lambda^2 + h_1\lambda + h_0)e^{-(\mu+\lambda)\tau_1} = 0, \end{aligned} \tag{4.15}$$

where $q = e^{-\mu\tau_1}, h_0 = q\gamma(l_0 + n_0\delta), h_1 = q\gamma(l_1 + n_1\delta), h_2 = q\gamma(l_2 + n_2\delta), h_3 = q\gamma(l_3 + \delta)$.

Suppose the endemic equilibrium of system (4.1) is stable in the absence of delay (τ_2) to seek medical care, implying that $Re(\lambda) = \xi(0) < 0$. The bifurcation value of $\tau_{1_0} > 0$ occurs when $\lambda(\tau_{1_0}) = \xi(\tau_{1_0}) + iw(\tau_{1_0})$ is purely imaginary, for $\xi(\tau_{1_0}) = 0$. Hence, defining the eigenvalue $\lambda = wi$, with infection rate oscillation frequency ($w > 0$) and making a substitution in (4.15) and expressing the exponential in terms of trigonometric ratios, we get

$$\begin{aligned} Im &:= a_1 \cos w\tau_1 + a_2 \sin w\tau_1 = R_1, \\ Re &: a_2 \cos w\tau_1 - a_1 \sin w\tau_1 = R_2, \end{aligned} \tag{4.16}$$

where $a_1 = w(h_1 - h_3w^2), a_2 = w(\gamma w^3 - h_2 w) + h_0, R_1 = w(k_3w^2 - (w^4 + k_1))$, $R_2 = k_2w^2 - (k_4w^4 + k_0)$.

By eliminating τ_1 from equation (4.15), squaring and adding these two equations and putting $w^2 = z$, we obtain the Hopf frequency below

$$H(z) = z^5 + B_4z^4 + B_3z^3 + B_2z^2 + B_1z + B_0 = 0, \tag{4.17}$$

where $B_4 = k_4 - 2(k_3 + \gamma), B_3 = k_3^2 + 2[(k_1 + 2h_2\gamma) - (k_2k_4 + h_3^2)]$,
$B_2 = k_2 + 2[(2h_1h_3 + k_4k_0) - (k_1k_3 + 2h_0\gamma + h_2^2)], B_1 = k_1^2 + 2[2h_0h_2 - (h_1^2 + k_2k_0)]$,
$B_0 = 2h_0^2 + k_0^2$.

The two Propositions about stability and critical delay in Kirui et al. (2015) are written as lemmas

Lemma 4.4.1. *If the $B_i(i = 0, 1, 2, 3, 4)$ guarantee the Routh–Hurwitz criteria, then all eigenvalues of* (4.17) *have negative real parts for all delay $\tau_1 \geq 0$. Thus the endemic equilibrium P^* if it exists is locally asymptotically stable whenever $\tau_1 \geq 0$, provided the endemic steady state is stable in the absence of the latent period delay, specifically τ_1 won't affect the stability of the dynamical system, for equation* (4.17) *without positive real roots.*

Lemma 4.4.2. *If $B_i(i = 0, 1, 2, 3, 4)$ do not satisfy Routh–Hurwitz criteria, thus $B_0 < 0$ or $B_0 > 0$ implies that* (4.25) *has at least one positive root and suppose that, it has a pair of imaginary roots say $\pm iw_{1_0}$ for such a value of w_{1_0}.*

Consequently to obtain the main results in this work, we assume equation (4.17) has at least one positive root w_{1_0}. By squaring and summing together the imaginary and real parts in equation (4.16), we get

$$\begin{aligned} \tau_1 &= \frac{1}{w}\arccos\left(\frac{w^2(h_1 - h_3w^2)(k_3w^2 - (w^4 + k_1))}{w(h_1 - h_3w^2)^2 + (w(\gamma w^3 - h_2w) + h_0)^2}\right) \\ &+ \frac{1}{w}\arccos\left(\frac{(w(\gamma w^3 - h_2w) + h_0)(k_2w^2 - (k_4w^4 + k_0))}{w(h_1 - h_3w^2)^2 + (w(\gamma w^3 - h_2w) + h_0)^2}\right) \\ &+ \frac{2n\pi}{w}. \end{aligned} \tag{4.18}$$

By denoting

$$\begin{aligned}
\tau_{1_n}^{(m)} &= \frac{1}{w_{1_n}}\arccos\left(\frac{w_{1_n}^2(h_1-h_3w_{1_n}^2)(k_3w_{1_n}^2-(w_{1_n}^4+k_1))}{w_{1_n}(h_1-h_3w_{1_n}^2)^2+(w_{1_n}(\gamma w_{1_n}^3-h_2w_{1_n})+h_0)^2}\right)\\
&+ \frac{1}{w_{1_n}}\arccos\left(\frac{(w_{1_n}(\gamma w_{1_n}^3-h_2w_{1_n})+h_0)(k_2w_{1_n}^2-(k_4w_{1_n}^4+k_0))}{w_{1_n}(h_1-h_3w_{1_n}^2)^2+(w_{1_n}(\gamma w_{1_n}^3-h_2w_{1_n})+h_0)^2}\right)+\frac{2n\pi}{w_{1_n}},\\
m &= 1,2,\ldots,\tilde{m}, n\in\mathbb{N}
\end{aligned}$$

Thus we define

$$\tau_{1_0}=\tau_{n_0}^{(0)}=min_{1\leq n\leq 5}\{\tau_{1_n}^{(0)}\}, w_{1_0}=w_{n_0}. \tag{4.19}$$

and state the result as follows

Lemma 4.4.3. *If τ_{1_0} and w_{1_0} are defined as* (4.19) *and $H'(z=w^2)>0$. The endemic equilibrium point P^* is linearly asymptotically stable for $\tau_1<\tau_{1_0}$, unstable for $\tau_1>\tau_{1_0}$ and undergoes a Hopf–bifurcation at $\tau_1=\tau_{1_0}$.*

To ensure the occurrence of the Hopf–bifurcation, it is desirable to verify the transversality condition. Without loss of generality, the delay τ_1 is chosen as the bifurcation parameter. The essential condition for existence of the Hopf–bifurcation is that the threshold eigenvalues traverse the imaginary axis with non–zero velocity.

Proposition 4.4.1. *If $\Phi_2(w_{1_0})>0$, where $\Phi_2(w_{1_0})$ satisfies* (4.22)*, system*(4.1) *undergoes a Hopf–bifurcation at the endemic equilibrium as τ_1 increases through τ_{1_0}.*

Proof. (Transversality condition for Hopf–bifurcation)

Differentiating equation (4.15) with respect to τ_1 we obtain

$$\frac{d\tau_1}{d\lambda}=\frac{(5\lambda^4+4k_4\lambda^3+3k_3\lambda^2+k_1)e^{\lambda\tau_1}+(4\gamma\lambda^3+3h_3\lambda^2+2h_2\lambda+h_1)}{\gamma\lambda^5+h_3\lambda^4+h_2\lambda^3+h_1\lambda^2+h_0\lambda}-\frac{\tau_1}{\lambda} \tag{4.20}$$

$$\begin{aligned}
\operatorname{sign}\Big[\frac{(\mathrm{dRe}\lambda)}{\mathrm{d}\tau_1}\Big]_{\tau_1=\tau_{1_0}} &= \operatorname{sign}\Big[\mathrm{Re}(\frac{\mathrm{d}\lambda}{\mathrm{d}\tau_1})^{-1}\Big]_{\lambda=\mathrm{iw}_{1_0}} \\
&= \operatorname{sign}\Big[\mathrm{ReN}_1\Big] + \operatorname{sign}\Big[\mathrm{ReN}_2\Big] \\
&= \operatorname{sign}\Big[\frac{\mathrm{c}_3(\mathrm{c}_1\cos\mathrm{w}\tau_1 + \mathrm{c}_2\sin\mathrm{w}\tau_1) + \mathrm{c}_4(\mathrm{c}_1\sin\mathrm{w}\tau_1 + \mathrm{c}_2\cos\mathrm{w}\tau_1)}{\mathrm{c}_3^2+\mathrm{c}_4^2}\Big] \\
&+ \operatorname{sign}\Big[\frac{(\mathrm{h}_1 - 3\mathrm{h}_3\mathrm{w}^2) + \mathrm{c}_4\mathrm{w}(2\mathrm{h}_2 - 4\gamma\mathrm{w}^3)}{\mathrm{c}_3^2+\mathrm{c}_4^2}\Big]. \qquad (4.21)
\end{aligned}$$

with

$$\begin{aligned}
N_1 &= \frac{c_3(c_1\cos w\tau_{1_0} + c_2\sin w\tau_{1_0}) + c_4(c_1\sin w\tau_{1_0} + c_2\cos w\tau_{1_0})}{c_3^2+c_4^2} \\
&+ \frac{i(c_3(c_2\cos w\tau_1 + c_{1_0}\sin w\tau_{1_0}) - c_4(c_2 sinw\tau_{1_0} + c_1\cos w\tau_{1_0})}{c_3^2+c_4^2}, \\
N_2 &= \frac{(h_1 - 3h_3w^2) + c_4w(2h_2 - 4\gamma w^3) + i(c_3w(2h_2 - 4\gamma w^2) + (h_1 - 3h_3w^2))}{c_3^2+c_4^2}.
\end{aligned}$$

Any linear combination of a sine and cosine of equal periods is equal to a single sine with the same period however, with an infection rate oscillation phase shift Ψ (Sutton et al., 2007).

Therefore, we get

$$\begin{aligned}
\operatorname{sign}\Big[\frac{(\mathrm{dRe}\lambda)}{\mathrm{d}\tau_1}\Big]_{\tau_1=\tau_{1_0}} &= \operatorname{sign}\Big[\mathrm{Re}(\frac{\mathrm{d}\lambda}{\mathrm{d}\tau_1})^{-1}\Big]_{\lambda=\mathrm{iw}_{1_0}} \\
&= \frac{D_0\sin(w\tau_1 + \Psi_2) + (h_1 - 3h_3w^2) + c_4w(2h_2 - 4\gamma w^3)}{c_3^2+c_4^2},
\end{aligned}$$

where $c_1 = 5w^4 - 3k_3w^2 + k_1,\ c_2 = 4k_4w^3, c_3 = w(\gamma w^4 - h_2w^2 + h_0), c_4 = w^2(h_3w^2 - h_1)$,

$D_0 = \sqrt{(c_3c_1 + c_2c_1)^2 + (c_3c_2 + c_4c_1)^2}, D_0^1 = c_4w_{1_0}(2h_2 - 4\gamma w_{1_0}^3), \Psi_2 = \arctan\frac{c_3c_1 + c_4c_2}{c_3c_2 + c_4c_1}$,

Let

$$\begin{aligned}
\Phi_2(w_{1_0}) &= D_0\sin(w_{1_0}\tau_{1_0} + \Psi) + (h_1 - 3h_3w_{1_0}^2) \\
&+ c_4w_{1_0}(2h_2 - 4\gamma w_{1_0}^3) > 0 \qquad (4.22)
\end{aligned}$$

, if conditions $(w_{1_0}\tau_{1_0} + \Psi_2) \in (\pi, \frac{\pi}{2}), h_1 > 3h_3w_{1_0}^2$ and $h_2 > 2\gamma w_{1_0}^2$ hold. Clearly

$$\begin{aligned} \operatorname{sign}\Big[\frac{(\mathrm{dRe}\lambda)}{\mathrm{d}\tau_1}\Big]_{\tau_1=\tau_{1_0}} &= \operatorname{sign}\Big[\mathrm{Re}(\frac{\mathrm{d}\lambda}{\mathrm{d}\tau_1})^{-1}\Big]_{\lambda=\mathrm{iw}_{1_0}} \\ &= \frac{D_0\sin(w_{10}\tau_{1_0} + \Psi_2) + (h_1 - 3h_3w_{1_0}^2) + D_0^1}{c_3^2 + c_4^2}, \end{aligned}$$

has the same sign as $\Phi_2(w_{1_0})$. This completes the proof.

Therefore, Proposition 4.5.1 implies that given $m > 0$, the eigenvalue $\lambda_m(\tau_1)$ of the characteristic equation (4.15) close to τ_{1_m} crosses the imaginary axis from the left to the right as τ_1 continuously changes from a value less than τ_{1_m} to one greater than τ_{1_m}.

4.5.2 Delay only in seeking medical care by the infectious $(\tau_1 = 0, \tau_2 > 0)$

To understand the influence of time delay in seeking medical care, we set $\tau_1 = 0$ in equation (4.13) yielding

$$\begin{aligned} g(\lambda, e^{-\lambda\tau_2}) &= \lambda^5 + p_4\lambda^4 + p_3\lambda^3 + p_2\lambda^2 + p_1\lambda + p_0 \\ &+(q_4\lambda^4 + q_3\lambda^3 + q_2\lambda^2 + q_1\lambda + q_0)p\gamma\delta e^{-\lambda\tau_2} = 0, \end{aligned} \tag{4.23}$$

where $p = e^{-\mu\tau_2}, p_4 = k_4+\gamma, p_3 = k_3+l_3\gamma, p_2 = k_2+\gamma, p_1 = k_1+l_1\gamma, p_0 = k_0+l_0\gamma$
$q_4 = \delta p, q_3 = (m_3+\gamma+\delta)p, q_2 = (m_2\delta+n_2\gamma\delta), q_1 = (m_1+n_1\gamma\delta)p, q_0 = (m_0+n_0\gamma\delta)p$

Proposition 4.4.2. *The endemic equilibrium point P^* is locally asymptotically stable (LAS) for $\tau_2 < \tau_{2_0}$ where τ_{2_0} is the minimum positive value of*
$\bar{\tau}_{2_0} = \frac{1}{w_{2_0}} \arccos\left(\frac{(p_2w_{2_0}^2 - p_4w_{2_0}^4 - p_0)(q_4w_{2_0}^4 - q_2w_{2_0}^2 + q_0) + (q_3w_{2_0}^3 - q_1w_{2_0})(p_3w_{2_0}^3 - w_{2_0}^5 - p_1w_{2_0})}{p\gamma\delta\Big((q_4w_{2_0}^4 - q_2w_{2_0}^2 + q_0)^2 - (q_1w_{2_0} - q_3w_{2_0}^3)^2\Big)}\right).$

Proof. Let $\lambda = iw, w > 0$ be a root of equation (4.23) to obtain

$P(\lambda, \tau_2) = w^5 i + p_4 w^4 - p_3 w^3 i - p_2 w^2 + p_1 w i + p_0 + (q_4 w^4 - q_3 w^3 i - q_2 w^2 + q_1 w i + q_0) p\gamma\delta e^{-iw\tau_2}$.

Using Euler expansion, separating real and imaginary parts, we obtain

$$\begin{aligned} p\gamma\delta((q_4 w^4 - q_2 w^2 + q_0)\cos w\tau_2 + (q_1 w - q_3 w^3)\sin w\tau_2) &= p_2 w^2 - p_4 w^4 - p_0, \\ p\gamma\delta((q_1 w - q_3 w^3)\cos w\tau_2 + (q_4 w^4 - q_2 w^2 + q_0)\sin w\tau_2) &= p_3 w^3 - w^5 \\ &- p_1 w. \end{aligned} \tag{4.24}$$

Eliminating τ_2 from equation (4.25), by squaring and adding these two equations and put $w^2 = z$, we obtain the Hopf frequency below

$$z^5 + A_4 z^4 + A_3 z^3 + A_2 z^2 + A_1 z + A_0 = 0, \tag{4.25}$$

with coefficients in (4.25) in Appendix A3(c).

Let's denote $g(z) = z^5 + A_4 z^4 + A_3 z^3 + A_2 z^2 + A_1 z + A_0$. Since $\lim_{z\to+\infty} g(z) = +\infty$ and $A_0 < 0$, then equation (4.25) has at least one positive root. Assuming equation (4.25) has $\tilde{n}$ positive roots, given by $\tilde{n}(1 \leq \tilde{n} \leq 5)$, denote by $z_1 < z_2 < \ldots z_{\tilde{n}})$, respectively. Then, equation (4.25) has $\tilde{n}$ positive roots if

$$w_1 = \sqrt{z_1}, w_2 = \sqrt{z_2}, \ldots, w_{\tilde{n}} = \sqrt{z_{\tilde{n}}}.$$

From (4.25), the corresponding $\tau_{2_n} > 0$, for which the characteristic equation (4.13) has a pair of purely imaginary roots eliminating $\sin w\tau_2$ from the first and second equations (4.25) and making $\cos(w\tau_2)$ the subject we get

$$\cos(w\tau_2) = \frac{(p_2 w^2 - p_4 w^4 - p_0)(q_4 w^4 - q_2 w^2 + q_0) + (q_3 w^3 - q_1 w)(p_3 w^3 - w^5 - p_1 w)}{(q_4 w^4 - q_2 w^2 + q_0)^2 + (q_3 w^3 - q_1 w)(q_1 w - q_3 w^3) p\gamma\delta}.$$

Thus, denoting

$$\begin{aligned}\tau_{2_n}^{(k)} &= \frac{1}{w_n}\arccos\left(\frac{(p_2w_n^2-p_4w_n^4-p_0)(q_4w_n^4-q_2w_n^2+q_0)}{(q_4w_n^4-q_2w_n^2+q_0)^2+(q_3w_n^3-q_1w_n)(q_1w_n-q_3w_n^3)p\gamma\delta}\right)\\ &+ \frac{1}{w_n}\arccos\left(\frac{(q_3w_n^3-q_1w_n)(p_3w_n^3-w_n^5-p_1w_n)}{(q_4w_n^4-q_2w_n^2+q_0)^2+(q_3w_n^3-q_1w_n)(q_1w_n-q_3w_n^3)p\gamma\delta}\right)\\ &+ \frac{2\pi(k-1)}{w_n}, \end{aligned} \tag{4.26}$$

where

$n = 1, 2, \ldots \tilde{n}, k = 1, 2, \ldots,$ then $\pm iw_n$ are a pair of purely imaginary roots of the equation (4.13). This allows us to define the Hopf–bifurcation threshold time delay value as

$$\begin{aligned}\tau_{2_0} &= \frac{1}{w_{2_0}}\arccos\left(\frac{(p_2w_{2_0}^2-p_4w_{2_0}^4-p_0)(q_4w_{2_0}^4-q_2w_{2_0}^2+q_0)}{p\gamma\delta\Big((q_4w_{2_0}^4-q_2w_{2_0}^2+q_0)^2-(q_1w_{2_0}-q_3w_{2_0}^3)^2\Big)}\right)\\ &+ \frac{1}{w_{2_0}}\arccos\left(\frac{(q_3w_{2_0}^3-q_1w_{2_0})(p_3w_{2_0}^3-w_{2_0}^5-p_1w_{2_0})}{p\gamma\delta\Big((q_4w_{2_0}^4-q_2w_{2_0}^2+q_0)^2-(q_1w_{2_0}-q_3w_{2_0}^3)^2\Big)}\right) \end{aligned} \tag{4.27}$$

This completes the proof.

Proposition 4.4.3 *If conditions*

$5w_{2_0}^4(q_1+2q_2w_{2_0})+(3p_3w_{2_0}^2+p_1)(3q_3w_{2_0}^2+4q_3w_{2_0}^3) > 5w_{2_0}^4(3q_3w_{2_0}^2+4q_4w_{2_0}^3)+(q_1+2q_2w_{2_0})(3p_3w_{2_0}^2+p_1), \frac{q_3w_{2_0}^2}{q_1} > 1, \frac{w_{2_0}^4q_4+q_0}{q_2w_{2_0}^2} > 1$ *hold, such that* $\Phi_1(w_{2_0}) > 0$, *then system* (4.1) *undergoes a Hopf–bifurcation at the endemic equilibrium point as* τ_2 *increases through* τ_{2_0}, *where expressions of* $\Phi_1(w_{2_0})$ *satisfies equation* (4.30) .

Proof. In order to establish whether the endemic equilibrium point P^* actually under goes a Hopf–bifurcation at $\tau_2 = \tau_{2_0}$, we let $\lambda(\tau_2) = \beta(\tau_2) + iw(\tau_2)$ be a root of equation (4.13) near $\tau_2 = \tau_{2_0}^{(k)}$ and $\beta(\tau_2)^{(k)} = 0$, as $w(\tau_2)^{(k)} = w_{2_0}$. Making a substitution into the L.H.S of equation (4.13) and taking a derivative with respect

to λ, we have

$$\frac{d\tau_2}{d\lambda} = \frac{(5\lambda^4 + 4p_4\lambda^3 + 3p_3\lambda^2 + 2p_2\lambda + p_1)e^{\mu\lambda\tau_2}}{(q_4\lambda^5 + q_3\lambda^4 + q_2\lambda^3 + q_1\lambda^2 + q_0\lambda)p\gamma\delta} + \frac{(4q_4\lambda^3 + 3q_3\lambda^2 + 2q_2\lambda + q_1)}{p\gamma\delta(q_4\lambda^5 + q_3\lambda^4 + q_2\lambda^3 + q_1\lambda^2 + q_0\lambda)} - \frac{\tau_2}{\lambda}. \tag{4.28}$$

Computing the sign of $\frac{d[Re(\lambda)]}{d\tau_2}$, from the characteristic equation (4.13) and solving (4.28) at $\tau_2 = \tau_{2_0}$ with $\lambda = iw_{2_0}$ and expressing $\sin(w_{2_0}\tau_{2_0})$ and $\cos(w_{2_0}\tau_{2_0})$, we obtain $\text{sign}\Big[\frac{\mathrm{d(Re}\lambda)}{\mathrm{d}\tau_2}\Big]_{\tau_2=\tau_{2_0}} = \text{sign}\Big[\mathrm{Re}(\frac{\mathrm{d}\lambda}{\mathrm{d}\tau_2})^{-1}\Big]_{\lambda=\mathrm{iw}_{2_0}}$,

$$= \text{sign}\Big[\mathrm{Re}\frac{\mathrm{f}_1\cos\mathrm{d}_0 + \mathrm{f}_2\sin\mathrm{d}_0}{\mathrm{g}_1 + \mathrm{ig}_2} + \mathrm{Re}\frac{\mathrm{i}(\mathrm{f}_3\cos\mathrm{d}_0 + \mathrm{f}_4\sin\mathrm{d}_0)}{(\mathrm{g}_1 + \mathrm{ig}_2)} + \mathrm{Re}\frac{\mathrm{f}_5}{\mathrm{g}_1 + \mathrm{ig}_2} - \mathrm{Re}\frac{\tau_2}{\mathrm{iw}_{2_0}}\Big],$$

$$\begin{aligned} = \text{sign}\Big[\mathrm{Re}\frac{\mathrm{g}_1(\mathrm{f}_1\cos\mathrm{d}_0 + \mathrm{f}_2\sin\mathrm{d}_0) - \mathrm{ig}_2(\mathrm{f}_1\cos\mathrm{d}_0 + \mathrm{f}_2\sin\mathrm{d}_0)}{\mathrm{g}_1^2 + \mathrm{g}_2^2}\Big] + \\ \text{sign}\Big[\mathrm{Re}\frac{\mathrm{g}_2(\mathrm{f}_2\cos\mathrm{d}_0 + \mathrm{f}_4\sin\mathrm{d}_0) + \mathrm{ig}_1(\mathrm{f}_3\cos\mathrm{d}_0 + \mathrm{f}_4\sin\mathrm{d}_0)}{\mathrm{g}_1^2 + \mathrm{g}_2^2}\Big] \\ +\text{sign}\Big[\mathrm{Re}\frac{\mathrm{f}_5\mathrm{g}_1}{\mathrm{g}_1^2 + \mathrm{g}_2^2}\Big], \end{aligned} \tag{4.29}$$

with coefficients in Appendix A3(d).

With linear combination of a sine and cosine of equal periods being equal to a single sine with the same period, equation (4.29), gives

$$\text{sign}\Big[\frac{\mathrm{g}_1(\sqrt{\mathrm{f}_1^2 + \mathrm{f}_2^2}(\sin(\mathrm{d}_0 + \Psi_0))) + \mathrm{g}_2\sqrt{\mathrm{f}_2^2 + \mathrm{f}_4^2}(\sin(\mathrm{d}_0 + \Psi_1)) + \mathrm{f}_5\mathrm{g}_1}{\mathrm{g}_1^2 + \mathrm{g}_2^2}\Big],$$

with $\Psi_0 = \arctan\frac{f_1}{f_2}$, $\Psi_1 = \arctan\frac{f_2}{f_4}$ and $f_2 \neq 0, f_4 \neq 0$.

Let

$$\Phi_1(w_{2_0}) = g_1\sqrt{f_1^2 + f_2^2}\,(\sin(d_0 + \Psi_0)) + g_2\sqrt{f_2^2 + f_4^2}\,(\sin(d_0 + \Psi_1)) + f_5g_1 \tag{4.30}$$

If $\Phi_1(w_{2_0}) > 0$, with $(d_0 + \Psi_{\{i=0,1\}}) \in (\pi, \frac{\pi}{2}]$, then $\text{sign}\left[\frac{\text{d}(\text{Re}\lambda)}{\text{d}\tau_2}\right]_{\tau_2=\tau_{2_0}} > 0$, hence the transversality condition holds and the system undergoes Hopf–bifurcation.

4.5.3 Delay in latent period and seeking medical care ($\tau_1 = \tau_2 = \tau > 0$)

Making a substitution of $\tau_1 = \tau_2 = \tau$ in equation (4.13), we get

$$\begin{aligned} g(\lambda, e^{-\lambda\tau}) = \lambda^5 + k_4\lambda^4 + k_3\lambda^3 + k_2\lambda^2 + k_1\lambda + k_0 \\ +((s_4)\lambda^4 + s_3\lambda^3 + s_2\lambda^2 + s_1\lambda + s_0)e^{-\lambda\tau} \\ +(s_3'\lambda^3 + s_2'\lambda^2 + s_1'\lambda + s_0')e^{-2\lambda\tau} = 0. \end{aligned} \tag{4.31}$$

with $s_4 = (\gamma + \delta)e^{-\mu\tau}, s_3 = (\gamma l_3 + m_3\delta)e^{-\mu\tau}, s_2 = (l_2\gamma + m_2\delta)e^{-\mu\tau}, s_1 = (l_1\gamma + m_1\delta)e^{-\mu\tau}$,
$s_0 = (l_0\gamma + m_0\delta)e^{-\mu\tau}, s_3' = (\gamma\delta)e^{-2\mu\tau}, s_2' = n_2\delta\gamma e^{-2\mu\tau}, s_1' = n_1\gamma\delta e^{-2\mu\tau}, s_0' = n_0\gamma e^{-2\mu\tau}$.

In order to examine whether or not the endemic equilibrium loses stability and undergoes Hopf–bifurcation as an outcome with inclusion of the time delays, a pair of purely imaginary root of the transcendental equation (4.31) is found. Suppose the pair of the imaginary root is given as $\lambda = iv$ with infection rate oscillation frequency ($v > 0$), using Euler's expansion and making a substitution into equation (4.31), separating real and imaginary parts, we obtain

$$g_0 \cos v\tau + g_1 \sin v\tau + g_2 \sin 2v\tau = G_1, \tag{4.32}$$

$$-g_1 \cos v\tau + g_0 \sin v\tau + g_3 \sin 2v\tau = G_2. \tag{4.33}$$

where $g_0 = s_1 v - s_3 v^3, g_1 = s_2 v^2 - s_4 v^4 - s_0, g_2 = s_2 v^2, g_3 = s_3' v^3 + s_1' v,$
$G_1 = v^5 + (k_3 + s_3 + s_3')v^3 - (k_1 + s_1')v, G_2 = (k_2 + s_2')v^2 - (k_4 v^4 + k_0 + s_0').$
Squaring and adding equation (4.32) and (4.33), we get following equation

$$g_0^2 + g_1^2 - G_1^2 - G_2^2 = -\frac{1}{2}(g_2^2 + g_3^2)(1 - \cos 4v\tau). \tag{4.34}$$

suppose $\|\cos 4v\tau\| < 1$, equation (4.34) leads to

$$G_1^2 + G_2^2 - (g_0^2 + g_1^2) = 0, \tag{4.35}$$

which reduces to

$$\begin{aligned} v^{10} + (2(k_3 + s_3 + s_3') + k_4^2 - s_4^2)v^8 + ((k_3 + s_3 + s_3')^2 \\ +2(k_1 + s_1') - 2k_4(k_2 + s_2') + 2s_2 s_4 - s_3^2)v^6 \\ +(2(k_1 + s_1')(k_3 + s_3 + s_3') + 2k_4(k_0 + s_0') + 2s_1 s_3 - (s_2^2 + 2s_0 s_4))v^4 \\ +((k_1 + s_1')^2 + 2s_0 s_2 - 2(k_2 + s_2')(k_0 + s_0') - s_1^2)v^2 + (k_0 + s_0')^2 = 0. \end{aligned} \tag{4.36}$$

Let $z = v^2$ such that we obtain equation (4.36) in terms of z

$$L(z) = z^5 + u_4 z^4 + u_3 z^3 + u_2 z^2 + u_1 z + u_0, \tag{4.37}$$

with $u_4 = 2(k_3 + s_3 + s_3') + k_4^2 - s_4^2, u_3 = (k_3 + s_3 + s_3')^2 + 2(k_1 + s_1^1) - 2k_4(k_2 + s_2^1) +$
$(2s_2 s_4 - s_3^2), u_2 = 2(k_1 + s_1')(k_3 + s_3 + s_3') + 2k_4(k_0 + s_0') + 2s_1 s_3 - (s_2^2 + 2s_0 s_4),$
$u_0 = (k_0 + s_0')^2 u_1 = (k_1 + s_1')^2 + 2s_0 s_2 - 2(k_2 + s_2')(k_0 + s_0') - s_1^2.$

Since equation (4.37), has a high degree polynomial we compute the eigenvalues numerically by using parameter values in Table 4.1. The resulting polynomial is $z^5 - 295.18z^4 - 130.18z^3 + 92.52z^2 - 0.15038z + 2.6 \times 10^{-12} = 0.$
Therefore, the following eigenvalues are obtained

$z_1 = 295.62, z_2 = 0, z_3 = 0.001629, z_4 = 0.38024, z_5 = -0.8212.$

We observe that there is only one negative real root which does not guarantee stability of model (4.1) in the presence of time delays $\tau = \tau_1 = \tau_2 > 0$, thus by Lemma 4.4.2 there exists a pure imaginary root w_c such that a critical time delay τ_c is achieved for which there is death or birth of period oscillations (Hopf–bifurcation).

Equation (4.34) yields

$$\tau_c = \frac{1}{4v_0} \arccos\left(\frac{g_2^2 + g_3^2 + 2(g_0^2 + g_1^2 - (G_1^2 + G_2^2))}{g_2^2 + g_3^2}\right) + \frac{j\pi}{2v_0}; j = 0, 1, 3, \ldots (4.38)$$

with $\lambda = iv$ (a purely imaginary root of equation (4.31)), if condition $g_0^2 + g_1^2 = G_1^2 + G_2^2$ and $\tau \in [0, \tau_c)$ holds. Without loss of generality, let v_0 represent the value v_0 corresponding to τ_c. We thus state the result below:

Proposition 4.4.4 *If condition $g_0^2 + g_1^2 = G_1^2 + G_2^2$ holds, then the chronic steady state P^* is locally asymptotically stable for $\tau \in [0, \tau_c)$, unstable when $\tau > \tau_c$ and undergoes a Hopf–bifurcation.*

4.6 Model results and discussion

Here, MATLAB dde23 function is used to obtain numerical simulations of model (4.1). Parameter values in Table 4.1 are used in the simulation. The positive endemic equilibrium is $P^* = (S^*, V^*, E^*, C^*, I^*) = (2099, 6, 54, 2, 100)$. In the absence of delays $\tau_1 = \tau_2 = 0$, the characteristic polynomial equation (4.14) is

$$\lambda^5 + 0.7364\lambda^4 - 148.4007\lambda^3 - 4.9408\lambda^2 - 0.3965\lambda - 0.0001806.$$

The corresponding eigenvalues are: $\lambda_1 = 11.8366, \lambda_2 = -0.000472, \lambda_3 = -12.5357,$ $\lambda_{4,5} = -0.01641 \pm 04885i$. Therefore, since the eigenvalues have one positive

Table 4.1: Parameter values

Parameter	value/unit	Source
b	22 day^{-1}	estd
ν	2.53×10^{-5}	(Sutton et al., 2007)
γ	3.3333×10^{-1} day $^{-1}$	assumed
μ	2.0547×10^{-3}	estd
δ	3.3×10^{-1} day $^{-1}$	(Ngari et al., 2016)
ρ	1.096×10^{-2} day^{-1}	(Ngari et al., 2014)
ϕ	3.5714×10^{-2}day^{-1}	(Melegaro et al., 2010)
ζ	5.4794×10^{-4}day^{-1}	(Melegaro et al., 2010)
ϑ	0.54	(Lindstrand, 2016)
β	1.0102×10^{-4} day^{-1}	assumed
τ_1	1–3 days	(White et al., 2009)
τ_2	2 days	(Källander et al., 2008)

root and four negative roots, the endemic equilibrium changes state of stability from unstable to stable thus under goes a Hopf–bifurcation (see Figure 4.3). This implies that as time approaches infinity, the partial populations are stable and pneumococcal pneumonia can no longer cause harm to individuals. The numerical simulation of equation (4.15) yields the characteristic roots as: $\lambda_1 = 0, \lambda_2 = 14.4621i, \lambda_3 = -14.4416,$
$\lambda_4 = \pm 0.00041 + 0.3771i, \lambda_5 = \pm 0.0579 + 0.1335i$. As τ_1 increase from zero, there is a value $\tau_{1_0} > 0$ such that the endemic equilibrium is stable for $\tau_1 \in [0, \tau_{1_0}]$ and unstable for $\tau_1 > \tau_{1_0}$. At this critical value, the endemic equilibrium loses

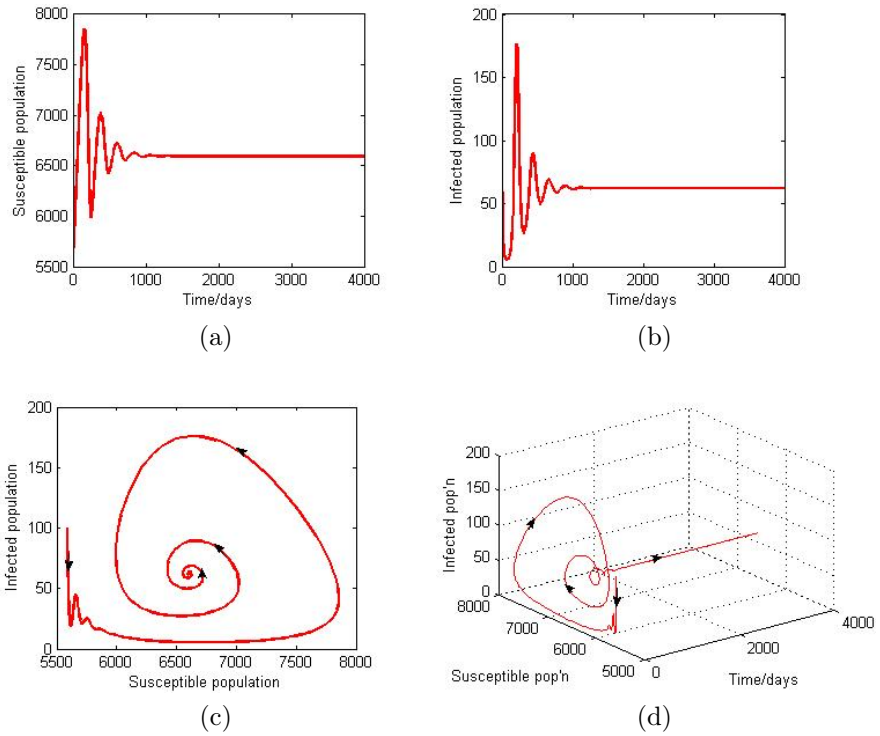

Figure 4.3: (a& b) Stability of the endemic equilibrium showing Hopf–bifurcation, with initial variables: $S(0) = 5586, V(0) = 22, C(0) = 64, I(0) = 11, E(0) = 100$. (c& d) The evolution of the infected, the susceptible and corresponding I-S portrait and 3-D phase trajectories, (with $R_0 = 15.4, R_0^u = 15.14, R_0^v = 0.271$ parameters:$\mu = 2.0547 \times 10^{-4}, \phi = 3.574 \times 10^{-2}$. The rest of the parameters remain fixed as in Table 4.1.

stability and Hopf–bifurcation arises. The real positive root is $w_{1_0} = 14.4621$ and the critical time delay $\tau_{1_0} = 0.109$ of a day ≈ 3 hrs.

Figure 4.4 shows the evolution of the susceptible and infected population of system (4.1). The low and high peaks in the number of susceptible and infected individuals indicate the season peak of the disease. If $\tau_1 < \tau_{10} = 0.109$ of a day ≈ 3 hrs, the partial populations of the susceptible and the infected are stable whereas if $\tau_1 > \tau_{10} = 0.109$ of a day ≈ 3hrs, the populations are unstable and it's hard to predict the future pattern of the disease prevalence. The numerical computation of equation (4.23) yields eigenvalues $\lambda_1 = 0, \lambda_2 = 0.06508i, \lambda_3 = -0.06522, \lambda_4 = -12.038, \lambda = -12.3263$.

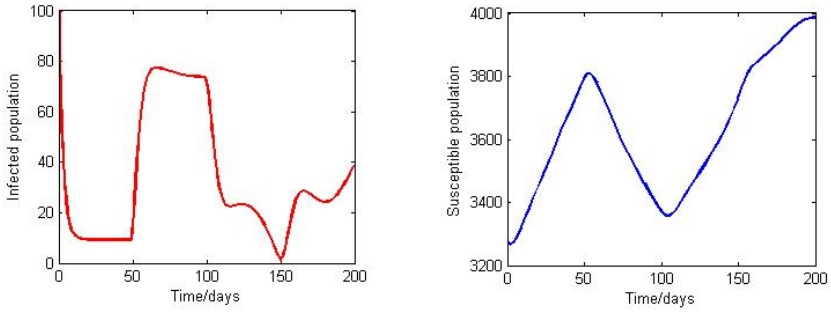

(a) (b)

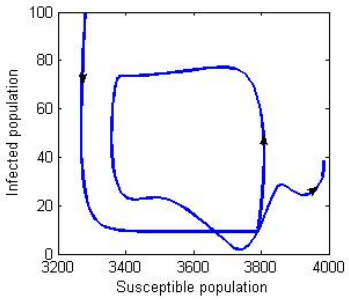

(c)

Figure 4.4: Simulation of model (4.1) for $\tau_2 = 0$ and $\tau_1 > 0$, with initial variable values: $(S(0), V(0), E(0), C(0), I(0)) = (3280, 30, 10, 10, 100)$. The rest of the parameters are as in Table 4.1.

The positive root $w_{20} = 0.06508$ and the critical time delay $\tau_{2_0} = 26$ days, hence system (4.1) is stable for $\tau_2 < 26$ days and unstable for $\tau_2 > \tau_{2_0}$. A characteristic polynomial (4.31) corresponding to two delays is solved to give the eigenvalues as; $\lambda_1 = 0, \lambda_2 = -17.1963, \lambda_3 = -0.6166, \lambda_4 = -0.04036, \lambda_5 = 0.9026i$, the real positive root $w_c = 0.9062$ and the critical time delay $\tau_c = 2.069$ days.

Figure 4.5 depicts the time series solution approaching their equilibrium point as time approaches infinity. This confirms the stability of the system when the value of time delay is less than $\tau_c = 2.069$ days and instability of the system if $\tau > \tau_c = 2.069$ days (see Proposition 4.5.3).

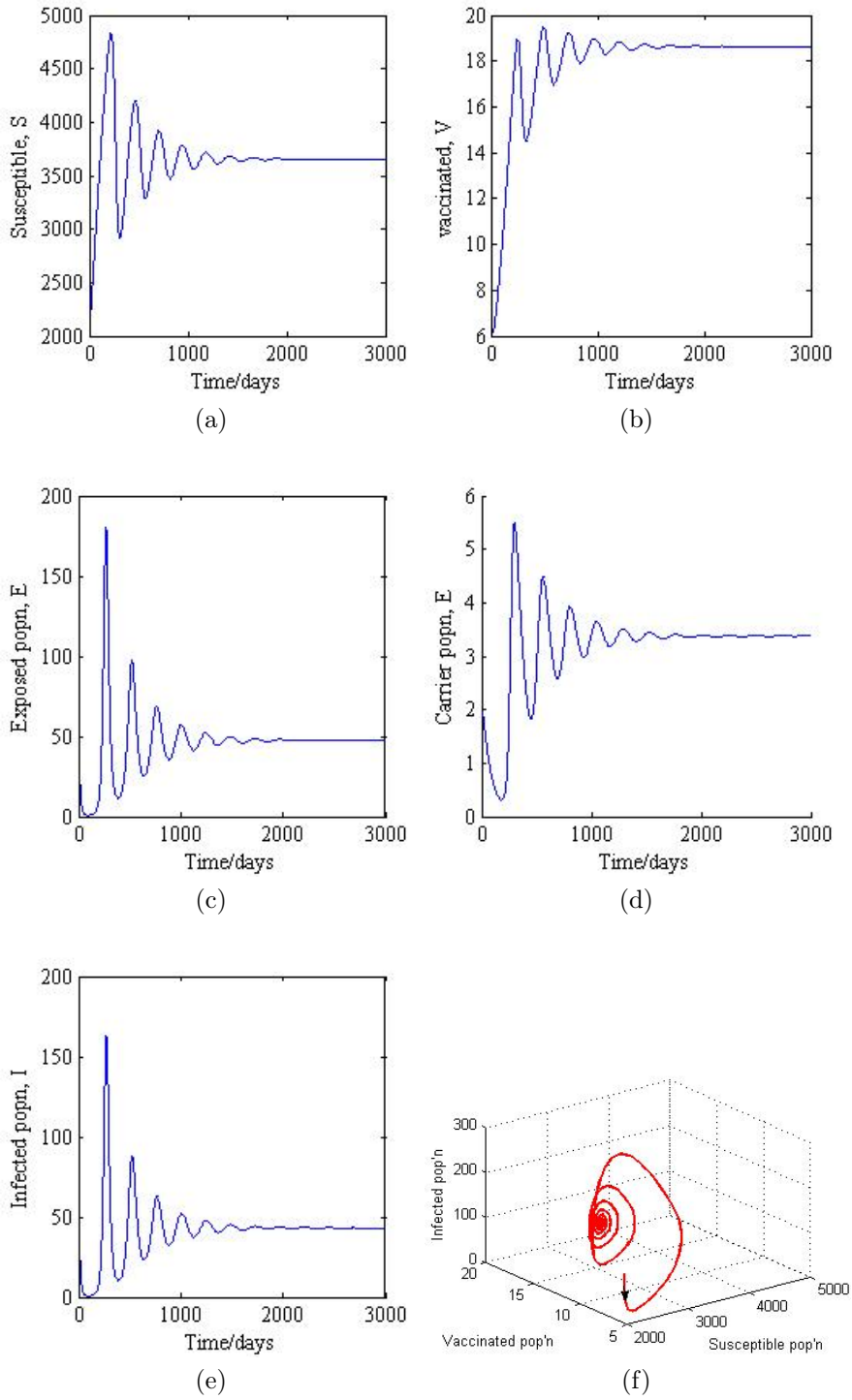

Figure 4.5: Stability of the endemic equilibrium P^* for $\tau_1 = \tau_2 = 2$ days. The rest of the parameters are as in Table 4.1.

To explore the effect of time delay τ_2 on pneumococcal pneumonia, we fix time delay $\tau_1 = 3$ days, and the parameter τ_2 is varied (Figure 4.6). The rate

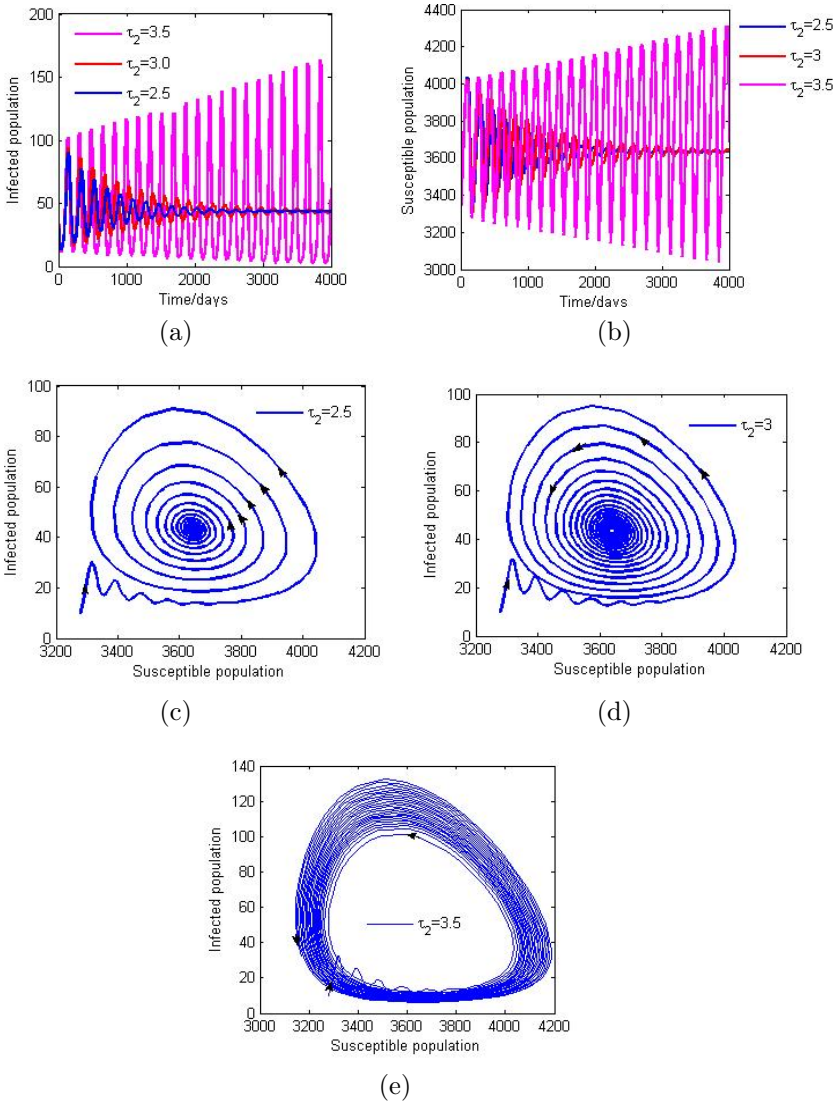

Figure 4.6: The effect of varying τ_2 on the dynamics of model (4.1). The delay τ_2 was chosen as $\tau_2 = 2.5, 3, 3.5$. All other parameters remain as stated in Table 4.1.

of convergence to stability of the endemic equilibrium point is attained with a reduction in the delay and a divergence is due to an increase in the delay that results into instability of the system. This gives rise to Hopf–bifurcation phenomenon.

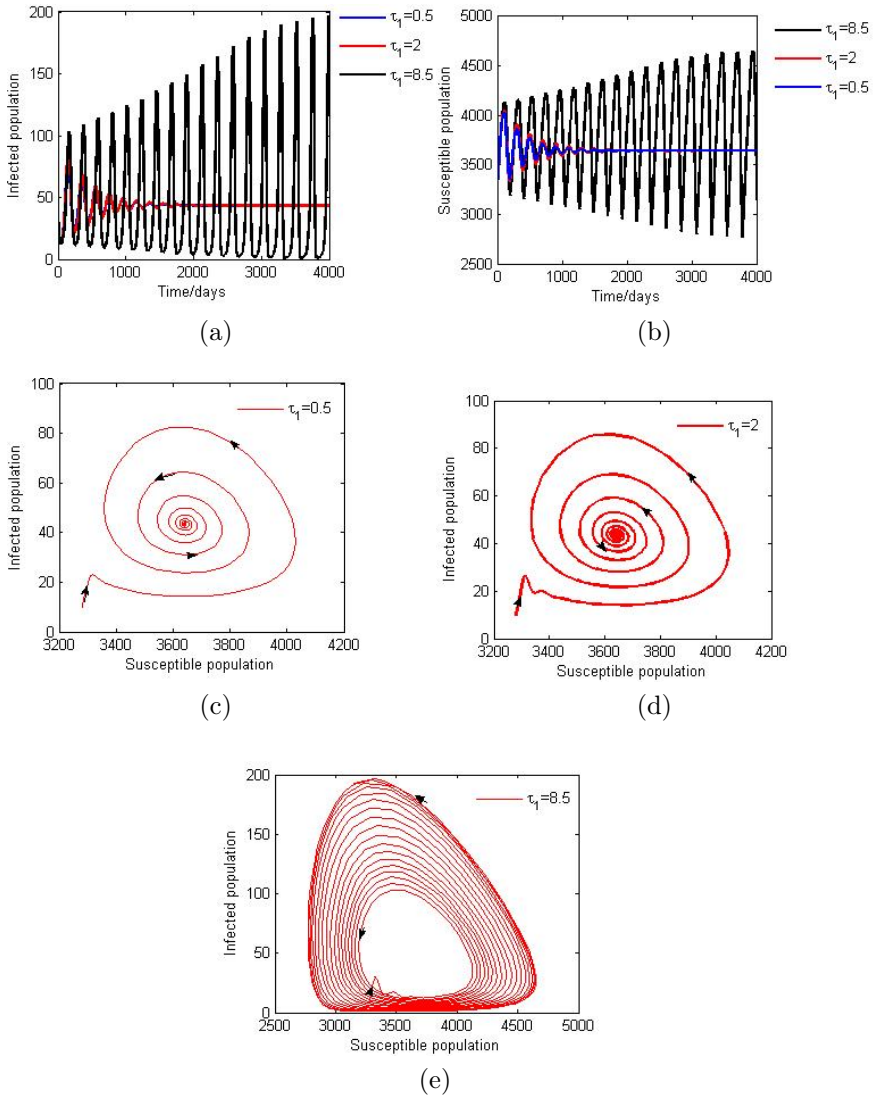

Figure 4.7: The effect of varying time delay τ_1 on the dynamics of model (4.1). The delay τ_1 was chosen as $\tau_1 = 0.5, 2, 8.5$. All the parameter values are the same as in Table 4.1.

In Figure 4.7, time delay τ_2 is fixed at 2 days in order to study the effect of time delay τ_1 on model (4.1). We observe an increase in the magnitude of the amplitude of oscillations as τ_1 increases, thus divergence from the endemic equilibrium occurs leading to unstable state. This implies that the disease will persist in the population with increased delays if there is no intervention instituted to reduce the delays. On the other hand a decrease in τ_1 guarantees the asymptotic stability of the endemic equilibrium which implies the disease can be eradicated

from the population.

In this Chapter, a mathematical model to study the effect of two time delays on the dynamics of pneumococcal pneumonia with vaccination is analyzed. The results show that, without delays ($\tau_1 = \tau_2 = 0$), the disease–free equilibrium P_0 is locally asymptotically stable if the control reproductive ratio $R_0 < 1$, whenever conditions $(\mu + \zeta)(\mu + \nu) > \zeta\nu$ and $R_0^v < 1$ hold, and unstable if $R_0 > 1$.

The results revealed that the endemic equilibrium is locally stable without delays and stable if the delays are under conditions. The transversality conditions for the existence of Hopf–bifurcation are stated and proved for three cases; (1) $\tau_1 = 0, \tau_2 = \tau > 0$, (2) $\tau_1 = \tau > 0, \tau_2 = 0$ and (3) $\tau_1 = \tau_2 = \tau > 0$. Critical values at which Hopf–bifurcation occur have been obtained. The results show that at critical values $\tau_{1_0} = 0.109 \approx 3$ hrs, $\tau_{2_0} = 26$ days and $\tau_c = 2.069$ days, the endemic equilibrium losses stability.

Basing on the numerical simulations obtained, we found out that when τ_1 , τ_2 are below the critical values τ_{1_0} and τ_{2_0} respectively, model (4.1) is asymptotically stable. Which implies that the number of individuals in the five subpopulations will be in ideal equilibrium and prevalence of pneumococcal pneumonia can easily be controlled. Conversely, if the value of the delays τ_1, τ_2 are greater than the critical values τ_{1_0} and τ_{2_0} respectively, a Hopf–bifurcation arises this phenomenon suggests persistent of pneumococcal pneumonia in the population. The number of individuals will fluctuate periodically, this is not helpful, effort should be put to control such a phenomenon.

We note that longer time delays destabilize the system and give rise to Hopf–bifurcations. This explains the oscillatory seasonal change of pneumococcal pneumonia disease

in human population whose immune systems are weak. Therefore, measures to reduce delays in latent and seeking medical care during pneumococcal pneumonia epidemic should be prioritized.

In the next Chapter, the effects of antibiotic resistance awareness and saturated treatment in the dynamics of pneumococcal pneumonia are discussed. Individuals have limited knowledge about antibiotic resistance during pneumococcal pneumonia treatment that has led to relapse of the disease and increased death in children below 5 years of age and the elderly.

CHAPTER 5

MODELING EFFECTS OF ANTIBIOTIC RESISTANCE AWARENESS AND SATURATED TREATMENT OF PNEUMOCOCCAL PNEUMONIA

5.1 Introduction

Antibiotic resistance is a major world wide threat to the provision of safe and effective health care. Evidence for treatment failures of antibiotic–resistant to pneumococcal pneumonia has been more difficult to document Schrag et al. (2001) and this limits developments in the control of the disease. Misuse of antimicrobials in developing countries is aided by their availability over the counter, without prescription and through unregulated supply chains (Ayukekbong et al., 2017).

In this Chapter, a model of pneumococcal pneumonia with antibiotic resistance awareness and saturated treatment is developed and analyzed in an attempt to reduce the incidence of pneumococcal pneumonia in humans.

5.2 Model formulation

The total population under consideration is $N(t)$, comprising four classes with the susceptible and infectious each partitioned into two. The susceptible class consists of; the aware individuals $S_a(t)$ that have had a chance to attend the

available antibiotic resistance awareness programs, and the unaware individuals $S_u(t)$ that have never heard of the prevailing programs or have heard of the existing programs but have not responded. The infectious class consists of; infected individuals receiving treatment $I(t)$, and infected individuals but resistant to first line treatment $R(t)$.

Thus unaware class is increased through a constant recruitment B and fading of information of aware individuals at a rate ξ. The Infection is spread through the interaction of infected and susceptible individuals. Considering a reduced incidence rate of the form, $g(I) = (\beta I - \frac{\beta_1 mI}{m+I})$, where $m > 0$ is the effect of media coverage on the contact transmission, $\beta > 0$ is the maximal effective contact rate before awareness and $\beta_1 > 0$ is the maximal reduced effective contact rate due to media alert in the presence of infective individuals. The transmission term has been considered because in real life, every individual will take precaution to protect themselves from infections as sooner as infected individuals with antibiotic resistant bacteria have been identified/reported in a wholly susceptible population which will reduce the disease spread. Again, with the rate of media awareness impact in both the numerator and denominator because infected individuals have to constantly be educated/reminded of proper prevention and control measures even after correct treatment has been administered. The fact that the coverage report about antibiotic resistance against existing treatment doesn't prevent spread of disease completely then $\beta \geq \beta_1 > 0$. The unaware individuals transfer to the aware class after receiving information through private individuals at a rate υ.

The transmission rate in this model is a bilinear incidence term $\beta_2 S_a I$ with $\beta_2 > 0$, is the contact rate between aware individuals and infected individuals. The infected class, is increased through the relapse of resistant individuals at a rate γ. It is assumed that infected individuals upon receiving the first line

of treatment tend not to complete the prescribed medication and develop resistant bacteria that may require costly treatment to be eliminated. A saturated treatment is considered because there exist delays in administering treatment by infected individuals and the medical resources may be limited. Suppose treatment to infected individuals is administered at a rate ϕ, and is either cleared of the pneumococcus or acquires resistance. Modifying the saturated treatment proposed in Zhang & Liu (2008) by incorporating, $\tau = \frac{1}{1+\phi D}$ which describes the effect of infected individuals delaying to seek treatment, where D is the number of days delayed in taking treatment (Obolski et al., 2015). Thus the saturated treatment we use in our model is of the form $T(I) = \frac{\phi I}{1+\tau I}$. However, if $\tau = 0$, the saturated treatment function becomes linear, that is $T(I) \approx \phi I$, if the number of infected individuals is minimal $T(I) \approx 0$, and if the number of infected individuals grows large, $T(I) \approx \phi$. The probability of acquiring resistance to first line treatment is p. Finally the rate of resistance acquisition upon treatment with the antibiotic is $p\phi$, and a fraction of infected individuals respond to treatment and recover from the disease, thus transfer to the aware class with a clearance rate $(1-p)\phi$.

Individuals who are treated incorrectly or individuals who do not take the right dose at the prescribed time become resistant to first line treatment and a correct treatment is administered after a delay period τ. Descriptions of state variables and epidemiological parameters are summarized in the nomenclature.

5.3 Model assumptions

The assumptions of the model are stated:

(i) All new recruitments (through birth and immigrants) are unaware.

(ii) Aware susceptible individuals transfer to unaware susceptible class due to

loss of memory or social factors.

(iii) Antibiotic resistance awareness is disseminated by private individuals and the media at rates υ and m respectively.

(iv) Antibiotic resistance is gained through mutations, due to exposure to antibiotics (Daşbaşı & Öztürk, 2016).

(v) The maximal effective contact rate before awareness to be greater than the maximal reduced contact rate due to the alert in the presence of infective individuals

(vi) Infected individuals are immediately treated with first line of treatment.

(vii) All subpopulations are decreased by a natural mortality rate μ.

With the assumptions, variables, parameters and the transition diagram in Figure 5.1, our proposed model for the dynamics of pneumococcal pneumonia is governed by the system of nonlinear ordinary differential equations got by applying the balance law of compartments stated as: rate of change=inflow transition rate−outflow transition rate that is: $\dot{X}$ = sum of inflow transition rates− sum of outflow transition rates.

$$\begin{aligned}
\dot{S}_u &= B + \xi S_a - (g(I) + \upsilon I + \mu)S_u, \\
\dot{S}_a &= \upsilon I S_u + (1-p)\Phi T(I) - (\beta_2 I + \xi + \mu)S_a, \\
\dot{I} &= g(I)S_u + \beta_2 S_a I + \gamma R - \Phi T(I) - (\mu + \delta)I, \\
\dot{R} &= p\Phi T(I) - (\gamma + \mu)R.
\end{aligned} \tag{5.1}$$

where

$T(I) = \frac{I}{1+\tau I}$ and $g(I) = (\beta I - \beta_1 \frac{mI}{m+I})$,

with initial conditions: $S_u(0) = S_{u0} \geq, S_a(0) = S_{a0} \geq 0$,

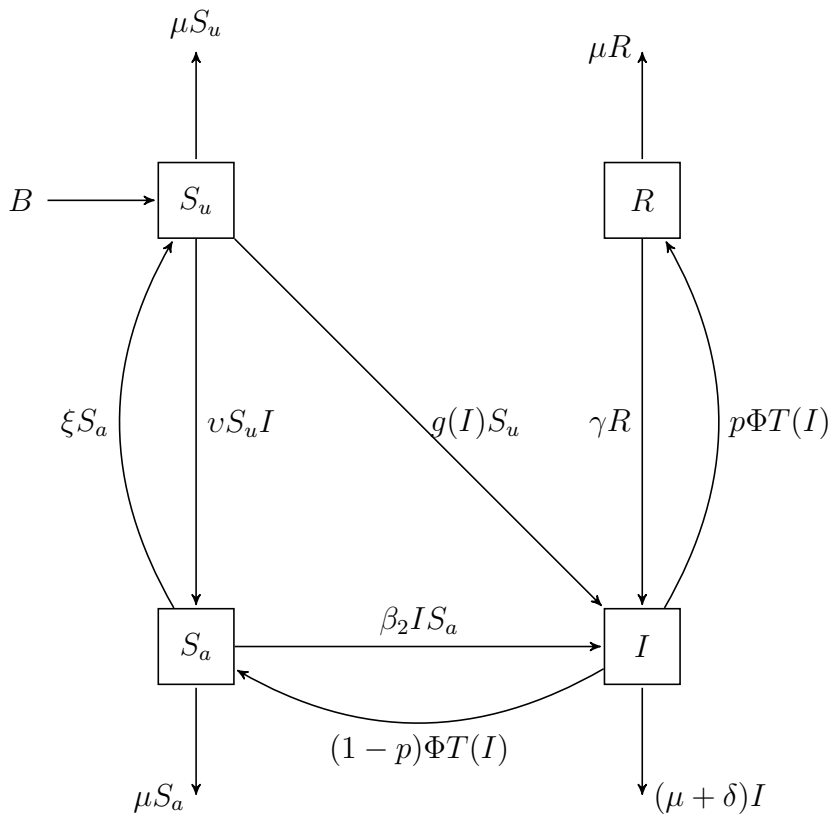

Figure 5.1: A transition diagram showing the dynamics of pneumococcal pneumonia,
with $T(I) = \frac{I}{1+\tau I}, g(I) = (\beta I - \frac{\beta_1 m I}{m+I})$.

$I(0) = I_0 \geq 0, R(0) = R^0 \geq 0$. Since model (5.1), describes human populations, all state variables and parameters are assumed positive for all $t \geq 0$.

Building on a mathematical model developed by Kizito & Tumwiine (2018), new compartments of susceptible and infective have been incorporated. Sub–dividing a compartment of susceptible into: aware individuals, unaware individuals; and the infectious into: infected individuals receiving treatment, and infected individuals resistant to first line treatment. A relapse of resistant individuals, a modified saturated treatment and a reduced disease transmission rate with the effect of antibiotic resistance awareness through media are also added.

5.3.1 Positivity of solution trajectories in model (5.1)

Lemma 5.2.1. Solutions of model (5.1) with initial conditions $S_u(0) = S_{u0} \geq$, $S_a(0) = S_{a0} \geq 0, I(0) = I_0 \geq 0$ and $R(0) = R^0 \geq 0$ are always non–negative for all $t \geq 0$.

Proof. Suppose $S_u(t), S_a(t), I(t), R(t)$ are solutions to model (5.1), then from the first equation of model (5.1), we have

$$\frac{dS_u}{dt} = B + \xi S_a - g(I)S_u - \upsilon I S_u - \mu S_u \geq -(g(I) + \upsilon I - \mu)S_u. \tag{5.2}$$

By using the technique of separation of variables we have

$$S_u(t) \geq S_{u0} \exp(-(\mu t + \int_0^t (g(I(\theta)) + \nu I(\theta))d\theta)) \geq 0. \tag{5.3}$$

Therefore, the solution of $S_u(t)$ in equation (5.3) is non–negative for all $t \geq 0$. Applying the same technique to the remaining variables of model (5.1) we get

$$\begin{aligned} S_a(t) \geq S_{a0} \exp(-(\xi + \mu) + \int_0^t \beta_2 I(\theta)d\theta) \geq 0, \\ I(t) = I_0 \exp(-(\mu + \delta)t) \geq 0 \end{aligned} \tag{5.4}$$

and

$$R(t) \geq R^0 \exp(-(\gamma + \mu)t) \geq 0. \tag{5.5}$$

Therefore, all solutions of $S_a(t), I(t)$ and $R(t)$ in equations (5.4) and (5.5) are non–negative for all times $t \geq 0$. This completes the proof.

5.3.2 Invariant region

Here we obtain a region in which the solution of model (5.1) is bounded. For this model the total population is $N = S_u + S_a + I + R$, such that the rate of change of the total population is

$$\frac{dN}{dt} = B - \mu N - \delta I, \tag{5.6}$$

$$\frac{dN}{dt} \leq B - \mu N. \tag{5.7}$$

Equation (5.7) corresponds to instances of no pneumococcal pneumonia related death. Therefore, we obtain

$$N \leq N_0 e^{-\mu t} + \frac{B}{\mu}(1 - e^{-\mu t}). \tag{5.8}$$

where, $N_0 = S_{u0} + S_{a0} + I_0 + R^0$.

Thus, from equation (5.8) we have

$$N(t) \leq \max(N_0, \frac{B}{\mu}) \tag{5.9}$$

Then, $0 \leq S_u + S_a + I + R \leq \frac{B}{\mu}$.

This implies that the region $D = \{(S_u, S_a, I, R) \in \mathbb{R}^4_+ \colon S_u + S_a + I + R = N \leq \frac{B}{\mu}\}$, which implies $N(t)$ is a bounded, and so are S_u, S_a, I and R.

5.3.3 Existence and uniqueness of the steady states

From model (5.1), equating the right hand side to zero. The Proposition 5.3.1 shall represent the existence and uniqueness of the endemic steady state.

Proposition 5.3.1. *If conditions* $(\gamma + \mu)(\mu + \delta) > \Phi(\gamma(p-1) - \mu)$, $B > I^* d$,

$(\upsilon I^* + \mu)(\beta_2 I^* + \xi + \mu) > \upsilon I^*(\beta_2 I^* + \xi)$ *and* $(\Phi + \mu + \delta)(\gamma + \mu) > p\Phi\gamma$ *hold, then model* (5.1) *will admit a unique endemic steady state,* $E^* = (S_u^*, S_a^*, I^*, R^*)$ if $R_0 > 1$.

Proof. Suppose $E^* = (S_u^*, S_a^*, I^*, R^*)$ is a steady state of model (5.1) satisfying the system below

$$\begin{aligned} B + \xi S_a^* - (g(I^*) + \upsilon I^* + \mu)S_u^* &= 0, \\ \upsilon I^* S_u^* + (1-p)\Phi T(I^*) - (\beta_2 I^* + \xi + \mu)S_a^* &= 0, \\ g(I^*)S_u^* + \beta_2 S_a^* I^* + \gamma R^* - \Phi T(I^*) - (\mu + \delta)I^* &= 0, \\ p\Phi T(I^*) - (\gamma + \mu)R^* &= 0. \end{aligned} \tag{5.10}$$

From equation (5.10) it follows that if we let $I^* = R^* = 0$ then we have the disease–free steady state $E_0^* = (S_u^0, S_a^0, I^0, R^0) = (\frac{\xi+\mu}{\upsilon}, \frac{B\upsilon - \mu\xi - \mu^2}{\mu\upsilon}, 0, 0)$ that exist for all epidemiological parameter values.

On the other hand, if $I^* \neq 0, R^* \neq 0$, then we have the endemic steady state $E^* = (S_u^*, S_a^*, I^*, R^*)$,

where

$$\begin{aligned} S_u^* &= \frac{(1+\tau I^*)^2(\beta_2 I^* + \xi + \mu)(B - I^* d) + (\beta_2 I^* + \xi)(1-p)\Phi I^*}{K(1+\tau I^*)}, \\ S_a^* &= \frac{\upsilon I^*(1+\tau I^*)^2(B - I^* d) + (1-p)\Phi I^*(\upsilon I^* + \mu)}{K(1+\tau I^*)}, \\ R^* &= \frac{p\Phi I^*}{(\gamma+\mu)(1+\tau I^*)}, \\ I^* &= I^{*+} = \frac{-r_1 + \sqrt{(r_1^2 - 4r_2 r_0)}}{2r_2}, \end{aligned}$$

with

$r_0 = m(\beta - \beta_1)S_u^* + m(\frac{\gamma\Phi p}{\gamma+\mu} + \Phi) - (\mu + \delta)$,

$r_1 = (\beta + \tau m(\beta - \beta_1))S_u^* + \tau(\beta - \beta_1)m + \frac{\gamma p\Phi}{\gamma+\mu} + \phi - (\mu + \delta)(1 + \tau m)$,

$r_2 = \tau(\beta S_u^* - (\mu + \delta))$

$d = (\gamma + \mu)((\gamma + \mu)(\mu + \delta) - \Phi(\gamma(p-1) - \mu))$,

$K = (\upsilon I^* + \mu)(\beta_2 I^* + \xi + \mu) - \upsilon I^*(\beta_2 I^* + \xi))$.

Therefore, there exists a unique endemic steady state E^* provided conditions $(\gamma+\mu)(\mu+\delta) > \Phi(\gamma(p-1)-\mu), B > I^*d, (\upsilon I^*+\mu)(\beta_2 I^*+\xi+\mu) > \upsilon I^*(\beta_2 I^*+\xi))$, $r_1 < 0$, $r_2 > 0$ and $r_0 < 0$ hold. This completes the proof.

5.3.4 The basic reproductive number

Computing the basic reproduction number, R_0 for model (5.1) by the method introduced by Van den Driessche and Watmough Van Den Driessche & Watmough (2002) according to which $R_0 = \rho(FV^{-1})$, where ρ is the spectral radius of a matrix (the maximum eigenvalue obtained from the matrix). Let $\mathbb{F}$ and $\mathbb{V}$ be vectors representing new infections and remaining transfer terms respectively

$$\mathbb{F} = \begin{pmatrix} g(S_u, I) + \beta_2 S_a I \\ \\ 0 \end{pmatrix}, \mathbb{V} = \begin{pmatrix} \Phi T(I) + (\mu + \delta)I - \gamma R \\ \\ (\gamma + \mu)R - p\Phi T(I) \end{pmatrix}. \quad (5.11)$$

The infected compartments are I and R, at disease–free steady state we obtain matrix Jacobian's F for $\mathbb{F}$ and V for $\mathbb{V}$ from (5.11) to have

$$F = \begin{pmatrix} (\beta - \beta_1)S_u^0 + \beta_2 S_a^0 & 0 \\ \\ 0 & 0 \end{pmatrix}, V = \begin{pmatrix} \Phi + \mu + \delta & -\gamma \\ \\ -p\Phi & \gamma + \mu \end{pmatrix}, \quad (5.12)$$

Thus, the next generation matrix for model (5.1) is evaluated as

$$FV^{-1} = \begin{pmatrix} \frac{((\beta-\beta_1)S_u^0+\beta_2 S_a^0)(\gamma+\mu)}{(\Phi+\mu+\delta)(\gamma+\mu)-p\gamma\Phi} & \frac{((\beta-\beta_1)S_u^0+\beta_2 S_a^0)\gamma}{(\Phi+\mu+\delta)(\gamma+\mu)-p\gamma\Phi} \\ 0 & 0 \end{pmatrix}. \tag{5.13}$$

Therefore, making substitutions of Su^0 and S_a^0, the basic reproduction number for model (5.1) is

$$R_0 \;=\; \rho(FV^{-1}) = \frac{(\gamma+\mu)\Big((\beta-\beta_1)\frac{\xi+\mu}{\upsilon}+\frac{\beta_2(B\upsilon-\mu\xi-\mu^2)}{\mu\upsilon}\Big)}{(\Phi+\mu+\delta)(\gamma+\mu)-p\Phi\gamma}. \tag{5.14}$$

5.3.5 Local stability behavior of the disease–free steady states

Proposition 5.3.2. *If condition* $\Phi+\mu+\delta) > p\Phi\gamma$ *hold, then the disease–free steady state* E_0^* *is locally asymptotically if* $R_0 < 1$ *and unstable for* $R_0 > 1$.

Proof. The Jacobian matrix of model (5.1) at E_0^* is given as

$$J(E_0) \;=\; \begin{pmatrix} -\mu & \xi & J_{13} & 0 \\ 0 & -(\xi+\mu) & J_{23} & 0 \\ 0 & 0 & J_{33} & \gamma \\ 0 & 0 & p\Phi & -(\gamma+\mu) \end{pmatrix}. \tag{5.15}$$

with

$$\begin{aligned} J_{13} &= -\frac{(\beta-\beta_1+\upsilon)(\xi+\mu)}{\upsilon}, \\ J_{23} &= \frac{((1-p)\Phi+\upsilon)(\xi+\mu)}{\upsilon} - \frac{\beta_2(B\upsilon-\mu\xi-\mu^2)}{\mu\upsilon}, \\ J_{33} &= \frac{(\beta-\beta_1)(\xi+\mu)}{\upsilon} + \frac{\beta_2(B\upsilon-\mu\xi-\mu^2)}{\mu\upsilon} - (\Phi+\mu+\delta). \end{aligned}$$

The characteristic polynomial of the matrix in (5.15) is given by

$$|J(E_0)-\lambda I| = \lambda^4 + m_3\lambda^3 + m_2\lambda^2 + m_1\lambda + m_0 = 0. \tag{5.16}$$

where $m_3 = \frac{(\beta_1-\beta)(\xi+\mu)}{\upsilon} + (4\mu+\phi+\delta+\gamma+\xi) - \frac{\beta_2(B\upsilon-\mu\xi-\mu^2)}{\mu\upsilon}$,

$m_2 = (\xi+\mu)\Big(\frac{(\beta_1-\beta)(\xi+\mu)}{\upsilon} - \frac{\beta_2(B\upsilon-\mu\xi-\mu^2)}{\mu\upsilon} + (\Phi+\mu+\delta) + (\gamma+\mu)\Big) + \mu\Big((\xi+\mu) + (\beta_1 - \frac{\beta(\xi+\mu)}{\upsilon} - \frac{\beta_2(B\upsilon-\mu\xi-\mu^2)}{\mu\upsilon} + (\Phi+\mu+\delta) + (\gamma+\mu)\Big) + \Big(\gamma+\mu\Big)\Big(\frac{(\beta_1-\beta)(\xi+\mu)}{\upsilon} - \frac{\beta_2(B\upsilon-\mu\xi-\mu^2)}{\mu\upsilon} + (\Phi+\mu+\delta)\Big) - \gamma p\Phi$

$m_1 = \mu\Big(\frac{(\xi+\mu)(\beta_1-\beta)(\xi+\mu)}{\upsilon} - \frac{\beta_2(B\upsilon-\mu\xi-\mu^2)}{\mu\upsilon} + (\Phi+\mu+\delta) + (\gamma+\mu)\Big)$

$+(\gamma+\mu)(\xi+\mu)\Big(\frac{(\beta-\beta_1)(\xi+\mu)}{\upsilon} + \frac{\beta_2(B\upsilon-\mu\xi-\mu^2)}{\mu\upsilon} - (\Phi+\mu+\delta)\Big) - \gamma p\Phi,$

$m_0 = -(\xi+\mu)\mu\left((\gamma p\Phi+\gamma+\mu)\Big(\frac{(\beta-\beta_1)(\xi+\mu)}{\upsilon} + \frac{\beta_2(B\upsilon-\mu\xi-\mu^2)}{\mu\upsilon} - (\Phi+\mu+\delta)\Big)\right).$

Therefore, the characteristic roots determined from polynomial equation (5.16) are

$\lambda_1 = -\mu, \quad \lambda_2 = -(\xi+\mu), \quad \lambda_3 = -\Big(\frac{f}{2} + \frac{(\gamma+\mu)}{2} + \frac{\sqrt{(f^2+2f(\gamma+\mu)+4p\gamma\Phi)}}{2}\Big),$

$\lambda_4 = -\Big(\frac{f}{2} + \frac{(\gamma+\mu)}{2} - \frac{\sqrt{(f^2+2f(\gamma+\mu)+4p\gamma\Phi)}}{2}\Big).$

with

$f = \frac{(\beta-\beta_1)(\xi+\mu)}{\upsilon} + \frac{\beta_2(B\upsilon-\mu\xi-\mu^2)}{\mu\upsilon} - (\Phi+\mu+\delta).$

Since all eigenvalues computed from polynomial equation (5.16) are negative, $\frac{f}{2} + \frac{(\gamma+\mu)}{2} > \frac{\sqrt{(f^2+2f(\gamma+\mu)+4p\gamma\Phi)}}{2}$, implying that $\frac{(\gamma+\mu)\Big(\frac{(\beta-\beta_1)(\xi+\mu)}{\upsilon} + \frac{\beta_2(B\upsilon-\mu\xi-\mu^2)}{\mu\upsilon}\Big)}{(\gamma+\mu)(\Phi+\mu+\delta)-p\Phi\gamma} < 1$, hence if condition $\Phi+\mu+\delta) > p\Phi\gamma$ hold, then $R_0 = \frac{(\gamma+\mu)\Big(\frac{(\beta-\beta_1)(\xi+\mu)}{\upsilon} + \frac{\beta_2(B\upsilon-\mu\xi-\mu^2)}{\mu\upsilon}\Big)}{(\gamma+\mu)(\Phi+\mu+\delta)-p\Phi\gamma} <$ 1, that is: $R_0 < 1$ implies that $\lambda_4 < 0$. Thus E_0^* is locally asymptotically stable.

Further, if $R_0 > 1$ then $\lambda_4 > 0$ which implies E_0^* is unstable. This completes the proof.

5.3.6 Local stability of endemic steady state

Proposition 5.3.4. *Suppose condition* $(\upsilon I^* + \mu)(\beta_2 I^* + \xi + \mu) > \upsilon I^*(\beta_2 I^* + \xi)$ *holds, then the endemic steady state* E^* *of model* (5.1) *is locally asymptotically stable in* D *for* $R_0 < 1$.

Proof. The variational matrix at E^* is given by

$$J(E^*) = \begin{pmatrix} a & \xi & c & 0 \\ \upsilon I^* & e & f & 0 \\ g & \beta_2 I^* & h & \gamma \\ 0 & 0 & l & -(\gamma+\mu) \end{pmatrix}. \tag{5.17}$$

where $a = -(\beta I^* - \frac{\beta_1 m I^*}{m+I^*} + \upsilon I^* + \mu)$, $f = -((p-1)\Phi - \upsilon S_u^* + \beta_2 S_a^*$, $e = -(\beta_2 I^* + \xi + \mu)$,
$c = -(\beta - \frac{\beta_1 m^2}{(m+I^*)^2} + \upsilon)S_u^*$, $g = (\beta I^* - \frac{\beta_1 m I^*}{(m+I^*)})S_u^*$, $l = \frac{p\Phi}{(1+\tau I^*)^2}$,
$h = \beta_2 S_a^* + (\beta - \frac{\beta_1 m^2}{(m+I^*)^2})S_u^* - \frac{\Phi}{(1+\tau I^*)^2} - (\Phi + \mu + \delta)$.
The characteristic equation associated to the variational matrix (5.17) is given by

$$|J(E^*) - \lambda I| = \lambda^4 + b_3\lambda^3 + b_2\lambda^2 + b_1\lambda + b_0 = 0. \tag{5.18}$$

with $b_3 = -(a + e + h - (\gamma + \mu))$,

$b_2 = h\Big(a + e\Big) - (\gamma + \mu)\Big(h + a\Big) + e\Big(a - (\gamma + \mu)\Big) - \Big(f\beta_2 I^* + \xi\upsilon I^* + \gamma l + cg\Big)$,

$b_1 = cg\Big(e - (\gamma + \mu)\Big) + f\beta_2 I^*\Big(a - (\gamma + \mu)\Big) + \Big(a + e\Big)\Big(\gamma l + h(\gamma + \mu)\Big) + \Big(h - (\gamma + \mu)\Big)\Big(\xi\upsilon I^* - ae\Big)$

$- \Big(\xi fg + c\upsilon\beta_2 I^{*2}\Big)$,

$b_0 = -\beta_2 I^*(\gamma+\mu)\Big(c\upsilon I^* - af\Big) - g(\gamma+\mu)\Big(\xi f - ce\Big) + \gamma l\Big(\xi\upsilon I^* - ae\Big)\Big(\gamma l + h(\gamma+\mu)\Big)$.

Evaluating the coefficients of polynomial equation (5.18) using parameter values in Table 5.2, we have

$b_3 = 2531.7, \quad b_2 = 10981, \quad b_1 = 3545.26, \quad b_0 = 2215.745.$

Thus polynomial equation (5.18), becomes

$\lambda^4 + 2531.7\lambda^3 + 10981\lambda^2 + 3545.26\lambda + 2215.745 = 0.$

Using polynomial function in MATLAB, the eigenvalues obtained are

$\lambda_1 = -0.7792, \lambda_2 = -248.64, \lambda_3 = -1.789 - 2.868i, \lambda_4 = -1.789 + 2.86i.$

Since $Re(\lambda_i) < 0$, the endemic steady state is locally asymptotically stable. This ends the proof.

5.4 Global stability of the equilibria

In this Section we deal with the global stability of steady states of model (5.1) using Lyapunov functionals with LaSalle's invariant principle. Since it is often hard to construct appropriate Lyapunov functions especially in epidemiological models with nonlinear and bilinear incidence rates, existing techniques for constructing Lyapunov functions have been improved see Vargas-De-León (2011). We propose the combination of quadratic and linear Lyapunov forms in the construction of Lyapunov function to prove a Theorem for global stability of disease–free steady state of the form

$U(x_1, x_2, x_3, x_4) = c\Big(\sum_{i=1}^{2} \frac{1}{2x_i^*}(x_i - x_i^*)^2\Big) + \sum_{i=3}^{4}(x_i - x_i^*)$.

where c is a positive constant, $\sum_{i=1}^{2} \frac{1}{2x_i^*}(x_i - x_i^*)^2$ represents a class containing susceptible population and $\sum_{i=3}^{4}(x_i - x_i^*)$ represents the remaining classes e.g infected and recovered. Whereas the Goh–Lotka–Voltera Logarithmic of the form $V(x_1, x_2, x_3, x_4) = c(\sum_{i=1}^{n}(x_i - x_i^* - x_i^* ln\frac{x_i}{x_i^*})$,
is used to prove the Theorem on global stability of the endemic steady state.

5.4.1 Global stability of the disease–free steady state

Theorem 5.4.1. *By Proposition 5.3.1, if the disease–free steady state E_0^* of model* (5.1) *is asymptotically stable, then E_0^* is globally asymptotically stable in D.*

Proof. Consider $U : D \to \mathbb{R}$ that is defined by

$$\begin{aligned} U(S_u, S_a, I, R) &= c\Big(\frac{1}{2S_u^0}(S_u - S_u^0)^2 + \frac{1}{2S_a^0}(S_a - S_a^0)^2 + (I - I_0)\Big) \\ &+ c(R - R^0). \end{aligned} \tag{5.19}$$

with $c = 1$. We find the derivative of the positive semidefinite function with respect to time along the solution of model system (5.1) to get

$$\begin{aligned} \frac{dU}{dt} &= \frac{S_u - S_u^0}{S_u^0}\dot{S}_u + \frac{S_a - S_a^0}{S_a^0}\dot{S}_a + \dot{I} + \dot{R}, \\ \frac{dU}{dt} &= \upsilon S_u I(\frac{S_a}{S_a^0} - \frac{S_u}{S_u^0}) + \xi S_a(\frac{S_u}{S_u^0} - \frac{S_a}{S_a^0}) + \frac{\phi I}{1+\tau I}(1-p)(2 + \frac{S_a}{S_a^0}) + \beta_2 S_a I(2 - \frac{S_a}{S_a^0}) \\ &+ (\beta - \frac{\beta_1 m}{m+I})(2 - \frac{S_u}{S_u^0})S_u I - \mu\Big(\frac{S_u^2}{S_u^0}(1 - \frac{S_u^0}{S_u}) + \frac{S_a^2}{S_a}(1 - \frac{S_a^0}{S_a}) + I + R\Big) - (\delta I + \gamma R), \\ \frac{dU}{dt} &\leq \beta_2 S_a I(2 - \frac{S_a}{S_a^0}) + \frac{S_a^2}{S_a}(1 - \frac{S_a^0}{S_a}) + (\beta - \frac{\beta_1 m}{m+I})(2 - \frac{S_u}{S_u^0})S_u I \\ &- \mu(I + R) - (\delta I + \gamma R). \end{aligned} \tag{5.20}$$

Lemma 5.4.1. *Let $a_1, a_2, \ldots, a_m$ be m positive numbers. The arithmetic mean $\bar{a} = \frac{a_1+a_2+\cdots+a_m}{m}$ is greater or equal to the geometric mean $\bar{a^*} = (a_1 \times a_2 \times \cdots \times a_m)^{\frac{1}{m}}$, that is $\bar{a} \geq \bar{a^*}$.* Applying Lemma 5.4.1 to equation (5.20), we have

$$\begin{aligned} \frac{dU}{dt} &\leq \beta_2 S_a I(2 - \frac{S_a}{S_a^0}) + \frac{S_a^2}{S_a}(1 - \frac{S_a^0}{S_a}) \\ &+ (\beta - \frac{\beta_1 m}{m+I})(2 - \frac{S_u}{S_u^0})S_u I. \end{aligned} \tag{5.21}$$

Thus, due to local stability of E_0 or E_1, then $\frac{dU}{dt} \leq 0$ for all $(S_u, S_a, I, R) \in D$. However, the strict equality $\frac{dU}{dt} = 0$ is valid for $S_u = S_u^0, S_a = S_a^0, I = 0$ and $R = 0$. Then the largest invariant set $\{(S_u, S_a, I, R) \in D : \frac{dU}{dt} = 0\}$ is reduced to the disease–free steady state E_0^*. Therefore, by the LaSalle's Invariance Principle LaSalle (1976) E_0^* is an attractive point that is globally asymptotically stable in D.□

5.4.2 Global stability of the endemic–steady state

Theorem 5.4.2. *If by Proposition 5.3.1, the unique endemic equilibrium of model* (5.1) *is asymptotically stable, then E^* is globally asymptotically stable in the interior of D.*

Proof. The Lyapunov function is defined as

$$\begin{aligned} W(S_u, S_a, I, R) &= c_1\Big(S_u - S_u^* - S_u^* \ln \frac{S_u}{S_u^*} + S_a - S_a^* - S_a^* \ln \frac{S_a}{S_a^*}\Big) \\ &+ c_2\Big(I - I^* - I^* \ln \frac{I}{I^*} + R - R^* - R^* \ln \frac{R}{R^*}\Big) \end{aligned} \tag{5.22}$$

with $c_1 = 1, c_2 = R_0 = \frac{(\gamma+\mu)}{(\Phi+\mu+\delta)(\gamma+\mu)-p\Phi\gamma}$.

Function W in (5.22) is defined, continuous and positive definite for all $S_u, S_a, I, R > 0$. Thus, the function $W(S_u, S_a, I, R)$ takes the value $W(S_u, S_a, I, R) = 0$ at the

steady state E^*, and the minimum value of $W(S_u, S_a, I, R)$ occurs at the endemic steady state E^*. We compute the derivative of W along the solution trajectories of model (5.1), as

$$\begin{aligned}
\dot{W} &= \dot{S}_u(1-\frac{S_u^*}{S_u}) + \dot{S}_a(1-\frac{S_a^*}{S_a}) + c_2\Big(\dot{I}(1-\frac{I^*}{I}) + \dot{R}(1-\frac{R^*}{R}\Big), \\
&= A(1-\frac{S_u^*}{S_u}) + \xi S_a^*(1-\frac{S_u^*}{S_u}) + g(I^*)S_u^*(\frac{S_u^*}{S_u}-1) + \upsilon I^* S_u^*(\frac{S_u^*}{S_u}-1) + \mu S_u^*(\frac{S_u^*}{S_u}-1) \\
&+ \upsilon I^* S_u^*(1-\frac{S_a^*}{S_a}) + (1-p)\phi T(I^*)(1-\frac{S_a^*}{S_a}) + \beta_2 I^* S_a^*(\frac{S_a^*}{S_a}-1) \\
&+ \xi S_a(\frac{S_a^*}{S_a}-1) + \mu S_a^*(\frac{S_a^*}{S_a}-1) + c_2\Big(g(I^*)S_u^*(1-\frac{I^*}{I}) + \beta_2 S_a^* I^*(1-\frac{I^*}{I}) \\
&+ \gamma R^*(1-\frac{I^*}{I}) + \phi T(I^*)(\frac{I^*}{I}-1) + (\mu+\delta)I^*(\frac{I^*}{I}-1) \\
&+ p\phi T(I^*)(1-\frac{R^*}{R}) + (\gamma+\mu)R^*(\frac{R^*}{R}-1)\Big). \qquad (5.23)
\end{aligned}$$

Since (S_u^*, S_a^*, I^*, R^*) is an endemic steady state of model (5.1), we have

$B = g(I^*)S_u^* + \upsilon I S_u^* + \mu S_u^* - \xi S_a^*$

and making a substitution of B in equation (5.23) and collecting like terms, we get

$$\begin{aligned}
\dot{W} &= I^* S_u^*\Big(\upsilon(1-\frac{S_a^*}{S_a}) + c_2(\beta - \frac{\beta_1 m}{m+I^*}\Big) - \mu(S_a(1-\frac{S_a^*}{S_a}) \\
&+ c_2 I^*\Big(1-\frac{I^*}{I}) + R^*(1-\frac{R^*}{R})\Big) + \frac{c_2\gamma R^{*2}}{R}(1-\frac{R}{R^*}\frac{I^*}{I}) \\
&+ \Phi T(I^*)p\frac{S_a^*}{S_a}(1-c_2\frac{R^*}{R}\frac{S_a}{S_a^*}) + \Phi T(I^*)(1-\frac{S_a^*}{S_a}) \\
&+ pc_2\Phi T(I^*) - \Phi T(I^*)c_2(1-\frac{I^*}{I}) - \delta c_2 I^*(1-\frac{I^*}{I}) \\
&+ \frac{\beta_2 S_a^{*2}}{S_a}(1-\frac{S_a}{S_a^*}\frac{I^*}{I}). \qquad (5.24)
\end{aligned}$$

$$\begin{aligned}\dot{W} &\leq \upsilon(1-\frac{S_a^*}{S_a})I^*S_u^* + R_0I^*\Big(1-\frac{I^*}{I}) + R^*(1-\frac{R^*}{R})\Big)\\ &+ \frac{R_0\gamma R^{*2}}{R}(1-\frac{R}{R^*}\frac{I^*}{I}) + \frac{\beta_2 S_a^{*2}}{S_a}(1-\frac{S_a}{S_a^*}\frac{I^*}{I})\\ &+ \Phi T(I^*)(1-\frac{S_a^*}{S_a}). \qquad (5.25)\end{aligned}$$

Hence since the arithmetic mean exceeds the geometric mean, we have
$(1-\frac{S_a^*}{S_a}) \leq 0$, $(1-\frac{R^*}{R}) \leq 0$ and $(1-\frac{I^*}{I}) \leq 0$.

We note that all model parameters are positive, therefore $\dot{W} \leq 0$ for $R_0 > 1$ and the equality holds if and only if $S_a^* = S_a$, $I^* = I$, $R^* = R$. Hence, W is a Lyapunov function on the interior of D, with the largest compact invariant subset of the set where $\dot{W} = 0$ is a singleton $\{(S_u, S_a, I, R) = S_u^*, S_a^*, I^*, R^*\}$. By LaSalle's invariance principle LaSalle (1976), it follows that the endemic equilibrium E^* of model (5.1) is globally asymptotically stable in the feasible region D if it exists.

5.4.3 Sensitivity analysis of model epidemiological parameters on the control reproduction number

In this section, model parameters are varied with respect to the control reproduction number, R_0 of model (5.1). Carrying out a sensitivity analysis of the model parameters will help us in identifying and verifying model epidemiological parameters that most affect the control reproduction number. Further, values obtained for sensitivity indexes indicate epidemiological parameters to be targeted for intervention purposes. The normalized forward sensitivity index technique is used to obtain the index of R_0 with respect to the parameters (Table 5.2). Hence, $\triangle_q^{R_0} = \frac{\partial R_0}{\partial q} \times \frac{q}{R_0}$, with R_0 =variable and q =A differentiable parameter.

Since the availability of literature and data especially on antibiotic resistance awareness of pneumococcal pneumonia is lacking, the qualitative predictions of our model (5.1) is dependent on estimating some of the epidemiological parameter

values Table 5.1.

Table 5.1: Parameters values

Parameter	Value/day^{-}1	Ref
B	5	assd
β	0.0417	(Opatowski et al., 2010)
β_1	0.0046	assd
β_2	0.000007498	assd
γ	0.00145	assd
μ	2.0×10^{-4}	(Kizito & Tumwiine, 2018)
m	0.5	assd
δ	0.1	(Ruhe & Hasbun, 2003; Henneman, 2012)
ξ	0.3	(Greenhalgh et al., 2015)
Φ	0.9	(Lipsitch, 2001)
D	1-14 days	(Pajuelo et al., 2018)
τ	0.2703	assd
p	$0 - 0.03$	(Obolski et al., 2015)
υ	0.0029	assd

From Table 5.2, the positive sign of sensitivity index of the control reproduction number with respect to the model parameters indicates that an increase (or decrease) in the value of each parameter in such a category will lead to an increase (or decrease) in the control reproduction number of the disease. Whereas the negative sign of sensitivity index of the control reproduction number with respect

Table 5.2: Sensitivity index (S.I) of R_0 w.r.t the parameters

Code	Parameter	S.I
1	β	+1.07189
2	β_1	-0.11824
3	β_2	+0.04635
4	p	+0.00079
5	ξ	+0.95282
6	υ	-0.95345
7	B	-0.13570
8	μ	-0.04621
9	δ	-0.10006
10	Φ	-0.89974
11	γ	+0.79958

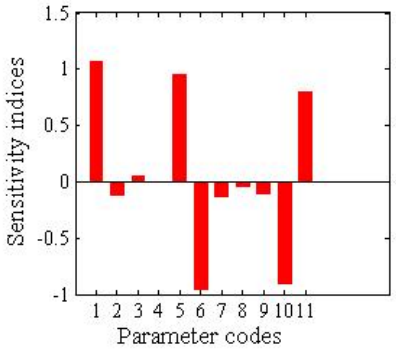

Figure 5.2: Sensitivity indices of R_0, in relation to epidemiological parameters.

to the model epidemiological parameters implies that, an increase (or decrease) in the value of the epidemiological parameter shall give rise to a corresponding decrease (or increase) in the control reproduction number. For instance in Figure 5.2 the sensitivity ($\triangle_{\xi}^{R_0} \approx 1$), means that, when ξ is increased (or decreased)

by 10%, increases or decreases R_0 by 10%. Further, Figure 5.2, shows that the control reproduction number is most sensitive to β, γ, ξ positively and υ, Φ negatively. Thus, with sensitivity analysis, one is able to get appropriate information on epidemiological parameters that can be targeted for intervention strategies that would help in preventing and controlling the transmission of pneumococcal pneumonia.

5.5 Model results and discussion

This Section deals with the numerical simulation results of model (5.1), that are carried out in MATLAB's standard solver for ODEs, the inbuilt function ode45. The function implements a Runge–Kutta method with variable time step for efficient computation. A discussion is also given. The epidemiological parameters chosen for the purpose of simulation are given in Table 5.1. The importance of R_0 is well demonstrated in all simulations. From Figure 5.3(a) the

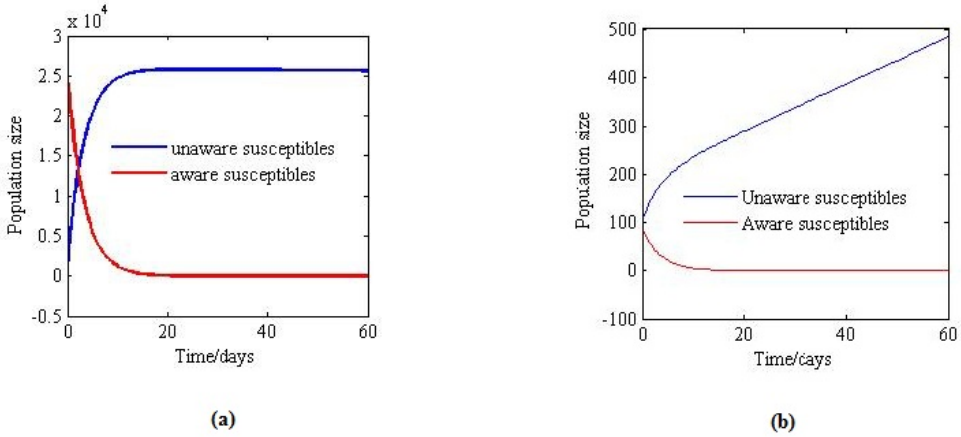

Figure 5.3: Stability of the disease–free steady state (a) With parameter values $\beta = 0.0001865$ and $\beta_1 = 0.00046$. (b) With parameter values $\beta = 0.0417, \gamma = 0.00145, \beta_1 = 0.046$ and $\beta_2 = 0.00007498$. Choosing initial values $S_u = 103, S_a = 24896, I = 0, R = 0$ and all the parameter values are the same as in Table 5.2

Unaware and Aware populations approach disease–free steady state with unaware

individuals maintaining a high number compared to the aware individuals. The control reproduction number is less than unity that is $R_0 = 0.3323 < 1$, thus the disease–free steady state is stable. The stability of the disease–free steady state means pneumococcus bacteria can completely be eliminated from the population and no more cases of pneumococcal pneumonia can be reported. Figure 5.3(b), shows that if $R_0 = 1.9258 > 1$, the disease–free steady state is unstable, implying that if one infected individual is introduced in a wholly susceptible population, infected cases would rise and more unaware individuals are at a risk of contracting pneumococcus bacteria. This would require control strategies to reduce the transmission of the disease at the earliest time possible.

Considering our main results in Section **??** and 5.4, Proposition 5.3.6 and Theorem 5.4.2 show that the endemic steady state is locally asymptotically stable since $Re(\lambda_i) < 0$ and globally stable if $R_0 > 1$. Figure 5.4(a), shows global stability

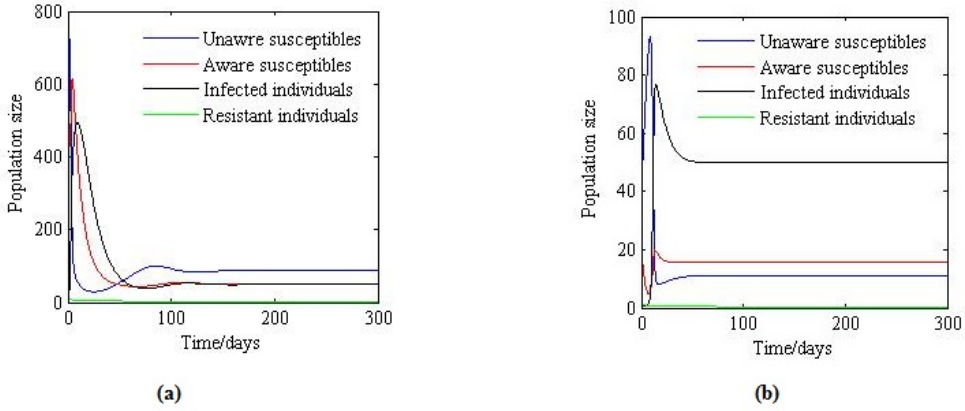

Figure 5.4: Stability of the endemic–steady state (a)Initial variables $S_u^* = 606, S_a^* = 581, I^* = 10, R^* = 8$. (b) Variables:$S_u^* = 40, S_a^* = 20, I^* = 1, R^* = 1$ Parameter values $\beta = 0.0417, \gamma = 0.00145, \beta_1 = 0.046$ and $\beta_2 = 0.00007498$. Initial values $S_u = 103, S_a = 24896, I = 0, R = 0$ and all the parameter values are the same as in Table 5.2

of all solution trajectories to an endemic steady state E^*. This implies that the pneumocccal pneumonia will continue to propagate in the population with few

infected individuals. Figure 5.4(b), shows that a unique endemic steady state is attained in the long run with more infected individuals. This implies that the pneumococcus bacteria could persist in the population, if no control measures are instituted to reduce the risks of acquiring the infections.

Figure 5.5(a), shows an exponential decay that is; the family of curves switches

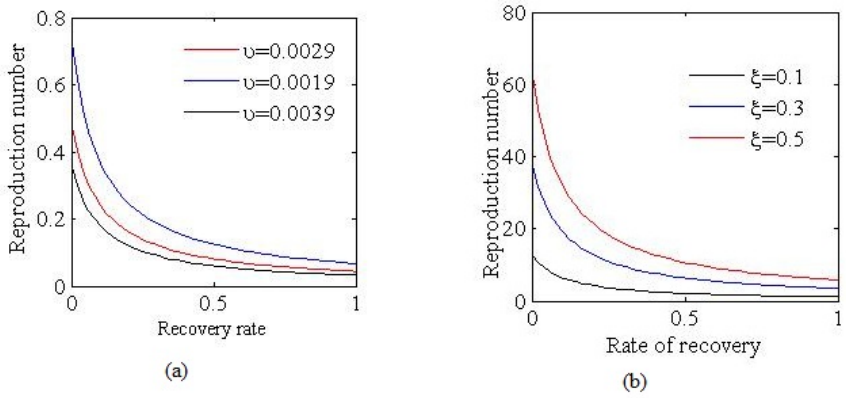

Figure 5.5: Effect of antibiotic resistance awareness and loss of information on awareness on the control reproduction number

due to the variation of private awareness from an increasing rate of growth to a decreasing rate, evidently suggesting the eradication of pneumococcus bacteria because of the presence of antibiotic resistance awareness and treatment.

Figure 5.5(b), shows effect of loss of information about antibiotic resistance awareness. An increase in the loss of information, implies an increase in numbers of infected individuals and the control reproduction number is high, however, due to the presence of treatment the disease is always eradicated from the population. On the other hand, reducing the loss of information implies that more individuals are aware of the transmission and are able to take control measures of the disease and reduce its spread.

Overall, a model for the effect of antibiotic resistance awareness and saturated treatment on the dynamics of pneumococcal pneumonia is developed and analyzed.

The basic reproduction number, R_0 for pneumococcal pneumonia prevalence, the conditions for existence and uniqueness of the equilibria are found. The result of Theorem 5.3.1, indicate that if $R_0 \leq 1$, the disease–free steady state E_0^* is locally asymptotically stable. Biologically, this means that pneumococcus bacteria cannot successfully invade the susceptible population thus, can easily be wiped out as time increases. This suggests that pneumococcal pneumonia can be controlled by ensuring R_0 is below unity. If $R_0 > 1$, then the disease–free steady state E_0^* is unstable, implying that the disease could manifest in the population and more cases might arise causing an epidemic.

The quadratic–linear and Goh–voltera Lyapunov functionals approaches are used to prove the global stabilities of the disease–free and endemic steady states respectively. The results show that the endemic steady state is globally stable if $R_0 > 1$.

To control pneumococcal pneumonia the results show that the family of decaying curves could help in providing mechanisms to design antibiotic awareness strategies about antibiotic resistance in order to reduce relapse of pneumococcal pneumonia. The threshold parameter R_0 could be reduced to less than unity if antibiotic resistance awareness and treatment are implemented simultaneously to ensure eradication of pneumococcus bacteria. Thus spread of pneumococcus pneumonia in the population will die out.

The next Chapter, gives the overall conclusion to the study and recommendations that could help in combating the severity of co–infection of IAV and pneumococcus and the pneumococcal pneumnia in humans.

CHAPTER 6

CONCLUSION AND RECOMMENDATIONS

6.1 Conclusion

In this study, it has been found out that influenza A virus and pneumococcus pathogens interaction with the epithelial target cells, result into acute infection known as bacterial pneumonia (pneumococcal disease) that is a concern to public health. The stability of steady states, co–existence and replacement of the two pathogens in the epithelial cell population calls for serious attention from public health sectors in order to avoid the 1918/1919 and 2009 pan endemic history repeating itself.

The models have shown achievement in predicting the outcome of IAV and pneumococcus co–infection within–host and the manifestation of pneumococcal pneumonia transmission between–host. The models strongly indicated that the spread of infection at largely depend on the contact rates with infected individuals within a population. The maximum number of bacteria an alveolar macrophage can catch, phagocytosis rate , number of infectious influenza A virus particles and pneumococcus liberated from lysis of infected cells and infection rates of pathogens are important parameters during the dynamics of IAV and pneumococcus co–infection. IAV and pneumococcus co–exist with–host affecting each other and give rise to a bifurcation state. The most virulent pathogen during the interaction of IAV and pneumococcus with the target cells is identified to be pneumococcus.

The model for pneumococcal pneumonia with time delay revealed that time delays in the latent stage and infected stage (delay by infected individuals to seek medical attention) during the spread of the disease give rise to Hopf–bifurcations. Larger delays lead to instabilities of the systems that maintains the infection in the population. Whereas small delays lead to the stability of the system implying that the infection can be wiped out in the population.

Pneumococcal pneumonia being a seasonal infection, it causes many death in children below five years of age and in the elderly. A mathematical model for pneumococcal pneumonia with antibiotic resistance awareness and saturated treatment revealed that such interventions are paramount in reducing the incidence in humans. For successful control of the disease in the population, it was found out that R_0 must be maintained below unity.

6.2 Recommendations

The findings from this study will be able to inform health providers, modelers, decision makers the level at which the co–infection is likely to affect the human population and devise appropriate policies and interventions to combat the disease. Health practitioners could develop educational workshops/conferences or training programmes to educate people about prevention and control strategies of influenza A and pneumococcal co–infection. Awareness programs through media and private awareness make individuals aware about the spread and control of a disease. Individuals are able to take various precautions (e.g. responding to vaccination programs, taking preventive medicine, vaccination, and taking medication timely and social distancing), to reduce their chances of being infected and re–infected

(relapsing).

For smooth control of pneumococcal pneumonia, there should not be much delay in seeking medical care by individuals, because there are high chances of individuals developing severe infections that require costly treatment. Organizing awareness campaign about antibiotic resistance during co–infections of viral–bacterial epidemics could be given priority to avoid persistence of the disease in the population.

This work will act as a podium for further research on 'viral–bacterial infections'. Researchers, should devise strategies to decrease the pathogen fitness R_{IP} to less than unity to help in prevention and control of pneumococcal establishment in a host that is already infected with influenza A virus. Disseminating up to date data on viral–bacterial interactions in humans within–host should be given priority.

6.3 Future research direction

Modeling viral–bacterial dynamics hasn't been given priority of study, that we believe new ideas in this study will improve research of infectious diseases. Indeed, there is much more research in modeling within–host co–infection that arise due to secondary infections than we could possibly cover here. However, we hope to have given a representative relish of the most innovative studies. Looking into the future, there are numerous areas where we feel modeling of within–host of dual pathogen interaction with an individual's internal systems can still make significant contributions. Clearly, as more quantitative data on the human host cells and immune response, both cellular and humoral, become available, it will be important to include these in the mechanistic in–host models of influenza A

virus and pneumococcus co–infection. This will be imperative to clarify the events during primary infection, and in the selection of appropriate vaccine in humans. Unifying the with–host and between–host co–infection models will give a better understanding of the spread of the disease.

Further, since time delays change the stability of dynamical systems it would be imperative to consider optimal control and cost effectiveness with time delays in the dynamics of pneumococcal pneumonia.

BIBLIOGRAPHY

Ackleh, A. S., & Allen, L. J. (2003). Competitive exclusion and coexistence for pathogens in an epidemic model with variable population size. *Journal of Mathematical Biology*, *47*(2), 153–168.

Agaba, G., Kyrychko, Y., & Blyuss, K. (2017). Time-delayed SIS epidemic model with population awareness. *Ecological Complexity*, *31*, 50–56.

Al Basir, F. (2018). Dynamics of infectious diseases with media coverage and two time delay. *Mathematical Models and Computer Simulations*, *10*(6), 770–783.

Al Basir, F., Ray, S., & Venturino, E. (2018). Role of media coverage and delay in controlling infectious diseases: A mathematical model. *Applied Mathematics and Computation*, *337*, 372–385.

Atkins, K. E., Lafferty, E. I., Deeny, S. R., Davies, N. G., Robotham, J. V., & Jit, M. (2017). Use of mathematical modelling to assess the impact of vaccines on antibiotic resistance. *The Lancet Infectious Diseases*, *18*(6), e204-e213.

Ayukekbong, J. A., Ntemgwa, M., & Atabe, A. N. (2017). The threat of antimicrobial resistance in developing countries: causes and control strategies. *Antimicrobial Resistance & Infection Control*, *6*(47), 1-8.

Baccam, P., Beauchemin, C., Macken, C. A., Hayden, F. G., & Perelson, A. S. (2006). Kinetics of influenza A virus infection in humans. *Journal of Virology*, *80*(15), 7590-7599.

Beauchemin, C. A., & Handel, A. (2011). A review of mathematical models of influenza A infections within a host or cell culture: lessons learned and challenges ahead. *BMC Public Health*, *11*(1), 1-15.

Beddington, J. R. (1975). Mutual interference between parasites or predators and its effect on searching efficiency. *The Journal of Animal Ecology*, 331–340.

Belser, J. A., Zeng, H., Katz, J. M., & Tumpey, T. M. (2011). Infection with highly pathogenic H7 influenza viruses results in an attenuated proinflammatory cytokine and chemokine response early after infection. *Journal of Infectious Diseases*, *203*(1), 40–48.

Bianca, C., Ferrara, M., & Guerrini, L. (2013). The time delays' effects on the qualitative behavior of an economic growth model. In *Abstract and applied analysis* (Vol. 2013).

Bichara, D., Iggidr, A., & Sallet, G. (2012). *Competitive exclusion principle for SIS and SIR models with n strains.* Unpublished doctoral dissertation, INRIA.

Bocharov, G., & Romanyukha, A. (1994). Mathematical model of antiviral immune response III. influenza A virus infection. *Journal of Theoretical Biology*, *167*(4), 323–360.

Bodnar, M. (2000). The nonnegativity of solutions of delay differential equations. *Applied Mathematics Letters*, *13*(6), 91–95.

Boianelli, A., Nguyen, V., Ebensen, T., Schulze, K., Wilk, E., & Sharma, N. (2015). Modeling influenza virus infection: a roadmap for influenza research. *Viruses*, *7*(10), 5274–5304.

Bosch, A. A., Biesbroek, G., Trzcinski, K., Sanders, E. A., & Bogaert, D. (2013). Viral and bacterial interactions in the upper respiratory tract. *Plos Pathogens*, *9*(1), 1-13.

Campo, R. E., Campo, C. E., Peter, G., Zuleta, J., Wahlay, N. A., & Cleary, T. (2005). Differences in presentation and outcome of invasive pneumococcal

disease among patients with and without HIV infection in the pre- HAARt era. *AIDS Patient Care & STDs*, *19*(3), 141–149.

Carrat, F., Vergu, E., Ferguson, N. M., Lemaitre, M., Cauchemez, S., & Leach, S. (2008). Time lines of infection and disease in human influenza: a review of volunteer challenge studies. *American Journal of Epidemiology*, *167*(7), 775–785.

Castillo-Chavez, C., Blower, S., Van Den Driessche, P., Kirschner, D., & Yakubu, A.-A. (2002). *Mathematical approaches for emerging and reemerging infectious diseases: an introduction* (Vol. 1). Springer Science & Business Media.

Castillo-Chavez, C., & Thieme, H. (1994). Asymptotically autonomous epidemic models.

Cauley, L. S., & Vella, A. T. (2015). Why is co-infection with influenza virus and bacteria so difficult to control? *Discovery Medicine*, *19*(102), 33-40.

Chang, D. B., & Young, C. S. (2007). Simple scaling laws for influenza A rise time, duration, and severity. *Journal of Theoretical Biology*, *246*(4), 621–635.

Chen, S., You, S., Liu, C., Chio, C., & Liao, C. (2012). Using experimental human influenza infections to validate a viral dynamic model and the implications for prediction. *Epidemiology & Infection*, *140*(9), 1557–1568.

Cheng, Y.-H., You, S.-H., Lin, Y.-J., Chen, S.-C., Chen, W.-Y., & Chou, W.-C. (2017). Mathematical modeling of postcoinfection with influenza A virus and streptococcus pneumoniae, with implications for pneumonia and COPD-risk assessment. *International Journal of Chronic Obstructive Pulmonary Disease*, *12*, 1973-1988.

Chertow, D. S., & Memoli, M. J. (2013). Bacterial coinfection in influenza: a grand rounds review. *Jama*, *309*(3), 275–282.

Chitnis, N., Hyman, J. M., & Cushing, J. M. (2008). Determining important parameters in the spread of malaria through the sensitivity analysis of a mathematical model. *Bulletin of mathematical biology*, *70*(5), 1272.

Chung, D. R., & Huh, K. (2015). Novel pandemic influenza A (H1N1) and community-associated methicillin-resistant Staphylococcus aureus pneumonia. *Expert Review of Anti-Infective Therapy*, *13*(2), 197–207.

Ciupe, S. M., & Heffernan, J. M. (2017). In-host modeling. *Infectious Disease Modelling*, *2*(2), 188–202.

Cooke, K. L., & Van Den Driessche, P. (1996). Analysis of an SEIRS epidemic model with two delays. *Journal of Mathematical Biology*, *35*(2), 240–260.

Cox, C. M., Blanton, L., Dhara, R., Brammer, L., & Finelli, L. (2011). 2009 Pandemic influenza A (H1N1) deaths among children-United states, 2009–2010. *Clinical Infectious Diseases*, *52*(S1), S69–S74.

Daşbaşı, B., & Öztürk, İ. (2016). Mathematical modelling of bacterial resistance to multiple antibiotics and immune system response. *SpringerPlus*, *5*(408), 1-17.

DeAngelis, D. L., Goldstein, R., & O'neill, R. (1975). A model for tropic interaction. *Ecology*, *56*(4), 881–892.

Din, Q., Ozair, M., Hussain, T., & Saeed, U. (2016). Qualitative behavior of a smoking model. *Advances in Difference Equations*, *2016*(1), 1-12.

Domínguez, Á., Ciruela, P., Hernández, S., García-García, J. J., Soldevila, N., & Izquierdo, C. (2017). Effectiveness of the 13-valent pneumococcal conjugate vaccine in preventing invasive pneumococcal disease in children aged 7-59 months. a matched case-control study. *Plos one*, *12*(8), e359-e369.

Elaiw, A., & Azoz, S. (2013). Global properties of a class of HIV infection models with Beddington–DeAngelis functional response. *Mathematical Methods in the Applied Sciences*, *36*(4), 383–394.

Erwin, S. H. (2017). *Mathematical models of immune responses to infectious diseases*. Unpublished doctoral dissertation, Virginia Tech.

Ferguson, L., Eckard, L., Epperson, W. B., Long, L.-P., Smith, D., & Huston, C. (2015). Influenza d virus infection in mississippi beef cattle. *Virology*, *486*, 28–34.

Gakkhar, S., & Chavda, N. (2012). A dynamical model for HIV–TB co-infection. *Applied Mathematics and Computation*, *218*(18), 9261–9270.

Ghoneim, H. E., Thomas, P. G., & McCullers, J. A. (2013). Depletion of alveolar macrophages during influenza infection facilitates bacterial superinfections. *The Journal of Immunology*, 1-11.

Gilchrist, M. A., Coombs, D., & Perelson, A. S. (2004). Optimizing within-host viral fitness: infected cell lifespan and virion production rate. *Journal of Theoretical Biology*, *229*(2), 281–288.

Gjorgjieva, J., Smith, K., Chowell, G., Sánchez, F., Snyder, J., & Castillo-Chavez, C. (2005). The role of vaccination in the control of SARS.

Greenhalgh, D., Rana, S., Samanta, S., Sardar, T., Bhattacharya, S., & Chattopadhyay, J. (2015). Awareness programs control infectious disease–Multiple delay induced mathematical model. *Applied Mathematics and Computation*, *251*, 539–563.

Griffiths, E. C., Pedersen, A. B., Fenton, A., & Petchey, O. L. (2014). Analysis of a summary network of co-infection in humans reveals that parasites interact

most via shared resources. *Proceedings of the Royal Society of London. Series B: Biological Sciences*, *281*(20132286), 1-9.

Guo, H., Li, M., & Shuai, Z. (2008). A graph-theoretic approach to the method of global Lyapunov functions. *Proceedings of the American Mathematical Society*, *136*(8), 2793–2802.

Hadjichrysanthou, C., Cauët, E., Lawrence, E., Vegvari, C., Wolf, F. de, & Anderson, R. M. (2016). Understanding the within-host dynamics of influenza A virus: from theory to clinical implications. *Journal of The Royal Society Interface*, *13*(119), 1-12.

Henneman, K. (2012). *Mathematical Modeling of Influenza and Secondary Bacterial Infection.* Unpublished doctoral dissertation, University of South Dakota.

Henriques-Normark, B., & Tuomanen, E. I. (2013). The pneumococcus: epidemiology, microbiology, and pathogenesis. *Cold Spring Harbor perspectives in medicine*, *3*(7), 1-15.

Hethcote, H. W. (2000). The mathematics of infectious diseases. *SIAM Review*, *42*(4), 599–653.

Hinrichsen, D., & Pritchard, A. J. (2005). *Mathematical systems theory I: modelling, state space analysis, stability and robustness* (Vol. 48). Springer Berlin.

Hirsch, M. W., Smale, S., & Devaney, R. L. (2012). *Differential equations, dynamical systems, and an introduction to chaos.* Academic press.

Hirsch, W. M., Hanisch, H., & Gabriel, J.-P. (1985). Differential equation models of some parasitic infections: methods for the study of asymptotic behavior. *Communications on Pure and Applied Mathematics*, *38*(6), 733–753.

Huang, G., Ma, W., & Takeuchi, Y. (2009). Global properties for virus dynamics model with beddington–deangelis functional response. *Applied Mathematics Letters*, *22*(11), 1690-1693.

Huang, G., Ma, W., & Takeuchi, Y. (2011). Global analysis for delay virus dynamics model with Beddington–DeAngelis functional response. *Applied Mathematics Letters*, *24*(7), 1199–1203.

Hussaini, N., Lubuma, J. M., Barley, K., & Gumel, A. (2016). Mathematical analysis of a model for AVL-HIV co-endemicity. *Mathematical Biosciences*, *271*, 80–95.

Iroh Tam, P.-Y., Sadoh, A. E., & Obaro, S. K. (2018). A meta-analysis of antimicrobial susceptibility profiles for pneumococcal pneumonia in sub-Saharan Africa. *Paediatrics and International Child Health*, *38*(1), 7–15.

Jiang, X., Yu, P., Yuan, Z., & Zou, X. (2009). Dynamics of an HIV-1 therapy model of fighting a virus with another virus. *Journal of Biological Dynamics*, *3*(4), 387–409.

Joseph, C., Togawa, Y., & Shindo, N. (2013). Bacterial and viral infections associated with influenza. *Influenza and other respiratory viruses*, *7*, 105–113.

Källander, K., Hildenwall, H., Waiswa, P., Galiwango, E., Peterson, S., & Pariyo, G. (2008). Delayed care seeking for fatal pneumonia in children aged under five years in Uganda: a case-series study. *Bulletin of the World Health Organization*, *86*, 332–338.

Kamal, R. P., Blanchfield, K., Belser, J. A., Music, N., Tzeng, W.-P., & Holiday, C. (2017). Inactivated H7 influenza virus vaccines protect mice despite low levels of neutralizing antibodies. *Journal of Virology*, *91*, 1-34.

Kandel, A., Bunke, H., & Last, M. (2007). *Applied graph theory in computer vision and pattern recognition.* Springer Science & Business Media.

Katz, M. A., Schoub, B. D., Heraud, J. M., Breiman, R. F., Njenga, M. K., & Widdowson, M.-A. (2012). *Influenza in Africa: uncovering the epidemiology of a long-overlooked disease.* Oxford University Press.

Khan, M. A., Islam, S., & Zaman, G. (2018). Media coverage campaign in Hepatitis B transmission model. *Applied Mathematics and Computation*, *331*, 378–393.

Kiem, S., & Schentag, J. J. (2013). Correlations between microbiological outcomes and clinical responses in patients with severe pneumonia. *Infection & Chemotherapy*, *45*(3), 283–291.

Kirui, W., Rotich, K. T., Jacob, B., & Lagat, C. R. (2015). Modeling the effects of time delay on HIV-1 in vivo dynamics in the presence of ARVs. *Science Journal of Applied Mathematics and Statistics*, *3*(4), 204-213.

Kizito, M., & Tumwiine, J. (2018). A mathematical model of treatment and vaccination interventions of pneumococcal pneumonia infection dynamics. *Journal of Applied Mathematics*, *2018*, 1-16.

Kollef, M. H., Sherman, G., Ward, S., & Fraser, V. J. (1999). Inadequate antimicrobial treatment of infections: a risk factor for hospital mortality among critically ill patients. *Chest*, *115*(2), 462–474.

Korobeinikov, A. (2007). Global properties of infectious disease models with nonlinear incidence. *Bulletin of Mathematical Biology*, *69*(6), 1871–1886.

Korobeinikov, A., & Maini, P. K. (2005). Non-linear incidence and stability of infectious disease models. *Mathematical Medicine and Biology: a Journal of the IMA*, *22*(2), 113–128.

Krishnapriya, P., Pitchaimani, M., & Witten, T. M. (2017). Mathematical analysis of an influenza A epidemic model with discrete delay. *Journal of Computational and Applied Mathematics*, *324*, 155–172.

Kuang, Y. (1993). *Delay differential equations: with applications in population dynamics* (Vol. 191). Academic press.

Laarabi, H., Labriji, E. H., Rachik, M., & Kaddar, A. (2012). Optimal control of an epidemic model with a saturated incidence rate. *Nonlinear Analysis: Modelling and Control*, *17*(4), 448–459.

Lakshmikantham, V., Leela, S., & Martynyuk, A. A. (1989). *Stability analysis of nonlinear systems*. Springer.

Lamb, K. E., Greenhalgh, D., & Robertson, C. (2011). A simple mathematical model for genetic effects in pneumococcal carriage and transmission. *Journal of Computational and Applied Mathematics*, *235*(7), 1812–1818.

LaSalle, J. P. (1976). *The stability of dynamical systems* (Vol. 25). Siam.

Lawi, G., Mugisha, J., & Ongati, O. N. (2013). Modeling co-infection of paediatric malaria and pneumonia. , *7*(9), 413-424.

Levy, B., Edholm, C., Gaoue, O., Kaondera-Shava, R., Kgosimore, M., & Lenhart, S. (2017). Modeling the role of public health education in Ebola virus disease outbreaks in Sudan. *Infectious Disease Modelling*, *2*(3), 323–340.

Li, L., Jin, Z., & Li, J. (2016). Periodic solutions in a herbivore-plant system with time delay and spatial diffusion. *Applied Mathematical Modelling*, *40*(7-8), 4765–4777.

Linda, J. A. (2007). *An introduction to mathematical biology.* Pearson Education Ltd.

Lindstrand, A. (2016). *Impact of pneumococcal conjugate vaccine on pneumococcal disease, carriage and serotype distribution: comparative studies in Sweden and Uganda*. Unpublished doctoral dissertation, Karolinska Institutet.

Lipsitch, M. (2001). Measuring and interpreting associations between antibiotic use and penicillin resistance in Streptococcus pneumoniae. *Clinical Infectious Diseases*, *32*(7), 1044–1054.

Liu, M., Chang, Y., & Zuo, L. (2016). Modelling the impact of media in controlling the diseases with a piecewise transmission rate. *Discrete Dynamics in Nature and Society*, *2016*, 1-6.

Lu, X., Wang, S., Liu, S., & Li, J. (2017). An SEI infection model incorporating media impact. *Mathematical Biosciences and Engineering*, *14*(5/6), 1317–1335.

Magombedze, G., Nduru, P., Bhunu, C. P., & Mushayabasa, S. (2010). Mathematical modelling of immune regulation of type 1 diabetes. *Biosystems*, *102*(2-3), 88–98.

Martcheva, M., Tuncer, N., & St Mary, C. (2015). Coupling within-host and between-host infectious diseases models. *Biomathematics*, *4*(2), 1-12.

Mathshidiso, M. (2018). Antibiotic resistance is a grave threat to future of global health.

May, R. M., & Anderson, R. M. (1983). Epidemiology and genetics in the coevolution of parasites and hosts. *Proceeding to the Royal Society London. Series B, Biological Sciences*, *219*(1216), 281–313.

May, R. M., & Nowak, M. A. (1995). Coinfection and the evolution of parasite virulence. *Proceeding of the Royal Society London B*, *261*(1361), 209–215.

Mbabazi, F. K., Mugisha, J. Y. T., & Kimathi, M. (2018). Modeling the within-host co-infection of influenza A virus and pneumococcus. *Applied Mathematics and Computation*, *339*, 488–506.

McArdle, A. J., Turkova, A., & Cunnington, A. J. (2018). When do co-infections matter? *Current Opinion in Infectious Diseases*, *31*(3), 209–215.

McCullers, J. A. (2004). Effect of antiviral treatment on the outcome of secondary bacterial pneumonia after influenza. *Journal of Infectious Diseases*, *190*(3), 519–526.

McCullers, J. A. (2006). Insights into the interaction between influenza virus and pneumococcus. *Clinical Microbiology Reviews*, *19*(3), 571–582.

McCullers, J. A. (2011). Preventing and treating secondary bacterial infections with antiviral agents. *Antiviral Therapy*, *16*(2), 123-135.

Melegaro, A., Choi, Y. H., George, R., Edmunds, W. J., Miller, E., & Gay, N. J. (2010). Dynamic models of pneumococcal carriage and the impact of the heptavalent pneumococcal conjugate vaccine on invasive pneumococcal disease. *BMC Infectious Diseases*, *10*, 1-15.

Metersky, M. L., Masterton, R. G., Lode, H., File Jr, T. M., & Babinchak, T. (2012). Epidemiology, microbiology, and treatment considerations for bacterial pneumonia complicating influenza. *International Journal of Infectious Diseases*, *16*(5), e321–e331.

Metzger, D. W., Furuya, Y., Salmon, S. L., Roberts, S., & Sun, K. (2015). Limited efficacy of antibacterial vaccination against secondary serotype 3 pneumococcal pneumonia following influenza infection. *The Journal of Infectious Diseases*, *212*(3), 445–452.

Mina, M. J., & Klugman, K. P. (2014). The role of influenza in the severity and transmission of respiratory bacterial disease. *The Lancet Respiratory Medicine*, *2*(9), 750-763.

Mina, M. J., Klugman, K. P., & McCullers, J. A. (2013). Live attenuated influenza vaccine, but not pneumococcal conjugate vaccine, protects against increased density and duration of pneumococcal carriage after influenza infection in pneumococcal colonized mice. *The Journal of Infectious Diseases*, *208*(8), 1281–1285.

Misra, A., Mishra, S., Pathak, A., Misra, P., & Naresh, R. (2012). Modeling the effect of time delay in controlling the carrier dependent infectious disease–cholera. *Applied Mathematics and Computation*, *218*(23), 11547–11557.

Misra, A., Sharma, A., & Singh, V. (2011). Effect of awareness programs in controlling the prevalence of an epidemic with time delay. *Journal of Biological Systems*, *19*(02), 389–402.

Morris, D. E., Cleary, D. W., & Clarke, S. C. (2017). Secondary bacterial infections associated with influenza pandemics. *Frontiers in Microbiology*, *8*(1041), 1-17.

Mosquera, J., & Adler, F. R. (1998). Evolution of virulence: a unified framework for coinfection and superinfection. *Journal of Theoretical Biology*, *195*(3), 293–313.

Nagy, L. D. (2011). *Epidemic models with pulse vaccination and time delay.* Unpublished master's thesis, University of Waterloo.

Nair, H., Brooks, W. A., Katz, M., Roca, A., Berkley, J. A., & Madhi, S. A. (2011). Global burden of respiratory infections due to seasonal influenza in young children: a systematic review and meta-analysis. *The Lancet*, *378*(9807), 1917–1930.

Ngari, C. G., Malonza, D. M., & Muthuri, G. G. (2014). A model for childhood pneumonia dynamics. *Journal of Life Sciences Research*, *1*(2), 31-40.

Ngari, C. G., Pokhariyal, G., & Koske, J. (2016). Analytical model for childhood pneumonia, a case study of Kenya. *British Journal of Mathematics & Computer Science*, *12*, 1-28.

Nthiiri, J. K., Lavi, G., & Mayonge, A. (2015). Mathematical model of pneumonia and HIV/AIDS co-infection in the presence of protection. *International Journal of Mathematical Analysis*, *9*(42), 2069–2085.

Obolski, U., Stein, G. Y., & Hadany, L. (2015). Antibiotic restriction might facilitate the emergence of multi-drug resistance. *Plos Computational Biology*, *11*(6), 1-15.

O'Brien, K. L., Wolfson, L. J., Watt, J. P., Henkle, E., Deloria-Knoll, M., & McCall, N. (2009). Burden of disease caused by Streptococcus pneumoniae in children younger than 5 years: global estimates. *The Lancet*, *374*(9693), 893–902.

Ojosnegros, S., Delgado-Eckert, E., & Beerenwinkel, N. (2012). Competition–colonization trade-off promotes coexistence of low-virulence viral strains. *Journal of The Royal Society Interface*, *9*(74), 2244-2254.

Okeke, I. N., Lamikanra, A., & Edelman, R. (1999). Socioeconomic and behavioral factors leading to acquired bacterial resistance to antibiotics in developing countries. *Emerging Infectious Diseases*, *5*(1), 18-27.

Opatowski, L., Baguelin, M., & Eggo, R. M. (2018). Influenza interaction with cocirculating pathogens and its impact on surveillance, pathogenesis, and epidemic profile: A key role for mathematical modelling. *Plos Pathogens*, *14*(2), 1-28.

Opatowski, L., Mandel, J., Varon, E., Boëlle, P.-Y., Temime, L., & Guillemot, D. (2010). Antibiotic dose impact on resistance selection in the community: a mathematical model of β-lactams and Streptococcus pneumoniae dynamics. *Antimicrobial Agents and Chemotherapy*, *54*(6), 2330–2337.

Pajuelo, M. J., Huaynate, C. A., Correa, M., Malpartida, H. M., Asayag, C. R., & Seminario, J. R. (2018). Delays in seeking and receiving health care services for pneumonia in children under five in the Peruvian Amazon: a mixed-methods study on caregivers' perceptions. *BMC Health Services Research*, *18*(149), 1-11.

Pawelek, K. A., Dor Jr, D., Salmeron, C., & Handel, A. (2016). Within-host models of high and low pathogenic influenza virus infections: The role of macrophages. *Plos One*, *11*(2), 1-16.

Pradeu, T. (2016). Mutualistic viruses and the heteronomy of life. *Studies in History and Philosophy of Science Part C: Studies in History and Philosophy of Biological and Biomedical Sciences*, *59*, 80–88.

Radin, J. M., Katz, M. A., Tempia, S., Talla Nzussouo, N., Davis, R., & Duque, J. (2012). Influenza surveillance in 15 countries in Africa, 2006–2010. *The Journal of Infectious Diseases*, *206*(S1), S14–S21.

Rao, P. R. S., & Kumar, M. N. (2015). A dynamic model for infectious diseases: The role of vaccination and treatment. *Chaos, Solitons & Fractals*, *75*, 34–49.

Redman, S., Spencer, E. A., & Sanson-Fisher, R. W. (1990). The role of mass media in changing health-related behaviour: a critical appraisal of two models. *Health Promotion International*, *5*(1), 85–101.

Rémy, V., Largeron, N., Quilici, S., & Carroll, S. (2015). The economic value of vaccination: why prevention is wealth. *Journal of Market Access & Health Policy*, *3*(1), 1-3.

Resti, M., Micheli, A., Moriondo, M., Becciolini, L., Cortimiglia, M., & Canessa, C. (2009). Comparison of the effect of antibiotic treatment on the possibility of diagnosing invasive pneumococcal disease by culture or molecular methods: a prospective, observational study of children and adolescents with proven pneumococcal infection. *Clinical Therapeutics*, *31*(6), 1266–1273.

Rigaud, T., Perrot-Minnot, M.-J., & Brown, M. J. (2010). Parasite and host assemblages: embracing the reality will improve our knowledge of parasite transmission and virulence. *Proceedings of the Royal Society B: Biological Sciences*, *277*(1701), 3693–3702.

Roberts, M., Andreasen, V., Lloyd, A., & Pellis, L. (2015). Nine challenges for deterministic epidemic models. *Epidemics*, *10*, 49–53.

Rodgers, G. L., & Klugman, K. P. (2016). Surveillance of the impact of pneumococcal conjugate vaccines in developing countries. *Human Vaccines & Immunotherapeutics*, *12*(2), 417–420.

Ruhe, J. J., & Hasbun, R. (2003). Streptococcus pneumoniae bacteremia: duration of previous antibiotic use and association with penicillin resistance. *Clinical Infectious Diseases*, *36*(9), 1132–1138.

Rynda-Apple, A., Robinson, K. M., & Alcorn, J. F. (2015). Influenza and bacterial super-infection: illuminating the immunologic mechanisms of disease. *Infection and Immunity*, *83*, 3764-3770.

Samanta, G., Sen, P., & Maiti, A. (2016). A delayed epidemic model of diseases through droplet infection and direct contact with saturation incidence and pulse vaccination. *Systems Science & Control Engineering*, *4*(1), 320–333.

Samuel, O., Edgar, D.-E., & Niko, B. (2012, April). Competition - colonization

trade-off promotes coexistence of low-virulence viral strains. *Royal Society Interface*, *9*(74), 2244-2254.

Schrag, S. J., Beall, B., Dowell, S., Organization, W. H., et al. (2001). *Resistant pneumococcal infections: the burden of disease and challenges in monitoring and controlling antimicrobial resistance* (Tech. Rep.). Geneva: World Health Organization.

Shi, W., Lei, F., Zhu, C., Sievers, F., & Higgins, D. G. (2010). A complete analysis of HA and NA genes of influenza A viruses. *Plos One*, *5*(12), 1-15.

Shrestha, S., Foxman, B., Dawid, S., Aiello, A. E., Davis, B. M., & Berus, J. (2013). Time and dose-dependent risk of pneumococcal pneumonia following influenza: a model for within-host interaction between influenza and streptococcus pneumoniae. *Journal of The Royal Society Interface*, *10*(86), 1-9.

Shuai, Z., & Driessche, P. van den. (2013). Global stability of infectious disease models using Lyapunov functions. *SIAM Journal on Applied Mathematics*, *73*(4), 1513–1532.

Smith, A. M. (2017). Quantifying the therapeutic requirements and potential for combination therapy to prevent bacterial coinfection during influenza. *Journal of Pharmacokinetics and Pharmacodynamics*, *44*(2), 81–93.

Smith, A. M., Adler, F. R., Ribeiro, R. M., Gutenkunst, R. N., McAuley, J. L., & McCullers, J. A. (2013). Kinetics of coinfection with influenza A virus and Streptococcus pneumoniae. *Plos Pathogens*, *9*(3), 1-13.

Smith, A. M., & Smith, A. P. (2016). A critical, nonlinear threshold dictates bacterial invasion and initial kinetics during influenza. *Scientific Reports*, *6*, 1-11.

Song, Y., & Wei, J. (2004). Bifurcation analysis for Chen's system with delayed feedback and its application to control of chaos. *Chaos, Solitons & Fractals*, *22*(1), 75–91.

Sun, G.-Q., Wang, S.-L., Ren, Q., Jin, Z., & Wu, Y.-P. (2015). Effects of time delay and space on herbivore dynamics: linking inducible defenses of plants to herbivore outbreak. *Scientific Reports*, *5*, 1-10.

Sun, G.-Q., Xie, J.-H., Huang, S.-H., Jin, Z., Li, M.-T., & Liu, L. (2017). Transmission dynamics of cholera: Mathematical modeling and control strategies. *Communications in Nonlinear Science and Numerical Simulation*, *45*, 235–244.

Sutton, K. L., Banks, H. T., & Castillo-Chávez, C. (2007). *Estimation of invasive pneumococcal disease dynamics parameters and the impact of conjugate vaccination in Australia* (Tech. Rep.). North Carolina State University. Center for Research in Scientific Computation.

Thieme, H. (2003). Mathematics in population biology. *Princeton and Oxford: Princeton University Press Google Scholar*.

Tilahun, G. T., Makinde, O. D., & Malonza, D. (2017). Modelling and optimal control of pneumonia disease with cost-effective strategies. *Journal of Biological Dynamics*, *11*(1), 400–426.

Van Den Driessche, P., Wang, L., & Zou, X. (2007). Modeling diseases with latency and relapse. *Mathematical Biosciences and Engineering*, *4*(2), 205-219.

Van Den Driessche, P., & Watmough, J. (2002). Reproduction numbers and sub-threshold endemic equilibria for compartmental models of disease transmission. *Mathematical Biosciences*, *180*(1), 29-48.

Van Den Driessche, P., & Watmough, J. (2008). Further notes on the basic reproduction number. In *Mathematical epidemiology* (pp. 159–178). Springer.

Vargas-De-León, C. (2011). On the global stability of SIS, SIR and SIRS epidemic models with standard incidence. *Chaos, Solitons & Fractals*, *44*(12), 1106–1110.

Waheed, M. T., Sameeullah, M., Khan, F. A., Syed, T., Ilahi, M., & Gottschamel, J. (2016). Need of cost-effective vaccines in developing countries: What plant biotechnology can offer? *SpringerPlus*, *5*(1), 1-9.

Wahl, B., O'Brien, K. L., Greenbaum, A., Majumder, A., Liu, L., & Chu, Y. (2018). Burden of Streptococcus pneumoniae and Haemophilus influenzae type B disease in children in the era of conjugate vaccines: global, regional, and national estimates for 2000–15. *The Lancet Global Health*, *6*(7), e744–e757.

Walker, C. L. F., Rudan, I., Liu, L., Nair, H., Theodoratou, E., Bhutta, Z. A., et al. (2013). Global burden of childhood pneumonia and diarrhoea. *The Lancet*, *381*(9875), 1405-1416.

Watanabe, Y., Ibrahim, M. S., Suzuki, Y., & Ikuta, K. (2012). The changing nature of avian influenza A virus (H5N1). *Trends in Microbiology*, *20*(1), 11–20.

Weinberger, D. M., Harboe, Z. B., Viboud, C., Krause, T. G., Miller, M., & Mølbak, K. (2014). Pneumococcal disease seasonality: incidence, severity and the role of influenza activity. *European Respiratory Journal*, *43*(3), 833–841.

White, A. N., Ng, V., Spain, C. V., Johnson, C. C., Kinlin, L. M., & Fisman, D. N. (2009). Let the sun shine in: effects of ultraviolet radiation on invasive pneumococcal disease risk in Philadelphia, Pennsylvania. *BMC Infectious Diseases*, *9*(1), 196.

Xing, Y., Song, L., Sun, G.-Q., Jin, Z., & Zhang, J. (2017). Assessing reappearance factors of H7N9 avian influenza in China. *Applied Mathematics and Computation*, *309*, 192–204.

Xu, R., & Ma, Z. (2010). Global stability of a delayed SEIRS epidemic model with saturation incidence rate. *Nonlinear Dynamics*, *61*(1-2), 229–239.

Xu, R., Wang, Z., & Zhang, F. (2015). Global stability and Hopf bifurcations of an SEIR epidemiological model with logistic growth and time delay. *Applied Mathematics and Computation*, *269*, 332–342.

Yang, X., Chen, L., & Chen, J. (1996). Permanence and positive periodic solution for the single-species nonautonomous delay diffusive models. *Computers & Mathematics with Applications*, *32*(4), 109–116.

Zhang, X., & Liu, X. (2008). Backward bifurcation of an epidemic model with saturated treatment function. *Journal of Mathematical Analysis and Applications*, *348*(1), 433–443.

Zhao, H., Lin, Y., & Dai, Y. (2014). An sirs epidemic model incorporating media coverage with time delay. *Computational and Mathematical Methods in Medicine*, *2014*, 1-10.

Zhao, H., & Zhao, M. (2017). Global Hopf bifurcation analysis of an susceptible-infective-removed epidemic model incorporating media coverage with time delay. *Journal of Biological Dynamics*, *11*(1), 8–24.

Zhonghua, Z., & Yaohong, S. (2010). Qualitative analysis of a SIR epidemic model with saturated treatment rate. *Journal of Applied Mathematics and Computing*, *34*(1-2), 177–194.

Zuo, L., & Liu, M. (2014). Effect of awareness programs on the epidemic outbreaks with time delay. *Abstract and Applied Analysis*, *2014*, 1-8.

APPENDICES

Appendix A1: Coefficients to polynomial equation (3.37)

$h_6 = 1, h_5 = (\mu_{vb} + (\alpha_v + \delta_b) - (k_0 + k_3 + k_5 + k_6), h_4 = L_4 + \xi_4, h_3 = L_3 + \xi_3, h_2 = L_2 + \xi_2, h_1 = L_1 + \xi_1, h_0 = L_0 + \xi_0$

$L_4 = k_0\Big(k_3 + k_5 - (\alpha_b + \delta_v) - \mu_{vb} + k_6\Big) + k_3\Big(k_5 - \mu_{vb} + k_6 - (\alpha_b + \delta_v)\Big) + k_5(-\mu_{vb} - k_6(\mu_{vb} + \alpha_b) + \mu_b(\alpha_b + \delta_v) - k_4\tau_v n_v,$

$L_3 = \beta_v^* I_b \tau_{vb} n_{vb}(k_0 + k_3 + k_6 + k_5) + (\mu_{vb}k_6(k_5 - k_0 + (\alpha_b + \delta_v) - k_3) + k_0\mu_{vb}((\alpha_b + \delta_v) - k_5) - (\alpha_b + \alpha_v)(-\mu_{vb} + k_6) + k_4\beta_b B^* \tau_{vb} n_{vb},$

$L_2 = k_0k_3k_5(-\mu_{vb}+k_6-(\alpha_b+\delta_v))-\beta_v^* I_b\beta_v^* V^*\tau_{vb}n_{vb}(k_0+k_6+k_3)+k_6k_0(\beta_v^* I_b^*\tau_{vb}n_{vb}-k_0k_3k_6(\mu_{vb}+(\alpha_b+\delta_v))-\beta_b S^*\beta_b B^*\tau_b n_b(-(\alpha_b+\delta_v)-\mu_{vb}+k_3)+\beta_b S^*\tau_b n_b(k_4\tau_v n_v+\beta_v^* I_b\tau_{vb}n_{vb})+k_6k_5\mu_{vb}\tau_v n_v-k_1\tau_{vb}n_{vb}(k_2\beta_b^* B^* + \beta_b B^*\beta_v^* V^*),$

$L_1 = \tau_b n_b\beta_b S^*\mu_{vb}(\alpha_b+\delta_v)-\beta_b S^*\beta_v^* I_b^*\tau_b n_b\tau_{vb}n_{vb})(k_3+k_0)+\beta_v^* V^*\tau_{vb}n_{vb}(k_1\beta_b B^*+k_0\beta_v^* I_b^*)(k_6+k_3)+\tau_{vb}n_{vb}\beta_b^* B^*(k_1k_2-k_0k_4)(k_5+k_6)+\beta_b S^*\tau_b n_b(k_4\beta_b^* B^*\tau_{vb}n_{vb}+k_1k_2\tau_v n_v)+k_0k_3k_5\mu_{vb}(k_6-(\alpha_b+\delta_v))-\beta_b S^*\beta_b^* B^*\mu_{vb}\tau_b n_b(k_3-(\alpha_b+\delta_v))+k_3k_5k_6(\alpha_b+\delta_v)(k_0-\mu_{vb})-\beta_b^* I_v^*\tau_{vb}n_{vb}(k_1\beta_b B^*\tau_b n_b)-k_4\beta_b S^*\tau_b n_b\tau_v n_v(k_0-\mu_{vb})+k_2\beta_b S^*\tau_b^2 n_b^2\tau_v n_v,$

$L_0 = \beta_v^* I_b\tau_{vb}n_{vb}\tau_b n_b\beta_b^2 S^*B^*+k_3\tau_{vb}n_{vb}(k_1\beta_b B^*+k_0\beta_v^* I_b)(\beta_b^*\tau_b n_b-\beta_v^* k_6)+k_0\beta_b\tau_b n_b-k_1k_2k_5k_6+k_0k_4k_5k_6-k_0k_3k_5k_6\beta_v^* I_b\tau_{vb}n_{vb}-k_3\tau_b n_b\beta_b S^*\mu_{vb}(\alpha_b+\delta_v),$

$\xi_4 = -(\alpha_b + \delta_v) + k_6\delta_v - (\beta_v^*\tau_{vb}n_{vb} + \beta_b S^*\tau_b n_b)$

$\xi_3 = k_4\tau_v n_v\Big(k_0 + k_5 - \mu_{vb} + k_6 + k_3\Big) + \beta_b S^*\tau_b n_b(k_0 - \mu_{vb} - (\alpha_b + \delta_v)) - k_5(\alpha_b + \delta_v)(-\mu_{vb} + k_0 + k_3 + k_6) + k_0k_3(-\mu_{vb} + k_6 - (\alpha_b + \delta_v) + k_5) + k_5k_6(k_3 + k_0) + k_1k_2\tau_v n_v - \beta_b S^*\beta_b B^*\tau_b n_b - k_3k_5\mu_{vb} - k_0k_6(\alpha_b + \delta_v) - \beta_v^* I_b\beta_v^* V^*\tau_{vb}n_{vb}\Big),$

$\xi_2 = k_5\mu_{vb}(\alpha_b+\delta_v)(k_0+k_6)+k_1k_2\tau_v n_v(k_5+k_6-\mu_{vb})-k_0k_5k_6\Big(\alpha_b+\delta_v)+(k_0+k_3)\Big)+(k_3\mu_{vb}(\alpha_b+\delta_v) + k_4(\beta_b^* B^*\tau_{vb}n_{vb} - k_0\tau_v n_v))(k_5 + k_6 + k_0) + k_5\mu_{vb}\tau_v n_v(k_4) + k_0\beta_v^*\tau_{vb}n_{vb}(k_5 + k_3 + k_6) + k_6\beta_v^*\tau_{vb}n_{vb}(k_5+k_3)+\beta_b S^*\tau_b n_b\Big(-(\alpha_b+\delta_v)(k_0-\mu_{vb})+k_3(k_0-(\alpha_b+\delta_v)-\mu_{vb})\Big)-k_0\mu_{vb}(\beta_b S^*\tau_b n_b+k_6(\alpha_b + \delta_v)) - \beta_v^* I_b\tau_b n_b(-\beta_b^* I_v^*\tau_v n_v + \beta_b^* I_v^*\tau_{vb}n_{vb}) - k_4\mu_{vb}k_6\tau_v n_v + k_3k_5\beta_v^* V^*\tau_{vb}n_{vb}\Big),$

$\xi_1 = k_0k_3\beta_b S^*\tau_b n_b\Big(-\mu_{vb} - (\alpha_b + \delta_v)\Big) + k_0k_4k_6\tau_v n_v(-\mu_{vb} + k_5) + \mu_{vb}(\alpha_b + \delta_v)(k_3 + k_5) + \beta_b^* I_v^*\beta_v^* I_b^*\tau_b n_b\tau_v n_v(-\mu_{vb} + k_0) - \beta_v^* I_b^*\beta_b^* I_v^*\tau_{vb}n_{vb}\tau_b n_b + k_5(k_3\beta_v^* I_b^*\tau_{vb}n_{vb} - k_4\mu_{vb}\tau_v n_v)(k_6 + k_0) - \beta_b S^*\tau_b n_b\beta_b B^*\Big(k_4\tau_v n_v + \beta_v^* I_b^*\tau_{vb}n_{vb}\Big) - k_1k_2k_5\tau_v n_v(-\mu_{vb} + k_6) - k_1\beta_b B^*\tau_b n_b\Big(-\beta_b^* I_v^*\tau_v n_v\Big) + \beta_b S^*\tau_b n_b k_3\beta_b B^*(\alpha_b + \delta_v) - \beta_v^*\tau_{vb}n_{vb}(\beta_b^{*2}B^*\tau_b n_b + k_3k_6\beta_v^*) - k_6(k_4k_5\beta_b^* B^*\tau_{vb}n_{vb} + k_1k_2\mu_{vb}\tau_v n_v),$

$\xi_0 = (k_0\beta_b^* I_v^*\beta_v^* I_b + k_0k_4k_5k_6)(\beta_b^* B^*\tau_{vb}n_{vb}+\mu_{vb}\tau_v n_v)+k_3k_5k_6\mu_{vb}(\alpha_b+\delta_v)+k_0\tau_{vb}n_{vb}\tau_b n_b\beta_b S^*\beta_v^* I_b - k_1\tau_b^2 n_b^2\beta_b S^*(k_4\beta_b B^*+k_2\beta_v^* I_b)(\beta_b^* B^*\tau_{vb}n_{vb}+\mu_{vb}\tau_v n_v)(\mu_{vb}\tau_v n_v+\beta_b^* B^*\tau_{vb}n_{vb})(\beta_b^* I_v^*\beta_b B^*+k_2\beta_b B^*),$

Appendix A2: Illustrations of proving Theorem 3.7.4

We note that, function $L(X)$ satisfies

$\frac{\partial L(X)}{\partial S} = 1 - [\frac{\beta_v S^* V^*}{1+aS^*+bV^*}(\frac{1+a\phi+bV^*}{\beta_v\phi V^*}) + \frac{\beta_b S^* B^*}{\beta_b\phi B^*}]_{S^*}^{S},$

$\frac{\partial L(X)}{\partial S} = 1 - (\frac{S^*}{S}(\frac{1+aS+bV^*}{1+aS^*+bV^*} + 1) - \frac{S^*}{S^*}(\frac{1+aS^*+bV^*}{1+aS^*+bV^*} + 1))$

$\frac{\partial L(X)}{\partial S} = 1 - (\frac{S^*}{S}\frac{(1+aS+bV^*)}{1+aS^*+bV^*}) - \frac{S^*}{S} + 2)$

$\frac{\partial L(X)}{\partial S} = 3 - \frac{S^*}{S}\frac{1+aS+bV^*}{1+aS^*+bV^*} - \frac{S^*}{S} = 3 - \frac{f_1(S^*,V^*)}{f_1(S,V^*)} - \frac{S^*}{S}$

$\frac{\partial L(X)}{\partial I_v} = 1 - \frac{I_v^*}{I_v}, \frac{\partial L(X)}{\partial I_B} = 1 - \frac{I_b^*}{I_b}, \frac{\partial L(X)}{\partial I_{vb}} = 1 - \frac{I_{vb}^*}{I_{vb}}, \frac{\partial L(X)}{\partial B} = 1 - \frac{I_b^*}{B}, \frac{\partial L(X)}{\partial V} = 1 - \frac{V^*}{V}$

Let the vertices's corresponding to system (3.1) be given as

$L_1 = S - S^* - \int_{S^*}^{S}[\frac{f_1(S^*,V^*)}{f_1(\phi,V^*)} + \frac{f_2(S^*,B^*)}{f_2(\phi,B^*)}]d\phi$, $L_2 = (I_v - I_v^* - I_v^* lnI_v)$, $L_3 = (I_b - I_b^* - I_b^* lnI_b)$, $L_4 = (I_{vb} - I_{vb}^* - I_{vb}^* lnI_{vb}), L_5 = (B - B^* - lnB^*), L_6 = E(V - V^* - V^* lnV)$

By equating the R.H.S of model (3.1) to zero we get

$$\begin{aligned}
\Lambda &= \frac{\beta_v S^* V^*}{1 + aS^* + bV^*} + \beta_b S^* B^* + \mu_s S^*, \\
\frac{\beta_v S^* V^*}{1 + aS^* + bV^*} &= (\beta_b^* B^* + \mu_v) I_v^*, \\
\mu_b I_b^* &= \beta_b S^* B^* - \beta_v^* I_b^* V^*, \\
\mu_{vb} I_{vb}^* &= \beta_v^* I_b^* V^* + \beta_b^* I_v^* B^*, \\
(\alpha_v + \delta_b + \frac{\gamma_a m A}{A + nB^*}) B^* &= rB^*(1 - \frac{B^*}{K}) + \tau_b n_b I_b^* \\
(\alpha_b + \delta_v) V^* &= \tau_v n_v I_v^* + \tau_{vb} n_{vb} I_{vb}^*.
\end{aligned} \tag{1}$$

Using system (1) and substituting for Λ in equation (3.44), we have

$$\begin{aligned}
\dot{L}_1 &= \Big(3 - \frac{f_1(S^*,V^*)}{f_1(S,V^*)} - \frac{S^*}{S}\Big)\Big(\frac{\beta_v S^* V^*}{1 + aS^* + bV^*} + \beta_b S^* B^* + \mu_s S^*\Big) \\
&- \Big(3 - \frac{f_1(S^*,V^*)}{f_1(S,V^*)} - \frac{S^*}{S}\Big)\Big(\frac{\beta_v SV}{1 + aS + bV} + \beta_b SB + \mu_s S\Big)
\end{aligned} \tag{2}$$

We consider Vertex 2

$$\begin{aligned}\dot{L}_2 &= (1-\frac{I_v^*}{I_v})\left(\frac{\beta_v SV}{1+aS+bV}-\beta_b^* BI_v-\mu_v I_v\right),\\ &= \frac{\beta_v SV}{1+aS+bV}+\beta_b^* I_v^* B+\mu_v I_v^*\\ &- \beta_b^* BI_v-\mu_v I_v-\frac{\beta_v SVI_v^*}{(1+aS+bV)I_v}. \end{aligned} \tag{3}$$

We substitute $\mu_v I_v^*$ from system (1) to obtain

$$\begin{aligned}\dot{L}_2 &= \beta_b^* BI_v^*+\frac{I_v^* f_1(S,V)}{f_1(S^*,V^*)}+\beta_b^* I_v^* B^*\left(1-\frac{BI_v}{B^* I_v^*}\right)\\ &- \mu_v I_v-f_1(S^*,V^*)\left(1-\frac{f_1(S,V)}{f(S^*,V^*)}\right). \end{aligned} \tag{4}$$

In equation (4) the arithmetic mean is greater than the geometric mean then we get

$$\dot{L}_2 \leq \beta_b^* I_v^* B^*(1-\frac{I_v B}{I_v^* B^*}) \tag{5}$$

Suppose we let: $I_v^* = I_v$, and $B^* = B$, then $\dot{L}_2 = 0$ and if we let $f(y) = 1-y+\ln y < 0$ then $\dot{L}_2 \leq \beta_b^* I_v^* B^*(1-\frac{I_v B}{I_v^* B^*}+\ln\frac{I_v B}{I_v^* B^*})$

Consider vertex 3

$$\begin{aligned}\dot{L}_3 &= \Big(1-\frac{I_b^*}{I_b}\Big)\Big(\beta_b SB-\beta_v^* VI_b-\mu_b I_b\Big),\\ &= \beta_b SB+\beta_v I_b^* V+\mu_b I_b^*-\beta_v^* VI_b-\mu_b I_b-\frac{\beta_b SBI_b^*}{I_b}. \end{aligned} \tag{6}$$

We substitute for $\mu_b I_b^*$ from system (1) in equation (6) to get

$$\dot{L}_3 = \beta_b SB-\mu_b I_b-\beta_v^* I_b^* V^*\Big(1-\frac{V}{V^*}\Big)+\beta_b S^* B^*\Big(1-\frac{I_b^* SB}{I_b S^* B^*}\Big). \tag{7}$$

Since the arithmetic mean is greater than the geometric mean then we have

$$\dot{L}_3 \leq \beta_b S^* B^* \Big(1 - \frac{I_b^* SB}{I_b S^* B^*}\Big). \tag{8}$$

Hence if we let: $I_b^* = I_b, S = S^*$ and $V^* = V$, then $\dot{L}_3 = 0$. Let $f(x) = 1 - x + \ln x < 0$ such that

$$\dot{L}_3 \leq \beta_b S^* B^* \Big(1 - \frac{I_b^* SB}{I_b S^* B^*} + ln \frac{I_b^* SB}{I_b S^* B^*}\Big) \tag{9}$$

Consider vertex 4

$$\frac{\partial L_4}{\partial I_{vb}} = 1 - \frac{I_{vb}^*}{I_{vb}} \tag{10}$$

and

$$\dot{L}_4 = \Big(1 - \frac{I_{vb}^*}{I_{vb}}\Big)\Big(\beta_v^* I_b V + \beta_b^* I_v B - \mu_{vb} I_{vb}\Big). \tag{11}$$

Expanding the expression we get

$$\dot{L}_4 = \beta_v^* I_b V + \beta_b^* I_v B - \mu_{vb} I_{vb} - \frac{\beta_v^* I_b V I_{vb}^*}{I_{vb}} - \frac{\beta_b^* I_v B I_{vb}^*}{I_{vb}} + \mu_{vb} I_{vb}^*, \tag{12}$$

substituting for $\mu_{vb} I_{vb}^*$ from system (1) in equation (12), we obtain

$$\dot{L}_4 = \beta_v^* I_b V + \beta_b^* I_v B - \mu_{vb} I_{vb} + \beta_v^* I_b^* V^* + \beta_b^* I_v^* B^* - \frac{\beta_v I_b V I_{vb}^*}{I_{vb}} - \frac{\beta_b^* I_v B I_{vb}^*}{I_{vb}} \tag{13}$$

$$\begin{aligned}\dot{L}_4 &= -\Big(\mu_{vb}I_{vb} - \beta_v^* I_b V - \beta_b^* I_v B\Big) + \beta_b^* I_v^* B^*\Big(1 - \frac{I_v B I_{vb}^*}{I_v^* B^* I_{vb}}\Big) \\ &+ \beta_v^* I_b^* V^*\Big(1 - \frac{I_b^* V I_{vb}^*}{I_b V^* I_{vb}}\Big). \qquad (14)\end{aligned}$$

By comparison between the arithmetical and the geometrical means in equation (14), $\dot{L}_4$ is negative definite hence

$$\dot{L}_4 \leq \beta_b^* I_v^* B^*(1 - \frac{I_v B I_{vb}^*}{I_v^* B^* I_{vb}}) + \beta_v^* I_b^* V^*(1 - \frac{I_b^* V I_{vb}^*}{I_b V^* I_{vb}}). \qquad (15)$$

Let $y = \frac{I_v B I_{vb}^*}{I_V^* B^* I_{vb}}$ and $f(y) = 1 - y + \ln y$ such that $f(y) = 0$ for $y = 1$ and $f(y) < 1$ if $y > 1$, and let $x = \frac{I_b^* V I_{vb}^*}{I_b V^* I_{vb}}$ such that $f(x) = 1 - x + \ln x < 0$ for $x = 1$ and $f(x) < 0$ if $x > 1$.

This implies that

$$\begin{aligned}\dot{L}_4 &\leq \beta_b^* I_v^* B^*\Big(1 - \frac{I_v B I_{vb}^*}{I_V^* B^* I_{vb}} + \ln \frac{I_v B I_{vb}^*}{I_V^* B^* I_{vb}}\Big) \\ &+ \beta_v I_b^* V^*\Big(1 - \frac{I_b^* V I_{vb}^*}{I_b V^* I_{vb}} + \ln \frac{I_b^* V I_{vb}^*}{I_b V^* I_{vb}}\Big). \qquad (16)\end{aligned}$$

Hence $\dot{L}_4 = 0$ iff $I_b = I_b^*, V = V^*, I_{vb} = I_{vb}^*$ and $I_v = I_v^*$

Consider vertex 5

$$\begin{aligned}\frac{\partial L_5}{\partial B} &= 1 - \frac{B^*}{B}, \\ \dot{L}_5 &= \Big(1 - \frac{B^*}{B}\Big)\Big(rB(1 - \frac{B}{K}\Big) + \tau_b n_b I_b - \Big(\alpha_v + \delta_b + \frac{\gamma_a m A}{A + hB})B\Big). \qquad (17)\end{aligned}$$

Expanding the equation (17) we obtain

$$\begin{aligned}\dot{L}_5 &= rB\Big(1 - \frac{B}{K}\Big) + \tau_b n_b I_b - \Big(\alpha_v + \delta_b + \frac{\gamma_a m A}{A + hB}\Big)B - rB^*\Big(1 - \frac{B}{K}\Big) - \tau_b n_b I_b \frac{B^*}{B} \\ &+ \Big(\alpha_v + \delta_b + \frac{\gamma_a m}{A + hB^*}\Big)B^*. \qquad (18)\end{aligned}$$

We make a substitution of $\Big(\alpha_v + \delta_b + \frac{\gamma_a m}{A+hB^*}\Big)B^*$ from system (1) to obtain

$$\begin{aligned}\dot{L}_5 &= rB\Big(1-\frac{B}{K}\Big) + \tau_b n_b I_b - (\alpha_v + \delta_b + \frac{\gamma_a m}{A+hB})B - rB^*\Big(1-\frac{B}{K}\Big) \\ &- \tau_b n_b I_b \frac{B^*}{B} + rB^*\Big(1-\frac{B^*}{K}\Big) + \tau_b n_b I_b^*. \end{aligned} \tag{19}$$

Hence simplifying equation (19) yields

$$\begin{aligned}\dot{L}_5 &= -\Big(B\Big(\alpha_v + \delta_b + \frac{\gamma_a m A}{A+hB}\Big) - rB\Big(1-\frac{B}{K}\Big) - \tau_b n_b I_b\Big) \\ &+ rB^*\Big(1-\frac{B^*}{K}\Big)\Big(1-\frac{B(1-\frac{B}{K})}{B^*(1-\frac{B^*}{K})}\Big) + \tau_b n_b I_b^*\Big(1-\frac{I_b B^*}{I_b^* B}\Big) \end{aligned} \tag{20}$$

Therefore, using the comparison between the arithmetical and geometrical means we get

$\dot{L}_5 \leq rB^*(1-\frac{B^*}{K})(1-\frac{B(1-\frac{B}{K})}{B^*(1-\frac{B^*}{K})}) + \tau_b n_b I_b^*(1-\frac{I_b B^*}{I_b^* B})$

Using the same arguments as in the previous equations we see that $\dot{L}_5 = 0$ for $B = B^*$ and $I_B = I_b^*$ and $\dot{L}_5 < 0$ by comparison of the arithmetic and geometric means.

Consider vertex 6

$$\begin{aligned}\frac{\partial L_6}{\partial V} &= 1 - \frac{V^*}{V}, \\ \dot{L}_6 &= (1-\frac{V^*}{V})(\tau_v n_v I_v + \tau_{vb} n_{vb} I_{vb} - (\alpha_b + \delta_v)V). \end{aligned} \tag{21}$$

Equation (21) simplifies to

$$\begin{aligned}\dot{L}_6 &= \tau_v n_v I_v + \tau_{vb} n_{vb} I_{vb} - V\Big(\alpha_b + \delta_v\Big) - \frac{\tau_v n_v I_v V^*}{V} - \frac{\tau_{vb} n_{vb} I_{vb} V^*}{V} \\ &+ \Big(\alpha_b + \delta_v\Big)V^* \end{aligned} \tag{22}$$

We substitute $(\alpha_b + \delta_v)V^*$ from system (1), to have

$$\begin{aligned} \dot{L}_6 &= \tau_v n_v I_v + \tau_{vb} n_{vb} I_{vb} - V\ Big(\alpha_b + \delta_v\Big) - \frac{\tau_v n_v I_v V^*}{V} \\ &- \frac{\tau_{vb} n_{vb} I_{vb} V^*}{V} + \tau_v n_v I_v^* + \tau_{vb} n_{vb} I_{vb}^* \end{aligned} \tag{23}$$

that reduces to:

$\dot{L}_6 = -((\alpha_b + \delta_v)V - \tau_v n_v I_v - \tau_{vb} n_{vb} I_{vb}) + \tau_v n_1 I_v^*(1 - \frac{I_v V^*}{I_v^* V}) + \tau_{vb} n_{vb} I_{vb}^*(1 - \frac{V^* I_{vb}}{V I_{vb}^*})$

Since the arithmetic mean is greater than the geometric mean this implies that;

$\dot{L}_6 \leq \tau_v n_v I_v^*(1 - \frac{I_v V^*}{I_v^* V}) + \tau_{vb} n_{vb} I_{vb}^*(1 - \frac{V^* I_{vb}}{V I_{vb}^*})$

Hence given $I_v = I_v^*, I_{vb} = I_{vb}^*$ and $V = V^*$, then $\dot{L}_6 = 0$ and $\dot{L}_6 < 0$

Appendix A3: Detailed mathematical coefficient terms used in Chapter 4 with corresponding computed values obtained by using parameters from Table 4.1

Appendix A3(a): Coefficient terms in the transcendental equation (4.13)

$k_4 = -(a_1 + a_5 + a_8 + a_{11} + a_{14})$,
$k_3 = (a_8(a_1 + a_5) + a_{11}(a_5 + a_1 + a_8 + a_{14}) + a_{14}(a_5 + a_1 + a_8) + a_1 a_5 - a_{12} a_{13} - a_2 a_4)$,
$k_2 = (a_2 a_4(a_8 + a_{11} + a_{14}) + a_{12} a_{13}(a1 + a_5 + a_8) - a_1 a_5(a_8 + a_{11} + a_{14}) - a_1 a_8(a_{11} + a_{14}) - a_{11}(a_5 a_8 + a_1 a_{14}) - a_{14}(a_5 a_8 + a_5 a_{11}) + a_8 a_{11}))$,
$k_1 = (a_8 a_{11}(a_1 a_5 - a_2 a_4) + a_1 a_5(a_8 a_{14} + a_{11} a_{14}) - a_2 a_4 a_{14}(a_8 + a_{11}) + a_{12} a_{13}(a_2 a_4 - a_1 a_5 - a_1 a_8 - a_5 a_8) + a_{11} a_{14}(a_1 a_8 + a_5 a_8)), k_0 = a_8(a_{11} a_{14} - a_{12} a_{13})(a_2 a_4 - a_1 a_5)$,
$l_3 = -(a_5 + a_{11} + a_{14} + a_1 + a_9), l_2 = (a_1(a_5 + a_{11} + a_{14}) + a_5(a_{11} + a_{14})) + (a_1 a_9 - a_3 a_7 + a_5 a_9 + a_9 a_{11})$,
$l_1 = (a_2 a_4(a_{14} + a_{11}) - a_1 a_5(a_{11} - a_{14}) - a_{11} a_{14}(a_1 - a_5) + a_{12} a_{13}(a_5 + a_1)) + (a_3 a_7(a_5 + a_{11}) + a_2(a_4 a_9 - a_6 a_7) - a_9 a_{11}(a_1 + a_5) - a_1 a_5 a_9), l_0 = (a_{12} a_{13}(a_2 a_4 - a_1 a_5) - a_{11} a_{14}(a_2 a_4 + a_1 a_5))) + a_7 a_{11}(a_2 a_6 - a_3 a_5) + a_9 a_{11}(a_1 a_5 - a_2 a_4)), m_3 = (a_1 + a_5 + a_8 + a_{11})$,
$m_2 = (a_1 a_5 - a_2 a_4 + a_1 a_8 + a_1 a_{11} + a_5 a_8 + a_5 a_{11} + a_8 a_{11})$,
$m_1 = (a_2 a_4 a_8 - a_1 a_5 a_{11} + a_2 a_4 a_{11} - a_1 a_8 a_{11} - a_5 a_8 a_{11} - a_1 a_5 a_8))$,
$m_0 = a_8 a_{11}(a_1 a_5 - a_2 a_4), n_2 = ((a_5 + a_{11} + a_1) + a_{11} a_{14} - a_{12} a_{13} - a_2 a_4)$,
$n_1 = (a_{11}(a1 + a_5) + a_1 a_5 - a_2 a_4), n_0 = a_{11}(a_2 a_4 - a_1 a_5))$.

Hence $a_1 = -0.01218, a_2 = 5.479 \times 10^{-4}, a_3 = -0.1764, a_4 = 2.53 \times 10^{-}5,$
$a_5 = 0.008057, a_6 = -0.0003596, a_7 = 0.0101, a_9 = 445, a_{10} = 0.005455, a_{11} = -0.01302,$
$a_{12} = 0.0003596, a_{13} = 0.01096, a_{14} = -0.03777, a_{15} = -0.3319, a_{16} = 0.33196,$
$a_{17} = 0.3279,\ k_4 = -0.07308, k_3 = 0.001759, k_2 = -0.00008172, k_1 = 0.0005897,$
$k_0 = 9.833^{-11}, l_3 = -445.2, l_2 = -14.81, -1.1915, l_0 = -0.0005686,\ m_3 = -0.03531,$
$m_2 = 0.0004299, m_1 = 0.00006202, m_0 = 00002674, n_2 = -0.3277, n_1 = 0.0003616,$
$n_0 = 0.000001277.$

Appendix A3(b): Coefficient terms in the characteristic equation (4.14)

$b_4 = k_4 + \gamma + \delta, b_3 = k_3 + l_3\gamma + m_3\delta, b_2 = k_2 + l_2\gamma + m_2\delta + n_2\gamma\delta, b_1 = k_1 + l_1\gamma + m_1\delta + n_1\gamma\delta,$
$b_0 = l_o\gamma + m_0\delta + n_0\gamma\delta,$ hence $b_4 = 0.7364, b_3 = -148.4007, b_2 = -4.9408, b_1 = -0.3965, b_0 = -0.0001806.$

Appendix A3(c): Coefficient terms in equation (4.25)

$A_4 = (p_2^2 - p^2\gamma^2\delta^2 q_4 - 2p_3), A_3 = (2p_1 + p_3^2 - 2p_2p_4 - p^2\gamma\delta^2(q_3^2 - 2q_4q_2)),$
$A_2 = (p_2^2 - 2p_1p_2 - p^2\gamma^2\delta^2(2q_4q_0 + q_2^2 - 2q_1q_3)), A_1 = p_1 - p^2\gamma^2\delta^2(q_1 - 2q_2q_0),$
$A_0 = -q_0^2p^2\gamma^2\delta^2,$
hence $A_4 = 296.9, A_3 = 22018, A_2 = 0.3754, A_1 = -0.3966, A_0 = -2585 \times 10^{-11}.$

Appendix A3(d): Coefficient terms in Transversality condition of equation 4.29

$d_0 = w_{2_0}\tau_2, f_1 = 5w_{2_0}^4 - (3p_3w_{2_0}^2 + p_1), f_2 = 4p_4w_{2_0}^3 - 2p_2w_{2_0}, f_3 = 2p_2w_{2_0} - 4p_4w_{2_0}^3,$
$f_4 = 5w_{2_0}^4 - 3p_3w_{2_0}^2, g_1 = p\gamma\delta(q_3w_{2_0}^4 - q_1w_{2_0}^2), g_2 = p\gamma\delta(q_4w_{2_0}^5 + q_0w_{2_0} - q_2w_{2_0}^3),$
$f_5 = q_1 + 2q_2w_{2_0} - (3q_3w_{2_0}^2 + 4q_4w_{2_0}^3),$
hence
$p = 0.9939, p_4 = 0.4064, p_3 = -148.4, p_2 = 0.3333, p_1 = -0.3966, p_0 = -0.0001895,$
$q_4 = 0.3279, q_3 = 0.6280, q_2 = -0.003463, q_1 = 0.00004153, q_0 = 0.00002672,$

Appendix A3(e): Critical value for seeking medical care τ_{2_0}

By applying L'Hopitals rule to the arccos function of equation (4.27), let

$y = \arccos(Z)$, $Z = \frac{(p_2 w_{2_0}^2 - p_4 w_{2_0}^4 - p_0)(q_4 w_{2_0}^4 - q_2 w_{2_0}^2 + q_0) + (q_3 w_{2_0}^3 - q_1 w_{2_0})(p_3 w_{2_0}^3 - w_{2_0}^5 - p_1 w_{2_0})}{p\gamma\delta\left((q_4 w_{2_0}^4 - q_2 w_{2_0}^2 + q_0)^2 - (q_1 w_{2_0} - q_3 w_{2_0}^3)^2\right)}$,

$$\frac{d(y)}{dw_{2_0}} = -\frac{(2p_2 w_{2_0} - 4p_4 w_{2_0}^3 - p_0)(q_4 w_{2_0}^4 - q_2 w_{2_0}^2 + q_0) + (p_2 w_{2_0}^2 - p_4 w_{2_0}^4 - p_0)(4q_4 w_{2_0}^3 - 2q_2 w_{2_0})}{p\gamma\delta\left(2(q_4 w^4 - q_2 w^2 + q_0))(4q_4 w^3 - 2q_2 w) - 2(q_1 w - q_3 w^3)(q_1 - 3q_3 w^2)\sqrt{1 - Z^2}\right)}$$

$$- \frac{(p_3 w_{2_0}^3 - w_{2_0}^5 - p_1 w_{2_0})(3q_3 w_{2_0}^2 - q_1) + (q_3 w_{2_0}^3 - q_1 w)(3p_3 w_{2_0}^2 - 5w_{2_0}^4 - p_1)}{p\gamma\delta\left(2(q_4 w_{2_0}^4 - q_2 w_{2_0}^2 + q_0))(4q_4 w_{2_0}^3 - 2q_2 w_{2_0}) - 2(q_1 w_{2_0} - q_3 w_{2_0}^3)(q_1 - 3q_3 w_{2_0}^2)\sqrt{1 - Z^2}\right)} = 0.174$$

Appendix A4: Matlab codes used in simulations

Appendix A4(a): Matlab codes for figures in Chapter 3

```
function mbabazi1()
clear all;
clc;
lambda = 10^3;
mu1=0.0625;
mu2 = 8.9 * 10^-1;
n1 = 1.0 * 10^2;
a=0.001;
b=0.002;
beta1 = 2.7 * 10^-5;
delt1=4;
alp2 = 3.2 * 10^-4;
tau1 = 1.2 * 10^-1;
r=27;
tau2 = 1.1 * 10^-2;
K = 2.3 * 10^7;
gamma=1.25;
m=400;
delt2 = 3.2 * 10^-1;
alp1 = 10^-1;
n2 = 10^4;
h=5.0;
A = 10^6;
beta2=0.012;
mu3 = 1.34 * 10^-1;
mu4 = 5.2 * 10^-10;
```

$tau3 = 2.4 * 10^-3;$
n3=25.1;
$beta3 = 7.3 * 10^-8;$
$beta4 = 4.1 * 10^-6;$
options=odeset('RelTol',10^-4,'$AbsTol'$,$[10^-4; 10^-4; 10^-4; 10^-4; 10^-4; 10^-4]$);
$[T, y] = ode45(@pmemodel, [08], [4.8 * 10^2; 10; 1; 10; 10^2; 10^7]$,options)
figure(10)
hold on
plot(T,abs(log(y(:,4))),'b','linewidth',1)
hold off
xlabel('Time,t/days');ylabel('Co-infected cell populaton/log-scale');
%figure(11)
%hold on
%plot(T,y(:,4),'r','linewidth',1)
%hold off
%xlabel('Time,t/days');ylabel('Co-infected cell populaton');
%figure(1)
%hold on
%plot(T,abs(log(y(:,1))),'r','linewidth',1)
%plot(T,abs(log(y(:,4))),'g',T,abs(log(y(:,5))),'b',T,abs(log(y(:,6))),'r','linewidth',1)
%%xlabel('Time,t/days');ylabel(' infected cell population/log-scale');
%figure(2)
%hold on
%plot(T,y(:,1),'b','linewidth',1)
%plot(T,abs(log(y(:,1))),'r',T,abs(log(y(:,4))),'b',T,abs(log(y(:,3))),'y',T,abs(log(y(:,2))),'–','linewidth',1)
%hold off
%xlabel('Time,t/days');ylabel(' uninfected cell population/log-scale');
%figure(3)
%hold on
%plot(T,abs(log(y(:,4))),'b',T,abs(log(y(:,1))),'r','linewidth',1)
%hold off
%xlabel('Time,t/days');ylabel(' cell population');
%figure(4)
%hold on
%plot(T,y(:,4),'r',T,y(:,1),'b','linewidth',1)
%hold off
%xlabel('Time,t/days');ylabel('cell population');
%figure(5)
%hold on
%plot(y(:,5), y(:,6),'b','linewidth',1)
%hold off
%xlabel('Density of pneumococcal');ylabel('Density of IAV');
%figure(6)
%hold on
%plot(y(:,5), y(:,6),'r','linewidth',1)

```
%hold off
%ylabel('Density of pneumococcal');xlabel('Density of IAV');
%figure(8)
%hold on
%plot(T,y(:,1),'r',T,y(:,4),'b',T,y(:,3),'y',T,y(:,2),'g','linewidth',1)
%hold off
%xlabel('Time,t/days');ylabel('cell population');
%figure(10)
%hold on
%plot(T,abs(log(y(:,4))),'b',T,abs(log(y(:,3))),'r',T,abs(log(y(:,2))),'g','linewidth',1)
%hold off
%xlabel('Time,t/days');ylabel('cell population/log-scale');
%figure(12)
%hold on
%plot(T,abs(log(y(:,3))),'b','linewidth',1)
%hold off
%xlabel('Time,t/days');ylabel('Density of newly infected cells/log-scale');
%xlabel('Time,t/days');ylabel('cell population/log-scale');
%figure(2)
%plot(abs(log(y(:,5))), abs(log(y(:,6))),'r','linewidth',1)
%ylabel('Density of SP/log-scale');xlabel('Density of IAV/log-scale');
%figure(2)
%hold on
%plot(T,y(:,2),'b',T,y(:,3),'r',T,y(:,4),'g','linewidth',1)
%hold off
%xlabel('Time,t/days');ylabel(' cell population');
%figure(2)
%hold on
%plot(T,abs(log(y(:,4))),'b',T,abs(log(y(:,1))),'r','linewidth',1)
%hold off
%xlabel('Time,t/days');ylabel(' cell population');
%figure(3)
%hold on
%plot(T,abs(log(y(:,5))),'b',T,abs(log(y(:,1))),'r',T,abs(log(y(:,6))),'g','linewidth',1)
%hold off
%xlabel('Time,t/days');ylabel(' cell population/log-scale ');
%figure(4)
%hold on
%plot(T,abs(log(y(:,1))),'r',T,abs(log(y(:,4))),'b','linewidth',1)
%hold off
%xlabel('Time,t/days');ylabel(' cell population/log-scale');
%figure(5)
%hold on
%plot(T,abs(log(y(:,1))),'r',T,abs(log(y(:,4))),'b',T,abs(log(y(:,3))),'y',T,abs(log(y(:,2))),'–','linewidth',1)
%hold off
```

%xlabel('Time,t/days');ylabel(' cell population/log-scale ');
%figure(2)
%hold on
%plot(T,y(:,4),'b','linewidth',1)
%hold off %xlabel('Time,t/days');ylabel('coinfected cells, $I_v b(t)$');
%figure(3)
%hold on
%plot(T,y(:,5),'b',T,y(:,5),'g',T,y(:,1),'r','linewidth',1)
%hold off
%xlabel('uninfected,S(t)');ylabel('Proportion of cells infected with , B(t) and B(t)');
%figure(3)
%hold on
%plot(T, y(:,2),'r','linewidth',1)
%hold off
%xlabel('Time,t/hours');ylabel('Proportion of cells infected with IAV, $I_v(t)$');
%figure(3)
%hold on
%plot(T,y(:,1),'r',T,y(:,4),'b','linewidth',1)
%hold off
%xlabel('Time,t/hours');ylabel('Proportion of cells, S(t) and Ivb(t)')
function dy=pnemodel(t,y)
dy=zeros(6,1);
$dy(1) = lambda - (beta1 * y(1) * y(6))./(1 + a * y(1) + b * y(6)) - beta2 * y(1) * y(5) - mu1 * y(1);$
$dy(2) = (beta1 * y(1) * y(6))./(1 + a * y(1) + b * y(6)) - beta4 * y(5) * y(2) - mu2 * y(2);$
$dy(3) = beta2 * y(1) * y(5) - mu3 * y(3) - beta3 * y(6) * y(3);$
$dy(4) = beta4 * y(5) * y(2) + beta3 * y(6) * y(3) - mu4 * y(4);$
$dy(5) = r * y(5) * (1 - y(5)./K) + tau2 * n2 * y(3) - (gamma * m * A * y(5))./A + h * y(5) -$
$(alp1 + delt2) * y(5);$
$dy(6) = tau1 * n1 * y(2) + y(4) * n3 * tau3 - (alp2 + delt1) * y(6);$
end
end

Appendix A4(b): dde23 codes for figures in Chapter 4

function DFE()
clear all;
clc;
$nu = 2.53 * 10^-2;$
$b = 22;$
$beta = 1.0102 * 10^-5;$
$mu = 2.0547 * 10^-3;$
$zeta = 5.4794 * 10^-4;$
$gamma = 3.3333 * 10^-2;$
$rho = 0.01096 * 10^-2;$

$phi = 3.57144 * 10^-1;$
$vartheta = 5.4 * 10^-1;$
$delt = 0.033;$
$options = odeset('RelTol', 10^-4,' AbsTol', [10^-4; 10^-4; 10^-4; 10^-4; 10^-4]);$
$[T, y] = ode45(@pnemodel, [0400], [10604; 103; 0; 0; 0], options)$
figure(2)
hold on
$plot(T, y(:, 1),' b', T, y(:, 2),' r',' linewidth', 1);$
hold off
xlabel('Time/days');ylabel('Population Size')
function dy =pnemodel(t, y)
$dy = zeros(5, 1);$
$dy(1) = b + zeta * y(2) + phi * y(5) - (nu + mu + beta * y(5)) * y(1);$
$dy(2) = nu * y(1) - (mu + zeta) * y(2) - beta * vartheta * y(5) * y(2);$
$dy(3) = beta * y(5) * y(1) - (gamma + mu) * y(3);$
$dy(4) = beta * vartheta * y(5) * y(2) - (rho + mu) * y(4);$
$dy(5) = rho * y(4) + gamma * y(3) - (delt + mu + phi) * y(5);$
end
end

{**driver for figure 3**
$sol = dde23('figure3',' 1', [3280, 30, 10, 10, 100], [0, 200]);$
$V = sol.y;$
$y1 = V(1, :);$
$y2 = V(2, :);$
$y3 = V(3, :);$
$y4 = V(4, :);$
$y5 = V(5, :);$
plot(sol.$x, y1,' r')$
$plot(y1, y5);$}
function v = figure3(t, y, Z)
ylag1=Z(:,1);
v=zeros(5,1);
$nu = 2.53 * 10^-5;$
$b = 22;$
$betar = 1.0102 * 10^-4;$
$mu = 2.0547 * 10^-3;$
$xi = 5.4794 * 10^-4;$
$gamma = 3.3333 * 10^-1;$
$rho = 0.01096;$
$phi = 3.5714 * 10^-2;$
$tau1 = 1;$
$vartheta = 5.4 * 10^-1;$
$delta = 0.33;$
$v(1) = b + xi * y(2) + phi * y(5) - (nu + mu + betar * y(5)) * y(1);$

$v(2) = nu * y(1) - (mu + xi) * y(2) - betar * vartheta * y(5) * y(2);$
$v(3) = betar * y(5) * y(1) - gamma * exp(-mu * tau1) * Z(3,1) - mu * y(3);$
$v(4) = betar * vartheta * y(5) * y(2) - (rho + mu) * y(4);$
$v(5) = rho * y(4) + gamma * exp(-mu * tau1) * Z(3,1) - (delta + mu + phi) * y(5);$

{**driver for figure 4**
sol=dde('fulgef2', '2', $[106, 10, 1, 1, 5], [0, 100]$);
$V = sol.y;$
$y1 = V(1,:);$
$y2 = V(2,:);$
$y3 = V(3,:);$
$y4 = V(4,:);$
$y5 = V(5,:);$
plot$(sol.x, sol.y(5,:), 'r', 'LineWidth', 1.5);$
function$v = fulgef2(t, y, Z)$
ylag2=Z(:,2);
v=zeros(5,1);
$nu = 2.53 * 10^-5;$
$b = 22;$
$betar = 1.0102 * 10^-3;$
$mu = 2.0547 * 10^-3;$
$xi = 5.4794 * 10^-4;$
$gamma = 3.3333 * 10^-1;$
$rho = 1.096 * 10^-2;$
$phi = 3.5714 * 10^-2;$
$tau2 = 2;$
$vartheta = 5.4 * 10^-1;$
$delta = 3.3 * 10^-1;$
function $dy = pnemodel(t, y)$
$y = zeros(5, 1);$
$dy(1) = b + xi * y(2) + phi * y(5) - (nu + mu + betar * y(5)) * y(1);$
$dy(2) = nu * y(1) - (mu + xi) * y(2) - betar * vartheta * y(5) * y(2);$
$dy(3) = betar * y(5) * y(1) - gamma * y(3) - mu * y(3);$
$dy(4) = betar * vartheta * y(5) * y(2) - (rho + mu) * y(4);$
$dy(5) = rho * y(4) + gamma * y(3) - delta * exp(-mu * tau2) * y(5) - (mu + phi) * y(5);$
end
end

{**driver for figure 4**
sol=dde23('figure3', $[23], [3280, 22, 100, 5, 11], [0, 4000]$)
$V = sol.y;$
$y1 = V(1,:);$
$y2 = V(2,:);$
$y3 = V(3,:);$
$y4 = V(4,:);$

$y5 = V(5,:);$
plot3(sol.$x, y1, y5,' b'$,'LineWidth',1)}
function v = figure3(t, y, Z)
ylag1=Z(:,1);
ylag2=Z(:,2);
v=zeros(5,1);
$nu = 2.53 * 10^{-}5;$
$b = 22;$
$betar = 1.0102 * 10^{-}4;$
$mu = 2.0547 * 10^{-}4;$
$xi = 5.4794 * 10^{-}4;$
$gamma = 3.3333 * 10^{-}1;$
$rho = 0.01096;$
$phi = 3.5714 * 10^{-}2;$
$tau1 = 2;$
$tau2 = 3;$
$vartheta = 5.4 * 10^{-}1;$
$delta = 0.33;$
$v(1) = b + xi * y(2) + phi * y(5) - (nu + mu + betar * y(5)) * y(1);$
$v(2) = nu * y(1) - (mu + xi) * y(2) - betar * vartheta * y(5) * y(2);$
$v(3) = betar * y(5) * y(1) - gammaexp(-mu * tau1) * Z(3,1) - mu * y(3);$
$v(4) = betar * vartheta * y(5) * y(2) - (rho + mu) * y(4);$
$v(5) = rho * y(4) + gamma * exp(-mu * tau1) * Z(3,1)$
$- delta * exp(-mu * tau2) * Z(5,2) - (mu + phi) * y(5);$

{**driver for figure 5**
sol=dde23('figure5',[22], [2099, 6, 54, 2, 100], [0, 3000])
V=sol.y;
y1=V(1,:);
y2=V(2,:);
y3=V(3,:);
y4=V(4,:);
y5=V(5,:);
plot3(y1, y2, y5)}
function v = figure5(t, y, Z)
ylag1=Z(:,1);
ylag2=Z(:,2);
v=zeros(5,1);
$nu = 2.53 * 10^{-}5;$
$b = 22;$
$betar = 1.0102 * 10^{-}4;$
$mu = 2.0547 * 10^{-}3;$
$xi = 5.4794 * 10^{-}4;$
$gamma = 3.3333 * 10^{-}1;$
$rho = 1.096 * 10^{-}2;$

$phi = 3.5714 * 10^-2;$
$tau1 = 2;$
$tau2 = 3;$
$vartheta = 5.4 * 10^-1;$
$delta = 0.33;$
$v(1) = b + xi * y(2) + phi * y(5) - (nu + mu + betar * y(5)) * y(1);$
$v(2) = nu * y(1) - (mu + xi) * y(2) - betar * vartheta * y(5) * y(2);$
$v(3) = betar * y(5) * y(1) - gamma * exp(-mu * tau1) * Z(3,1) - mu * y(3);$
$v(4) = betar * vartheta * y(5) * y(2) - (rho + mu) * y(4);$
$v(5) = rho * y(4) + gamma * exp(-mu * tau1) * Z(3,1)$
$- delta * exp(-mu * tau2) * Z(5,2) - (mu + phi) * y(5);$

{**driver for figure 5**
sol=dde23('figure10', [0.5 2], [3280, 20, 20, 8, 10], [0,4000])
V=sol.y;
y1=V(1,:);
y2=V(2,:);
y3=V(3,:);
y4=V(4,:);
y5=V(5,:);
plot(y1,y5)}
function v = figure10(t, y, Z)
ylag1=Z(:,1); ylag2=Z(:,2); v=zeros(5,1); $nu = 2.53 * 10^-5;$
$b = 22;$
$betar = 1.0102 * 10^-4;$
$mu = 2.0547 * 10^-3;$
$xi = 5.4794 * 10^-4;$
$gamma = 3.3333 * 10^-1;$
$rho = 1.096 * 10^-2;$
$phi = 3.5714 * 10^-2;$
$tau1 = 0.5;$
$tau2 = 2;$
$vartheta = 5.4 * 10^-1;$
$delta = 0.33;$
$v(1) = b + xi * y(2) + phi * y(5) - (nu + mu + betar * y(5)) * y(1);$
$v(2) = nu * y(1) - (mu + xi) * y(2) - betar * vartheta * y(5) * y(2);$
$v(3) = betar * y(5) * y(1) - gamma * exp(-mu * tau1) * Z(3,1) - mu * y(3);$
$v(4) = betar * vartheta * y(5) * y(2) - (rho + mu) * y(4);$
$v(5) = rho * y(4) + gamma * exp(-mu * tau1) * Z(3,1)$
$- delta * exp(-mu * tau2) * Z(5,2) - (mu + phi) * y(5);$

{**driver for figure 5**
sol=dde23(figure14,'3',[10, 5, 5, 2, 4, 2], [0,14])
V=sol.y;
y1=V(1,:);

y2=V(2,:);
y3=V(3,:);
y4=V(4,:);
y5=V(5,:);
figure(1)
hold on
plot3(sol.x,y1,y5,'r','LineWidth',2)
hold off}
function v = figure14(t, y, Z)
ylag2=Z(:,2);
v=zeros(5,1);
$nu = 2.53 * 10^-5;$
$b = 22;$
$betar = 1.0102 * 10^-4;$
$mu = 2.0547 * 10^-3;$
$xi = 5.4794 * 10^-4;$
$gamma = 3.3333 * 10^-1;$
$rho = 1.096 * 10^-2;$
$phi = 3.5714 * 10^-3;$
$tau2 = 3;$
$vartheta = 5.4 * 10^-1;$
$delta = 0.33;$
$v(1) = b + xi * y(2) + phi * y(5) - (nu + mu + betar * y(5)) * y(1);$
$v(2) = nu * y(1) - (mu + xi) * y(2) - betar * vartheta * y(5) * y(2);$
$v(3) = betar * y(5) * y(1) - (gamma + mu) * y(3);$
$v(4) = betar * vartheta * y(5) * y(2) - (rho + mu) * y(4);$
$v(5) = rho * y(4) + gamma * y(3) - delta * exp(-mu * tau2) * Z(5, 2)$
$- (mu + phi) * y(5);$

{**driver for figure 5**
sol=dde23('figure30', [1.5 1.5], [5586, 22, 11, 64, 100], [0,4000])
V=sol.y;
y1=V(1,:);
y2=V(2,:);
y3=V(3,:);
y4=V(4,:);
y5=V(5,:);
plot(y1,y5)}
function v = figure30(t, y, Z) ylag1=Z(:,1); ylag2=Z(:,2); v=zeros(5,1); $nu = 2.53 * 10^-5;$
$b = 22;$
$betar = 1.0102 * 10^-4;$
$mu = 2.0547 * 10^-4;$
$xi = 5.4794 * 10^-4;$
$gamma = 3.3333 * 10^-1;$
$rho = 1.096 * 10^-2;$

$phi = 3.5714 * 10^-1;$
$tau1 = 1.5;$
$tau2 = 1.5;$
$vartheta = 5.4 * 10^-1;$
$delta = 0.33;$
$v(1) = b + xi * y(2) + phi * y(5) - (nu + mu + betar * y(5)) * y(1);$
$v(2) = nu * y(1) - (mu + xi) * y(2) - betar * vartheta * y(5) * y(2);$
$v(3) = betar * y(5) * y(1) - gamma * exp(-mu * tau1) * Z(3,1) - mu * y(3);$
$v(4) = betar * vartheta * y(5) * y(2) - (rho + mu) * y(4);$
$v(5) = rho * y(4) + gamma * exp(-mu * tau1) * Z(3,1) - delta * exp(-mu * tau2) * Z(5,2) -$
$(mu + phi) * y(5);$

Appendix A4(c): Matlab codes for figures in Chapter 5

function DFE3()
clear all;
clc;
A =5;
beta =0.0147;
$beta2 = 0.7498e - 5;$
beta1=0.046;
mu =0.0002;
delta=0.1;
$gamma = 1.45 * 10^-2;$
m=0.5;
phi =0.9;
tau =0.2703;
p=0.001;
xi=0.3;
upsilon=0.0039;
options=odeset('RelTol',10^-4,$'AbsTol'$, $[10^-4; 10^-4; 10^-4; 10^-4]$);
$[T, y] = ode45(@pnemodel, [0100], [200; 300; 20; 20], options)$
figure(3)
hold on
plot(y(:,1),y(:,3), 'r','linewidth',0.5)
hold off
xlabel('Unaware susceptible');ylabel('Infected')
function dy=pnemodel(t,y)
dy=zeros(4,1);
$dy(1) = A + xi * y(2) - y(1) * (beta * y(3) - beta1 * m * y(3)/(m + y(3)))$
$- upsilon * y(1) * y(3) - mu * y(1);$
$dy(2) = upsilon * y(1) * y(3) - mu * y(1) + (1 - p) * phi * y(3)/(1 + tau * y(3))$
$- (beta2 * y(3) + xi + mu) * y(2);$
$dy(3) = y(1) * (beta * y(3) - beta1 * m * y(3)/(m + y(3))) + beta2 * y(3) * y(2)$

$+ gamma * y(4) - phi * y(3)/(1 + tau * y(3)) - (mu + delta) * y(3);$
$dy(4) = p * phi * y(3)/(1 + tau * y(3)) - (gamma + mu) * y(4);$
end
end

function mbabazi()
clear all;
clc;
A =5;
$beta = 0.046 * 10^{-}1;$
beta2=0.0000749;
beta1=0.0046;
mu =0.0002;
delta=0.1;
$gamma = 1.45 * 10^{-}2;$
m=0.65;
phi =0.9;
tau =0.24;
p=0.02;
xi=0.3;
upsilon=0.0029;
options=odeset('RelTol',$10^{-}4,' AbsTol', [10^{-}4; 10^{-}4; 10^{-}4; 10^{-}4]);$
$[T, y] = ode45(@pnemodel, [0100], [20; 500; 20; 10], options)$
figure(1)
hold on
plot(T,abs(log(y(:,4))),'r','linewidth',2);
hold off
xlabel('Time/days');ylabel(' Population size')
%plot(T,abs(log(y(:,1))),'b',T,abs(log(y(:,2))),'y', T, abs(log(y(:, 3))),'k', T, abs(log(y(:, 4))),'r','linewidth',0.5)
%plot(T,abs(log(y(:,1))),'b', T, y(:, 2),'r','T, y(:,3),'g', T, y(:, 4),'p',linewidth',1);
%figure(2)
%hold on
%plot3(y(:,4),y(:,2),y(:,1));
%plot(T,y(:,1),'b',T, y(:,2),'r')
%plot(T,y(:,2),'b',T, y(:, 5),'r', T,y(:,1),'g','linewidth',0.5);
%hold off
%xlabel('Time/days');ylabel('Infected popn, I')
%xlabel('Time/days');ylabel('vaccinated, V')
function dy=pnemodel(t,y)
dy=zeros(4,1);
$dy(1) = A + xi * y(2) - y(1) * (beta * y(3) - beta1 * m * y(3)/(m + y(3)))$
$- upsilon * y(1) * y(3) - mu * y(1);$
$dy(2) = upsilon * y(1) * y(3) - mu * y(1) + (1 - p) * phi * y(3)/(1 + tau * y(3))$
$- (beta2 * y(3) + xi + mu) * y(2);$
$dy(3) = y(1) * (beta * y(3) - beta1 * m * y(3)/(m + y(3))) + beta2 * y(3) * y(2)$

$+ gamma * y(4) - phi * y(3)/(1 + tau * y(3)) - (mu + delta) * y(3);$
$dy(4) = p * phi * y(3)/(1 + tau * y(3)) - (gamma + mu) * y(4);$
end
end

Appendix A5: List of Publications

(1) Mbabazi,F.K., Mugisha, J.Y.T.,& Kimathi, M. (2018), Modeling the within–host co–infection of influenza A virus and pneumococcus. *Applied Mathematics and Computation*, 339, 488-506. *https://doi.org/10.1016/j.amc.2018.07.031*

(2) Mbabazi,F.K., Mugisha, J.Y.T.,& Kimathi, M. (2019), Hopf–bifurcation analysis of pneumococcal pneumonia with time delays. *Abstract and Applied Analysis,* 2019(1), 1-21. *https://doi.org/10.1155/2019/3757036*

(3) Mbabazi,F.K., Mugisha, J.Y.T.,& Kimathi, M, Modeling pneumococcal pneumonia with interventions: Awareness and saturated treatment *Under review*